Université de Montréal

Transcriptional activation by Sp1 and post-transcriptional repression by muscle-specific microRNA *miR-133* of expression of human *ERG1* and *KCNQ1* genes and potential implication in arrhythmogenesis

par

Xiaobin Luo

Programme des Sciences biomédicales

Département de Médecine
Faculté de Médecine

Thèse présentée à la Faculté des études supérieures
en vue de l'obtention du grade de Maîtrise
en Sciences biomédicales

Avril 2007

Université de Montréal
Faculté des études supérieures

Cette thèse intitulée :

Transcriptional activation by Sp1 and post-transcriptional repression by muscle-specific microRNA *miR-133* of expression of human *ERG1* and *KCNQ1* genes and potential implication in arrhythmogenesis

présentée par :

Xiaobin Luo

a été évaluée par un jury composé des personnes suivantes :

Dr. Bruce G. Allen
Président-rapporteur
Dr. Zhiguo Wang
Directeur de recherche
Dr. Alvin Shrier
Membre du jury

RÉSUMÉ

Les gènes *HERG1* et *KCNQ1* codent pour l'expression de sous-unités alpha canalaires perméables aux ions K^+. Ces protéines canal participent activement au processus de repolarisation des myocytes cardiaques comme dans le phénomène de « réserve de repolarisation » et ainsi constituent des acteurs déterminants dans l'apparition des arythmies. L'expression de ces gènes présente une disparité régionale dépendant à la fois de facteurs de différenciation mais aussi du profil physiopathologique du muscle cardiaque. Dans cette étude, nous avons identifié l'ensemble des régions promotrices et les sites d'initiation de la transcription de tous les isoformes de *HERG1* et *KCNQ1*. Nous avons aussi caractérisé un transactivateur commun, la protéine SP1 qui permet de contrôler leur transcription. Pour la première fois nous apportons des évidences expérimentales montrant que les gènes codant pour l'expression des canaux ioniques constituent des cibles de régulation pour les microARNs (miARNs): *miR-133* réprimait l'expression de *HERG1* et *KCNQ1* et *miR-1* réprimait l'expression de *KCNE1*. Les ARNm codant pour l'expression de l'ensemble des isoformes *HERG1* et *KCNQ1* étaient distribuées de façon asymétrique au sein du muscle cardiaque avec une prédominance dans les cavités de la partie droite du cœur en comparaison avec la partie gauche. Nous avons observé une hétérogénéité spatiale de la distribution de *KCNQ1* et *KCNE1* suivant trois axes (interventriculaire, transmural et apical-basal) avec une disparité notable entre les niveau d'expression des ARNm et des protéines correspondantes. Cette disparité était associée à une hétérogénéité dans la distribution spatiale de SP1 et *miR-1/miR-133*. Nos données ont ensuite permis de montrer clairement que des interactions entre SP1 et miR-1/miR-133 déterminent l'expression des gènes *HERG1* et *KCNQ1*, par la même, seul le profil d'expression régional de SP-1 et *miR-1/miR-133* pouvait expliquer la différence régionale reconnue des courants I_{Kr} et I_{Ks}, démasquant une implication potentielle dans la genèse des arythmies. Ainsi notre étude a permis de caractériser un nouvel aspect de la fonction cellulaire des miARNs visant à réguler l'électrophysiologie cardiaque. Offrant une explication des différences observées entre les quantités d'ARNm et les niveaux d'expression des protéines issus d'un même gène.

Mots-clés: HERG1, KCNQ1, Canaux potassiques, Sp1, microARNs, miR-1, miR-133, Arythmies, Différences régionales, Repolarisation.

ABSTRACT

HERG1 and *KCNQ1* genes encode two major repolarizing K^+ channel α-subunits that critically determine the repolarization rate and repolarization reserve in cardiac cells thereby the likelihood of arrhythmias. Expressions of these genes are regionally heterogeneous and change dynamically depending on differentiation status and pathological states of the heart. Here we identified the core promoter regions and transcription start sites for all *HERG1* and *KCNQ1* isoforms, and revealed Sp1 as a common transactivator for their transcriptions. We also demonstrated that the mRNA levels of all *HERG1* and *KCNQ1* isoforms are asymmetrically distributed within the heart, being predominant in the right relative to the left chamber. Notably, we for the first time experimentally validated ion channel genes as targets for microRNA regulation by showing the ability of *miR-133* to repress *HERG1* and *KCNQ1* and of *miR-1* to repress *KCNE1*. We further demonstrated the spatial heterogeneity of *KCNQ1* and *KCNE1* distributions along three axes (interventricular, transmural and apical-basal) and disparity between mRNA and protein expression of these genes, and the spatial heterogeneity of Sp1 and *miR-1/miR-133* distributions as well. Our data strongly indicate that the interplay between Sp1 and *miR-1/miR-133* determines the expression levels of *HERG1* and *KCNQ1* genes and the unique regional expression profiles of Sp1 and *miR-1/miR-133* may be one of the mechanisms for the well-recognized regional differences of I_{Kr} and I_{Ks}, which might have a potential implication in arrhythmogenesis. Moreover, our study unraveled a novel aspect of the cellular function of miRNAs in regulating cardiac electrophysiology and offered an explanation for disparities between mRNA and protein expressions of genes.

Keywords : HERG1, KCNQ1, Potassium channels, Sp1, microRNA, miR-1, miR-133, Arrhythmia, Regional difference, Repolarization.

TABLE OF CONTENT

LIST OF TABLES

LIST OF FIGURES

Chapter 3

LIST OF ABBREVIATIONS

AF: Atrial fibrillation

AP: Action potential

APD: Action potential duration

AVB: Atrioventricular block

AVN: Atrioventricular node

CACNA1C: L-type-calcium channel alpha 1C subunit

EAD: Early afterdepolarizaiton

EAG: *ether-a-go-go* related gene

Epi: Epicardial

Endo: Endocardial

HEK293: Human embryonic kidney 293 cell line

HERG: Human *ether- a-go-go* related gene

HERG1a: Human *ether- a-go-go* related gene isoform 1

HERG1b: Human *ether- a-go-go* related gene isoform 2

$I_{Ca,L}$: L-type calcium current/channel

I_K: Delayed rectifier potassium current/channel

I_{Kur}: Ultrarapidly-activated delayed rectifier potassium current/channel

I_{Na}: Voltage-gated sodium channel/channel

I_{to}: Transient outward potassium current/channel

I_{Kr}: Rapidly-activated delayed rectifier potassium current/channel

I_{Ks}: Slowly-activated delayed rectifier potassium channel/channel

I_{K1}: Inward recitifer potassium current/channel

Irx5: Iroquois homeobox transcription factor

K^+: Potassium

KCNQ1 (KvLQT1): Slow delayed rectifier K^+ channel alpha subunit member 1

KCNQ1a: Slow delayed rectifier K^+ channel alpha subunit member 1 isoform 1

KCNQ1b: Slow delayed rectifier K^+ channel alpha subunit member 1 isoform 2

K_V: Voltage-gated potassium

LQTS: Long QT syndrome

LA: Left atrium

LV: Left ventricle

LPC: Lysophosphatidylcholine

minK (KCNE1): Minimal potassium channel

MiRP1 (or KCNE2): MinK-related peptide 1

M-cell: Midmyocardial cells

Mid: Midmyocardial

miRNA(s): microRNA(s)

miR-1: microRNA-1

miR-133: microRNA-133

Mef2: Myocyte enhancer factor 2

Nkx2-5: NK2 class of homeobox transcription factor

NFAT: Nuclear factor of activated T-cells

NF-κB: Nuclear factor-kappa B

RA: Right atrium

RV: Right ventricle

RACE: Rapid amplification of cDNA ends

P-/GW-bodies: Processing bodies

SAN: Sinoatrial node

siRNAs: short interfering RNAs

Sp1: Stimulating protein 1

SCN5A: Sodium channel alpha subunit

SRF: Serum response factor

Stat3: Signal transducer and activator of transcription-3

SV40 promoter: Simian virus 40 (SV40) promoter

TK promoter: Thymidine kinase (TK) promoter

TdP: torsades de pointes

Tbx: T-Box transcription factor

TSS: Transcription start site

3'UTR: 3'-untranslated region

5'UTR: 5'-untranslated region

Special recognition is due as well to the administrative office at the Centre de Recherche de l'ICM, to the staff in the Faculte de medicine and the Faculte de medicine and the Faculte de etudies superieurs of the Universite de Montreal, for their help in my graduate studies and preparing for this thesis. I would like to extend my gratitude to Dr. Bruce G. Allen, Dr. Alvin Shrier for their kindness in spending time to review my thesis and providing insightful suggestions and constructive comments in my thesis.

I want to deeply thank my wonderful parents (Zhihong Wang and Shiguang Luo), my brother-in-law Chengwei and my sister Xiaolin for their endless care and love; to my girlfriend Ling who has been supporting me facing any obstacle and sharing our happiness; and to all others of my families. This work would not be done without their support.

Xiaobin Luo, April 2007

CONTRIBUTION OF AUTHORS

The following is a statement regarding the contribution of co-authors and myself to the four articles which have been published or submitted for publication, and included in this thesis.

1. **Luo X**, Xiao J, Lin H, Shan H, Yang B, Wang Z. (2007) Genomic structure, transcriptional control and tissue distribution of human *ERG1* and *KCNQ1* genes. ***FEBS Lett.*** (Submitted in August 2007).

Dr. Zhiguo Wang and I proposed the original research plan. I designed and performed the experiments, analyzed the data, and wrote the manuscript. Dr. Jiening Xiao and Dr. Huixian Lin were involved in the experiments related to cloning promoters of *HERG1a* and *HERG1b*. Dr. Hongli Shan and Dr. Baofeng Yang participated in experiments of Real-time RT PCR. Dr. Zhiguo Wang had the original idea and fully supervised the work and finalized the manuscript for publication.

2. **Luo X**, Xiao J, Lin H, Lu Y, Li B, Yang B, Wang Z. (2007) Transcriptional activation by stimulating protein 1 and post-transcriptional repression by muscle-specific microRNAs of I_{Ks}-encoding genes and potential implications in regional heterogeneity of their expressions. ***J Cell Physiol.*** 2007 Aug;212(2):358-67.

Dr. Zhiguo Wang and I proposed the original research plan. I designed and performed the experiments, analyzed the data, and wrote the manuscript. Dr. Jiening Xiao and Dr. Huixian Lin were involved in experiments of Western blot. Dr. Yanjie Lu, Dr. Baoxin Li and Dr. Baofeng Yang contributed to experiments of Real-time RT PCR. Dr. Zhiguo Wang fully supervised the work and finalized the manuscript for publication.

3. Xiao J, **Luo X**, Lin H, Zhang Y, Lu Y, Wang N, Zhang Y, Yang B, Wang Z. MicroRNA miR-133 Represses HERG K^+ Channel Expression Contributing to QT Prolongation in Diabetic Hearts. ***J Biol Chem.*** 2007 Apr 27;282(17):12363-7.

In this work, I designed and performed all experiments concerning the effect of *miR-133* on HERG in cell line, and analyzed the data for this part. Dr. Jiening Xiao performed the experiments and analyzed the data about the effect of miR-133 in diabetic rabbit and human myocytes. Dr. Huixian Lin and Ning Wang were involved in experiments of Western blot. Dr. Yanjie Lu, Ying Zhang and Dr. Baofeng Yang participated into experiments of HERG current recording under application of *miR-133* and its antisense. Dr. Yiqiang Zhang performed the Patch-clamp recording of HERG current in diabetic rabbit myocytes. Dr. Zhiguo Wang fully supervised the work and finalized the manuscript for publication.

DEDICATION

This thesis is dedicated to:

My mother, my father, my sister, my brother-in-law, and my girlfriend, for their love, patience, understanding, encouragements, and supports. Were it not for their sacrifice, this thesis may have never been completed.

PART I. INTRODUCTION AND REVIEW OF THE LITERATURE

1. Delayed rectifier potassium currents I_{Kr} and I_{Ks} in the heart

1.1 Overview of cardiac action potential

The normal electrophysiological behavior of the heart is determined by the orderly propagation of electrical impulses resulting in rapid depolarization and slow repolarization, thereby generating action potentials in individual myocytes[1]. The cardiac action potential (AP) reflects a balance between inward (depolarizing) and outward (repolarizing) currents. It consists of five phases. Phase 0 represents depolarization of the myocytes, in which voltage-gated sodium channels (I_{Na}) are rapidly activated to depolarize the cell membrane. Phase 1 of the cardiac AP occurs right after the peak of depolarization, which underlies an early rapid phase of the repolarization in ventricular and atrial cells. This rapid repolarization is due to the inactivation of I_{Na} and activation of transient outward potassium current (I_{to}). Following phase 1 is the long lasting plateau phase 2 repolarization, reflecting the balance between slowly decreasing inward depolarizing calcium ($I_{Ca,L}$) currents through L-type calcium channels and gradually increasing outward repolarizing potassium currents mainly through rapid delayed rectifier potassium current (I_{Kr}). The net amount of ions fluxing across the cell membrane during the plateau phase is small, resulting in high impedance. Therefore a relatively small change in the ion current can have a significant impact on the membrane potential thereby action potential duration (APD). Phase 3 repolarization is primarily due to activation of I_{Kr} and slow delayed rectifier potassium channels (I_{Ks}), along with inactivation of $I_{Ca,L}$. Phase 4 is the final stage of the cardiac action potential, during which the cell membrane return to its resting potential, which is accomplished by the outward potassium current (I_{K1}) through inward rectifier channels. Figure 1 shows the relationships among different cardiac ion channels and an AP.

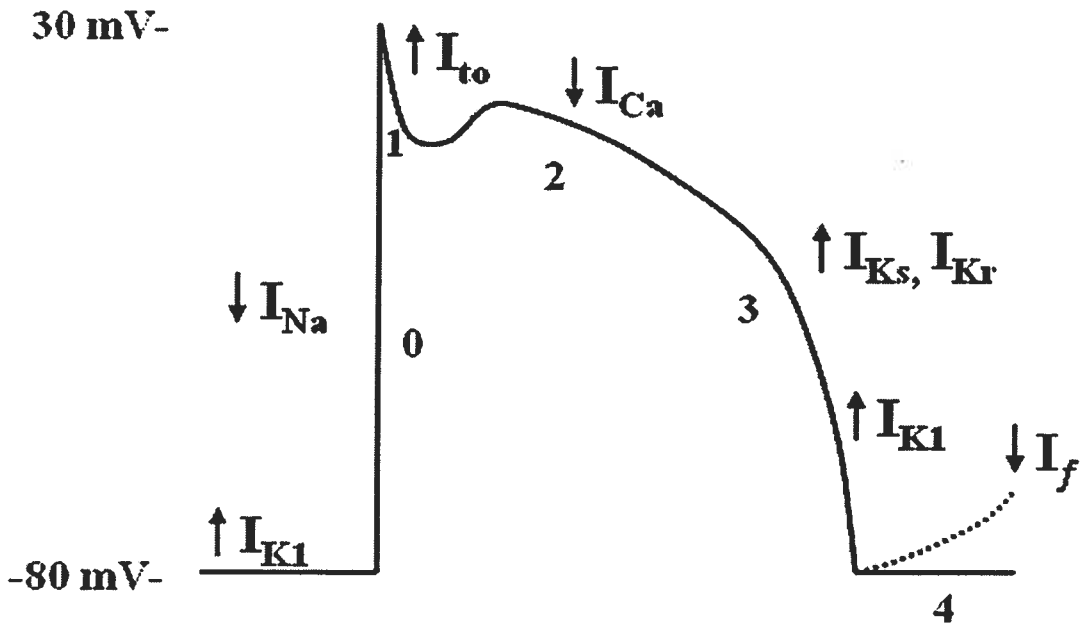

Figure 1. Cardiac action potential and ion channels. Typical ventricular action potential (AP) with inward currents (downward arrow) and outward currents (upward arrow). Numbers indicate various phases of an AP (Modified from Schram G, et al.[2])

The configuration and duration of AP differ in specific regions (e.g., atrium versus ventricle; apex versus basal, etc.) as well as in different layers within those regions (e.g., epicardium, midmyocardium and endocardium) [3-5] (as shown in Figure 2). These physiologic heterogeneities of cardiac AP are likely due to differential expression of ion channels. For example, smaller I_{Ks} accounts partly for longer APD in midmyocardium. Other factors, such as genetic defects (mutations in ion channel genes), sympathetic regulation, modulation by drugs and alterations in response to a variety of diseases (e.g., ischemia, myocardial infarction, hypertrophy, diabetes, etc.), can exaggerate these heterogeneities generating a substrate for arrhythmogenesis.

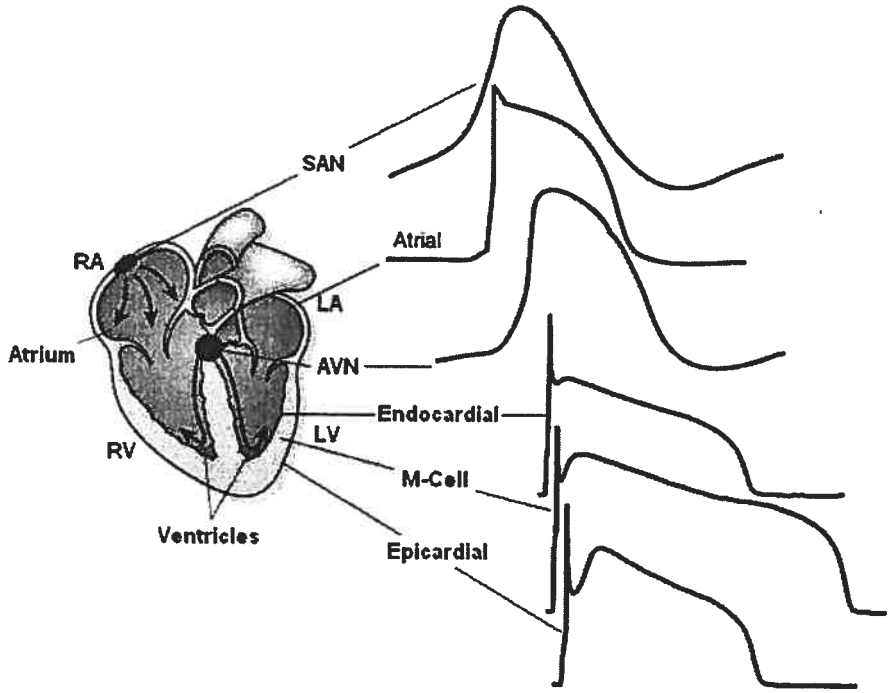

Figure 2. Action potential waveforms are variable in different regions of the heart. Schematic representation of the heart; AP waveforms recorded in different regions of the heart are illustrated.

1.2 Biophysical properties of rapid and slow delayed rectifier potassium channels

1.2.1 Overview of I_{Kr} and I_{Ks}

In cardiac myocytes, voltage-gated potassium (K_V) channels are the primary determinants of action potential repolarization. In general, based on differences in time- and voltage-dependent properties and pharmacological sensitivities, there are two types of cardiac K_V have been distinguished[6], transient outward potassium currents (I_{to}) and delayed rectifier potassium currents (I_K). I_{to} rapidly activates and inactivates when cell membrane depolarizes to positive potential around -30 mV, which underlies the early phase (phase 1) of the action potential in atrial and

ventricular cells[7]. I_K activate more slowly compared to I_{to} following initial depolarization. Three distinct components, I_{Kur}, I_{Kr} and I_{Ks}, comprise the delayed rectifier potassium current in the heart[8-11]. I_{Kur} activates extremely fast (named *ultrarapid*), almost instantaneously when compared to the other two components of I_K. I_{Kr} activates fast and exhibits a strong inward rectification, and I_{Ks} activates very slowly. While I_{Kr} and I_{Ks} are found in both of atial and ventricle myocytes in different species (except adult rodent), I_{Kur} exists only in atrial myocytes in most species (including human)[11-16], but not in human ventricular myocytes and Purkinje fibers, suggesting that it is a suitable target for specific treatment of atrial arrhythmias. Since my study is focusing on the regulation of pore forming α-subunits of I_{Kr} and I_{Ks} channels, for the rest of this chapter, I will mainly discuss these two major components.

1.2.2 Electrophysiological and pharmacological properties of I_{Kr} and I_{Ks}

1.2.2.1 I_{Kr} and I_{Ks} in general

I_{Kr} and I_{Ks} are distinguished by their kinetics of activation, deactivation and inactivation, and by their highly variable sensitivity to drug blockers. They were first distinguishably recorded in guinea pig atrial and ventricular myocytes, basing on the distinct differences in time- and voltage-dependent properties[17-19]. They have also been found co-expressed in human atrial and ventricular myocytes[15;16;20;21], as well as in canine[4;22-25] and rabbit[26;27] ventricles and in canine Purkinje fibers[25]. In some species, for example, feline[28-31] and fetal mice[32] and rat[33], I_{Kr} composes the major repolarizing current, but it is rapidly supplanted postnatally by a very large I_{to}[33;34]. In contrast, the currents of I_{Kr} and I_{Ks} are undetectable in small adult rodent ventricles[35],

1.2.2.2 Electrophysiological and pharmacological properties of I_{Kr}

I_{Kr} channels activate during the upstroke (Phase 1) and plateau (Phase 2) phases of an AP. Activation of I_{Kr} starts with precipitous voltage dependence and its half-maximal activation appears approximately at the potential of -25 mV. The amplitude of I_{Kr} increases as the membrane potential arises to 0 mV, and then decreases upon further depolarization, resulting in a unique 'bell' shape of the current-voltage relationship. I_{Kr} activates rapidly and inactivates faster at more positive potential, and thus limits the time that the channels stay in the open state, showing strong inward rectification[36]. On repolarization the rate of recovery from inactivation through the open state is much more rapid then deactivation, which results in a large outward current in the voltage negative to 0 mV and provides a basis for promoting phase 3 repolarization.

I_{Kr}/HERG was originally classified to be a component of I_K due to its specific sensitivity to methanesulfonanilide class III antiarrhythmic agent E-4031[37], dofetilide and d-sotalol[38]. I_{Kr}/HERG is also blocked by class I antiarrhythmic agents such as propafenone[39], quinidine[40], flecainide[41] and mexiletine[42], as well as some other non-cardiovascular drugs (e.g. cisapride[43], terfenadine[44], astemizole[45]). Blockage of I_{Kr}/HERG channels by pharmacological agents is pro-arrhythmic, which will potentially produce marked QT prolongation and distinctive ventricular tachycardia, *torsades de pointes*, or acquired long QT syndrome (LQTS).

1.2.2.3 Electrophysiological and pharmacological properties of I_{Ks}

Compared to I_{Kr}, I_{Ks} activates much more slowly when cell membrane depolarizes to above -30 mV. Its half-maximal activation is around +20 mV[15;37;46-48]. I_{Ks} activates much slowly, and an extremely long depolarization period is required for it to reach the steady-state level. I_{Ks} mainly serves as a "repolarization reserve" in cardiac repolarization in both human atria and ventricles[49;50], preventing excessive APD prolongation and development of arrhythmogenic early afterdepolarizations[49],

particularly when I_{Kr} is substantial depressed by drugs or in the presence of cardiac disease.

I_{Ks} is resistant to blockade by methanesulfonanilide antiarrhythmic agents[37], but selectively blocked by chromanols (293B, HMR-1556)[51;52]. I_{Ks} specific blockers have been developed but not commercialized because of the potential risk of *torsades de pointes*. It has been shown that there is a tendency of developing a homogeneous APD prolongation in ventricular tissue by blocking I_{Ks}[53].

1.2.3 Contributions of I_{Kr} and I_{Ks} to repolarization

The relative contributions of I_{Kr} and I_{Ks} to repolarization have been broadly studied in different species for the last two decades. In guinea pig ventricular myocytes, similar amplitudes of these two currents were recorded when the membrane potential was set to the potential corresponding to plateau phase of repolarization, indicating their equal contributions to the repolarization[37]. Blockade of either I_{Kr} or I_{Ks} caused a similar moderate prolongation of repolarization, whereas concomitant blockade of both I_{Kr} and I_{Ks} led to a much greater prolongation[54]. In rabbit and dog ventricular myocytes, the relatively amplitude of I_{Kr} under the similar condition (membrane potential depolarized to $^{+}30$ or $^{+}40$ mV) is larger than I_{Ks}[25;55], which implicates that the overall contribution of I_{Kr} to ventricular repolarization is greater than that of I_{Ks}. Therefore, in dog and rabbit (perhaps in human), I_{Kr} may be more important than I_{Ks} in determining ventricular repolarization. However, interestingly, when repolarization is delayed pharmacologically or pathologically, the prolonged APD will favor activation of I_{Ks} to restrict the excessive APD prolongation, reducing the risk of early afterdepolarization (EAD).

2. Molecular composition of I_{Kr} and I_{Ks}

2.1 Overview of molecular composition of I_{Kr} and I_{Ks}

The molecular identity of I_{Kr} and I_{Ks} remained unknown until revealed by molecular genetic analysis of an inherited disease, long QT syndromes. HERG encodes subunits to form channel complex constituting I_{Kr}. KCNQ1 and KCNE1 encode subunits that co-assemble to form channels that mediate I_{Ks}. Mutations in any of these genes can cause LQTS, a disorder of cardiac repolarization that predisposes to lethal ventricular arrhythmias.

2.2 Molecular composition of I_{Kr}

HERG (Human *ether-a-go-go*) is a member of the *ether-a-go-go* (*EAG*) channel family originally cloned from a hippocampal cDNA library and was found to be highly expressed in human heart tissue[56]. Several independent heterologous expression studies confirmed that HERG encodes the α-subunit underlying I_{Kr}[57;58]. HERG has the same channel structure as the other voltage-gated ion channels[59-60]. Four repeats of six transmembrane domains (S1-S6) constitute each HERG channel with a reentrant 'pore-loop' between S5-S6 to form the channel pore[60;59;61-63]. The biophysical properties of expressed HERG are nearly identical to those of native I_{Kr} in cardiac myocytes[57;37]. Some studies also proposed that additional channels subunits, minK (KCNE1) or Mink-related peptide 1 (MiRP1 or KCNE2) may associate with the pore-forming α subunit (HERG) to form the native I_{Kr}[64-66]. Although this notion is further potentiated by the finding of mutations in KCNE2 gene are associated with congenital and acquired LQTS[65;67], but it still remains somewhat uncertain and are challenged by other studies. For examples, Weerapura et al. reported that the biophysical and pharmacological properties of HERG channel without the co-expression of MiRP1 were quite similar with I_{Kr} recorded in guinea pig[68]. And meanwhile, some other studies have also failed to confirm the biophysical interactions between HERG and MiRP1[69]. Mutations in pore-forming α-subunit

(HERG) or in putative regulatory subunit Mink-related peptide 1 (MiRP-1) of I_{Kr} channels are associated with congenital (LQT2 and LQT6) and acquired long QT syndrome, which carries increased risk of life-threatening cardiac arrhythmias[57;65;70].

Taken together, I_{Kr} is composed primarily of the pore-forming α-subunit HERG which might be associated with a function-altering β-subunit MiRP1 or minK, but the β-subunits underlying I_{Kr}, and their interactions with HERG are still under controversy, and remain to be further investigated.

2.3 Molecular composition of I_{Ks}

The pore-forming α-subunit KCNQ1 (formerly called KvLQT1) together with β-subunit mink (KCNE1) forms the slow delayed rectifier potassium channel (I_{Ks}) when co-expressed in heterogeneous systems, while expressing any of them alone can not produce I_{Ks}-like current[47;71-74]. KCNQ1 was originally identified with the purpose of searching for a gene associated with LQTS by the positional cloning approach[72]and is found to express strongly in the pancreas and the heart[72]. KCNQ1 has 676 amino acids which consists of six transmembrane domains and forms typical pore loop structure[71;75;76]. MinK is a single transmembrane protein containing 129 amino acids, and functions as the regulatory accessory to increase the macroscopic current amplitude by slowing the channel activation kinetics and shifting the activation at more positive potential[66;73;77]. Loss-of-function mutations in either KCNQ1 or minK cause forms of LQTS (LQTS1 and LQTS5, respectively)[47;62;71;72;78;79].

2.4 Isoforms of *HERG1* and *KCNQ1*

2.4.1 Isoforms of *HERG1*

In mammalian heart, N-terminal splice variants of ERG have been found in both human and mouse[80;81]. The long isoform 1a (HERG1a) has 396 amino acids in the N-terminus, whereas the short isoform 1b (HERG1b) has only 36 amino acids in

the N-terminus[80;81]. The lacking part of isoform 1b is important for the slow deactivation process of isoform 1a[80-84]. A recent study proposed that cardiac I_{Kr} channels are minimally composed of HERG1a and HERG1b α-subunits that co-assemble in the membrane[83]. Interestingly, HERG1b subunits co-expressed in heterologous systems preferentially form heteromultimers with HERG1a and modify the deactivation gating properties previously attributed to the HERG1a N-terminus[84]. A study carried out by Nerbonne *et al* using specific antibodies against the N- and C-termini of HERG in human, rat and mouse, showed that HERG1a is expressed in adult hearts of all three species, but there is no detectable expression of HERG1b[85]. However, HERG1b was shown to contribute to I_{Kr} channel function in the neonatal hearts[86]. These findings indicate that there is a developmental change in ERG isoform expression.

2.4.2 Isoforms of *KCNQ1*

Isoform 1 (long isoform) and isoform 2 (short isoform) are the two major splice variants in the heart when detected at the mRNA level[87-89]. Two isoforms are different in their N-termini, with deletion of nearly the whole N terminus of isoform 2[87-90]. When expressed in a heterologous context, the isoform 2 protein functions as a dominant negative isoform[87]. Notably, a detectable amount of protein originating from isoform 2 transcript has never been reported in cardiac tissue[91]. For convenience, here we designate the two major isoforms KCNQ1a (long isoform or isoform 1) and KCNQ1b (short isoform or isoform 2).

3. Regional heterogeneities of I_{Kr} and I_{Ks}

There exist marked differences in the densities of I_{Kr} and I_{Ks} in different myocardial cell types, which contribute to the regional properties of AP waveforms in the heart. These intrinsic regional heterogeneities of I_{Kr} and I_{Ks} help to maintain the normal heterogeneous property of cardiac AP through out the heart, and thereby assure the proper propagation of electrical signal. The regional differences are

reflected in sinoatrial node (SAN), atrioventricular node (AVN), apex versus base, left atrium (LA) versus right atrium (RA), left ventricle (LV) versus right ventricle(RV)) or layers (epicardial (Epi), midmyocardial (Mid) and endocardial (Endo)) of the atria and ventricles.

3.1 Transmural differences of I_{Kr} and I_{Ks}

Two independent studies have shown that the density of I_{Kr} in cells isolated from guinea pig left ventricular free walls was higher in epicardial than in midmyocardial or in endocardial myocytes, whereas both I_{Kr} and I_{Ks} densities at the base of the heart were smaller in sub-endocardial myocytes than those in mid-myocardial and sub-epicardial myocytes[92;93]. In dog ventricles, I_{Ks} density was found significantly higher in epicardial and endocardial cells than in midmyocardial (M) cells, whereas, I_{Kr} density was comparable among those three layers[22]. The lower density of I_{Ks} in the M cells is supposed to contribute to the longer APD in midmyocardial region[22]. In rabbit ventricular cells, I_{Ks} density was shown to be significantly greater in epicardial myocytes than in endocardial myocytes, whereas the densities of I_{Kr} in these two layers were found to be similar[94].

3.2 Apex-base differences of I_{Kr} and I_{Ks}

A substantial electrophysiological difference between I_{Kr} and I_{Ks} was also recognized along the apico-basal axis of ventricle in some animal species, for example, in rabbit ventricular myocytes, I_{Ks} density was higher in base than in apex, whereas the density of I_{Kr} was found to be lower in the base that in the apex[55].

3.3 Inter-chamber differences of I_{Kr} and I_{Ks}

I_{Kr} is larger in left atrial free-wall than in right atrium, which accounts for the shorter APDs in this region in guinea pig[95]. Two recent studies have investigated the interventricular differences of I_{Kr} and I_{Ks} expression in canine hearts: the density of

I_{Kr} was found to be comparable between left and right ventricles, whereas I_{Ks} density was almost two-fold higher in right ventricle than in left ventricle[23;96].

3.4 Molecular bases underlying the regional heterogeneities of I_{Kr} and I_{Ks} (Discrepancy between mRNA and protein)

The molecular bases for the regional differences in I_{Kr} and I_{Ks} have been evaluated based on differential expressions of the channel subunits at both mRNA and protein levels. For example, ERG protein levels in dogs are greater in the LA than in the RA, consistent with a larger I_{Kr} in LA[95]. Human minK mRNA levels are not significantly different among epicardial, midmyocardial, and endocardial tissues[88]. However, KCNQ1b (isoform 2, dominant negative splice variant of KCNQ1) expresses more abundantly in the midmyocardium, potentially accounting for lower I_{Ks} in M cells[88]. In ferret, a larger I_{Ks} with more abundant *KCNQ1* transcripts are observed in RA than in LA, and ERG mRNA and protein expressions are more abundant in the apex than in the base, which is in accordance with I_{Kr} in these regions[28;29].

Notably, in addition to the regional difference of I_{Kr} and I_{Ks} subunits' expressions, there is also a consistent discrepancy between the protein and mRNA expressions of these genes. A typical example is the-well recognized heterogeneity of I_{Ks}. According to the previous studies, KCNQ1 and KCNE1 distribute with significant interventricular gradients (RV>LV) at both mRNA and protein levels, which is in agreement with I_{Ks} interventricular difference[97]. The protein levels of both KCNQ1 and KCNE1 are higher in apical than in basal area, despite that their mRNA levels are not significantly different[98]. KCNQ1 protein level is greater in Epi than in Mid[99], whereas that of KCNE1 is the opposite, and there is not transmural difference in mRNA levels of KCNQ1 and KCNE1[88].

Tremendous work has been done in the past decade regarding the ionic basis of electrical heterogeneity in different regions of the heart. However, the molecular bases responsible for these regional heterogeneities are still poorly understood: how

ion channel genes turn on or off, and what are the determining factors that control their differential expressions in the heart.

3.5 Implications of regional heterogeneities of I_{Kr} and I_{Ks} in arrhythmogenesis

Under normal physiological conditions, the regional difference is genetically programmed with a certain pattern with APD gradient from long to short following the sequence of activation of myocardial mass during an excitation, which constitutes an intrinsic protection mechanism against arrhythmias which could be induced due to radial and retrograde excitation propagation. Under pathological situations, the spatial heterogeneity is abnormally increased and the intrinsic pattern of spatial heterogeneity may also be broken. These changes render the heart a loss of the intrinsic antiarrhythmic mechanism and a vulnerability to arrhythmogenesis. For example, enlarged interventricular differences have been shown to cause acquired LQTS[100;101]. The spatial heterogeneity of cardiac repolarization is largely due to diversity and varying densities of repolarizing K^+ currents. I_{Kr} and I_{Ks} are the two most important repolarizing currents responsible for ventricular repolarization. It is therefore likely that regional heterogeneities of I_{Kr} and I_{Ks} play important roles in determining the spatial dispersion of electrical activities[22].

4. Alterations of delayed rectifier potassium channel (Age and diseases)

4.1 Age-dependent changes in I_{Kr} and I_{Ks}

Expression of both *HERG* and *KCNQ1* genes is dynamic depending on differentiation status and cell cycle of the cells, contributing importantly to the developmental evolution of myocardial AP morphology. For example, I_{Kr} is the sole component of delayed rectifier K^+ current in fetal day 18 mouse ventricles, yet both I_{Kr} and I_{Ks} can be observed on postnatal day 1. By day 3, I_{Ks} is the dominant component. With further development into adulthood, neither I_{Kr} nor I_{Ks} can be observed[32;102]. In canine heart, it was found that I_{Ks} is absent or minimal before age 4

weeks, at which time I_{Kr} is the major repolarizing current[95]. With progression toward adulthood, I_{Ks} appears and increases in density while I_{Kr} density diminishes. It appears that expressions of *HERG* and *KCNQ1* genes are tightly controlled by certain factors according to a defined genetic program related to morphogenesis during development. Therefore, understanding expression regulation of these genes will provide a better insight on this issue.

4.2 I_{Kr} and I_{Ks} under pathological conditions

The current densities of I_{Kr} and I_{Ks} in cardiomyocytes are modulated under a variety of pathological conditions in different species.

4.2.1 Congenital and acquired long QT syndromes

The long QT syndrome is a heart disease in which there is an abnormally long delay between the depolarization and repolarization of the ventricles of the heart. It is associated with syncope and sudden cardiac death due to ventricular arrhythmias[103]. It could be either congenital or acquired, depending on whether it is induced by mutations in genes or by medications[103;104]. Two clinical phenotypes of congenital LQTS have been recognized: The Romano-Ward syndrome (autosomal dominant)[105;106] and the Jervell-Lange-Nielsen syndrome (autosomal recessive)[107]. Romano-Ward syndrome is most common forms of congenital LQTS and is associated with mutations in I_{Kr}, I_{Ks}, and I_{Na} channels genes[57;72;108]. On the other hand, Jervell-Lange-Nielsen syndrome is relatively rare and is normally associated with deafness solely due to defects in I_{Ks}[107]. The LQTS-associated mutations in the K^+ channels decrease outward current through I_{Kr} or I_{Ks} by loss-of-function or dominant-negative mechanisms[57;72;108]. Acquired LQTS or drug-induced LQTS is more common than its congenital counterpart, mainly due to the sensitivity of I_{Kr} (HERG) to agents with class III antiarrhythmic action[109], antifungal or antihistamine agenes[110;111], and macrolide antibiotics[112;113]. Recent studies have demonstrated that a number of non-genetic and genetic risk factors[67;79;114] could increase susceptibility to

acquired form of LQTS. Non-genetic factors include female gender, hypokalemia, and other heart diseases[115;116].

To date, more than eight LQTS genes have been identified, which when genetically defected can lead to different forms of LQTS. Among these LQTS genes, *KCNQ1* and *HERG* are responsible for a majority (~85-90%) of cases of inherited LQTS, LQT1 and LQT2. Moreover, HERG protein is also a pharmacological target for a majority of acquired LQTS as a result of drug blockade.

4.2.2 Atrial fibrillation (AF)

The current densities of I_{Kr} and I_{Ks} do not change in animal models with atrial fibrillation (atrial tachypacing-induced)[117]. Thus far, voltage-clamp data regarding I_{Kr} and I_{Ks} in human atria have not been available[24]. However, several studies have reported alterations in I_{Kr} and I_{Ks} subunits in AF patients, including decreased mRNA expression of *ERG* and *KCNQ1* along with increased expression of minK[118;119] and decreased ERG and minK protein expression[120].

4.2.3 Hypertrophy

In hypertrophic rat hearts, both I_{Kr} and I_{Ks} were significantly decreased, resulting in significant prolongation of APD_{90} (90% repolarization)[121]. In chronic complete atrioventricular block (AVB)-induced rabbit hypertrophy model, a prominent QT prolongation and high incidence of spontaneous TdP and sudden cardiac death were observed, and both I_{Kr} and I_{Ks} were significantly smaller in AVB myocytes than in control[122]. Xu et al. reported a significant reduction of I_{Ks} density in both Epi- and Endo- left ventricular myocytes with no significant changes in I_{Kr} density, in rabbit left ventricular hypertrophy model[94]. Moreover, in AVB-induced hypertrophic dog hearts, Volders et al. found that I_{Kr} and I_{Ks} had a similar voltage dependence of activation and time course of deactivation in chronic AVB and control, whereas I_{Kr} density was similar in LV myocytes but smaller in RV myocytes of chronic AVB versus control, and I_{Ks} densities in both LV and RV cells were

significantly lower in chronic AVB than control[96]. However, due to the variations in species as well as the methods in creating hypertrophy animal models, some studies showed no significant changes in I_{Kr} and I_{Ks} under hypertrophic condition, for example, in a guinea pig model with aortic banding[123].

4.2.4 Ischemia

In a dog model of myocardial infarction, ventricular myocytes in the border zone 5 days after the coronary occlusion showed significantly less densities of both I_{Kr} and I_{Ks}, when compared with the non-infarcted region, and a significant decrease in mRNA of dERG and dminK were also observed in the infarcted hearts with no change of KCNQ1 mRNA[124]. During the very early phase of acute ischemia and infarction, I_{Kr} is increased[125;126], which might be due to the direct interaction between lysophosphatidylcholine (LPC) and HERG[127;128].

4.3.5 Heart failure

A recent study showed that sustained tachycardia and bradycardia downregulate I_{Ks} subunits (at both mRNA and protein levels), but bradycardia also suppresses ERG/I_{Kr}, causing prominent repolarization delays and spontaneous TdP. These results point to a crucial role for delayed-rectifier subunit remodeling in TdP susceptibility associated with rate-related cardiac remodeling. In a rabbit model of tachypacing-induced heart failure, both I_{Kr} and I_{Ks} were significantly down-regulated in ventricular myocytes, accompanying a significant prolongation of APD[129], whereas in tachypacing-induced heart failure dogs, only reduction of I_{Ks} density was observed in atrial myocytes[130;131]. Although the results of different studies often vary, the most consistent electrophysiological changes in the ventricles are APD prolongation, especially at slow heart rates, with a reduction in I_{to}, I_{Kr} and I_{Ks}, and I_{K1}.

4.3.6 Diabetes

Abnormal QT prolongation in diabetic patients has become a non-negligible clinical problem and has attracted increasing attention from basic scientists, because it increases the risk of lethal ventricular arrhythmias. In type-1 diabetic dog, the QTc interval and the ventricular action potential duration were moderately prolonged, accompanied by significant reduction in the density of I_{Ks}. No differences were observed in the density of I_{Kr}. Western blot analysis revealed a reduced expression of minK in diabetic dogs, while other channel proteins were unchanged (HERG, MiRP1) or increased (KvLQT1)[132]. However, another recent study, using rabbit model of type-1 diabetes, reported that a significant downregulation of I_{Kr} current density in diabetic heart and rERG is severely depressed in its expression at the protein level but not at the mRNA level[133].

4.3.7 Molecular mechanism underlying pathological changes of I_{Kr} and I_{Ks} (Discrepancy between mRNA and Protein)

The reduction of I_{Kr} and/or I_{Ks} under the pathological conditions described above may provide the substrates for arrhythmias in the diseased hearts through regional inhomogeneous prolongation of APD.

It is important to note that a phenomenon of disparate changes of I_{Kr} and I_{Ks} subunits expressions at protein and mRNA levels have been observed in failing hearts, ischemic myocardium and diabetic hearts. For example, several studies found that I_{Kr} current density was significantly diminished in myocytes from failing hearts and diabetic hearts that are electrophysiologically characterized by repolarization slowing and QT prolongation, despite that the mRNA level of *HERG* was barely altered under these conditions[129;131;133;134]. Another example is shown in infarcted heart, where the current density of I_{Ks} was reduced, with no detectable change in *KCNQ1* transcripts[124]. The molecular mechanism underlying this disparate expression pattern of mRNA and protein is largely unknown and needs to be further investigated.

5. Molecular regulation of HERG and KCNQ1 expression

Many factors, such as neural hormone, metabolic stress and medications, were shown to regulate the expressions of HERG and KCNQ1 via the complex signaling pathways. However, little is known concerning their gene regulations, especially on transcriptional and post-transcriptional levels.

5.1 Transcriptional regulation of ion channel-encoding genes

5.1.1 Importance and feasibility

Regulation of transcription is a complex set of events controlled by DNA sequences positioned in proximity to the genes (promoters) and by elements acting at a distance (enhancers). Promoters and enhancers that activate polymerase II transcribed mRNA genes are formed by a combinatorial puzzle of short sequences recognized by sequence-specific regulators. Generally, It is well accepted that an ideal model systems for the study of physiologically controlled transcriptional regulation will be monomeric proteins such as metabolic enzymes[135]. Ion channels, which are typically both heteromeric and multimeric membrane proteins, seem, at least at the first glance, to be very unlikely a suitable candidate for transcriptional regulation of their expression[190]. However, large amount of recent studies showed that, ion channel expression, either during the course of organogenesis or pathogenesis of the heart, seems to be mediated primarily at the level of transcription of their encoding α- or β-subunits[137-152]. Moreover, heart development is well governed by a core set of evolutionarily conserved transcription factors GATA families[153-159], Mef2[160], Tbx 5[161], Nkx2-5[157] and Hand2[157] which controls cardiac cell fates, the expression of genes encoding the contractile proteins, and the morphogenesis of cardiac structure[162-165]. These transcription factors also regulate each other's expression, forming a genetic network to program cardiac organogenesis[157]. Many other transcription factors such as NFAT[166], NF-κB[167] and Stat3[168] have also been shown to actively participate in developing many cardiac

diseases including hypertrophy, congenital heart failure, ischemia and etc.[166-174]. It is obvious that there is a missing link between the rapidly increasing knowledge of transcription factor function and the developmental and pathological changes of ion channel genes, prompting our further studies on detail analysis of the transcriptional control of ion channel genes[175-177].

Specificity and precision are two most important advantages of transcriptional regulation of gene expression, and are especially important for good control of ion channel genes expression[112]. In mammalian heart, various functionally distinct ion channels act in concert to maintain normal function of the heart. The functions of these channels are either non-overlapping or only partially overlapping[1;136], and, more importantly, different ion channels have their own distinct encoding genes. Expression of each ion channel gene can in principle be regulated independently at the transcriptional level by recruiting of multiple different transcription factors[157;178]. On the other hand, transcriptional regulation can produce precisely graded levels of gene expression[179]. Notably, the precise regulation of channel expression is very important for some channels, such as the channels contributing to the plateau phase of the action potential, where small changes in current level can result in large changes in the membrane potential[22;180-183].

5.1.2 Current progress in study of human ion channel promoters

To date, there have been only a few studies regarding the detail analysis of ion channel promoters in human, including *SCN5A* (encoding α-subunit of human sodium channel)[184], *CACNA1C* (also named Cav1.2, encoding α-subunit of human L-type Ca^{2+} channel)[185] and *KCNE1* (encoding β-subunit of human slow delayed rectifier potassium channel)[186;187]. A number of K^+ channels have been investigated on their genomic structures for transcriptional regulation, with their promoter regions identified and characterized. However, a majority of these studies were conducted with rat and mouse genes and the findings may not be applicable to human genes, considering large interspecies variations in the 5'-flanking regions of genes. Research on promoter elements of human K^+ channel pore-forming α-subunits has

been sparse despite a recent report describing the transcriptional control of several human *KCNE* genes (*KCNE*1-5) encoding a family of single-transmembrane-domain K^+ channel β-subunits that modulate the properties of several K^+ channel α-subunits[187].

5.1.3 The role of stimulating protein 1 (Sp1) in transcriptional regulation

In mammalian cells, Sp1 transcription factor is an extremely versatile protein which functions as transactivator to enhance gene transcription by direct binding to target DNA through its zinc finger protein motifs[188;189]. It was originally identified as the transcription factor which binds to multiple GC-boxes in the simian virus 40 (SV40) promoter[190;191] and the thymidine kinase (TK) promoter[192] to activate transcription. Sp1 is also known to activate very large number of genes, such as housekeeping, tissue-specific and cell cycle-regulated genes, and is required to prevent methylation of CpG islands[193;194]. Notably, one of the most important features for Sp1 to exert its transactivating action is to bind to promoters which contain GC-rich elements such as GC-box (GGGGCGGGG) or GT/CACCC-box (GGTGTGGGG)[188;189;190;191].

5.2 Post-transcriptional regulation of ion channel genes

In addition to transcriptional regulation, several other regulatory mechanisms are also involved in determining the ultimate level of protein expression, such as post-transcriptional regulation, translational regulation and post-translational modification (or protein maturation). Since my study is focusing on the gene regulation of the ion channel genes, I will mainly discuss the post-transcriptional regulation.

It has recently become increasingly apparent that small regulatory RNAs, including the short interfering RNAs (siRNAs) and microRNAs (miRNAs), are also important gene regulatory factors. MiRNAs are ~22 nucleotide (nt)-long RNA molecules which bind to partially complementary sequences within the 3'-

untranslated region (3'-UTR) of target mRNAs and suppress their translation with or without mRNA cleavage, resulting in gene silencing[195-197]. Although the exact silencing mechanism is not well known, more and more recent evidence indicates that miRNAs might repress gene expression by sequestering targeted mRNAs into processing bodies (P-/GW-bodies)[198;199], where the miRNAs-bound mRNAs are unavailable for protein synthesis but are subject to de-capping and degradation by resident nucleases[198;199].

MiRNAs were originally identified in nematodes[200], and soon thereafter they were also confirmed to exist endogenously in higher eukaryotes, including plants and mammals[195;197;201]. Most of the miRNAs are evolutionarily conserved[195;197]. Since the first cloning of miRNA, *line-4* miRNA, in 1993 by Lee et al.[200], miRNAs have attracted more and more researchers' interest in understanding the molecular details underlying miRNA-guided gene regulation, because of their robustness in nature, and important roles in global developmental regulation as well as in cell differentiation and proliferation[195;197].

More than 300 miRNAs have been identified to date, among which, microRNA-1 (*miR-1*) and microRNA-133 (*miR-133*) are known to be specifically and strongly expressed in adult cardiac and skeletal muscle and play an important role in regulating development of the heart[202;203]. Whether these miRNAs are involved in regulation of ion channel gene expression remained largely unknown.

6 References

1. Roden DM, Balser JR, George AL, Jr., Anderson ME. Cardiac ion channels. *Annu Rev Physiol.* 2002;64:431-475.

2. Schram G, Pourrier M, Melnyk P, Nattel S. Differential distribution of cardiac ion channel expression as a basis for regional specialization in electrical function. *Circ Res.* 2002;90:939-950.

3. Antzelevitch C, Fish J. Electrical heterogeneity within the ventricular wall. *Basic Res Cardiol.* 2001;96:517-527.

4. Liu DW, Gintant GA, Antzelevitch C. Ionic bases for electrophysiological distinctions among epicardial, midmyocardial, and endocardial myocytes from the free wall of the canine left ventricle. *Circ Res.* 1993;72:671-687.

5. Clark RB, Bouchard RA, Salinas-Stefanon E, Sanchez-Chapula J, Giles WR. Heterogeneity of action potential waveforms and potassium currents in rat ventricle. *Cardiovasc Res.* 1993;27:1795-1799.

6. Barry DM, Nerbonne JM. Myocardial potassium channels: electrophysiological and molecular diversity. *Annu Rev Physiol.* 1996;58:363-394.

7. Noble D, Tsien RW. Outward membrane currents activated in the plateau range of potentials in cardiac Purkinje fibres. *J Physiol.* 1969;200:205-231.

8. Fedida D, Eldstrom J, Hesketh JC, Lamorgese M, Castel L, Steele DF, Van Wagoner DR. Kv1.5 is an important component of repolarizing K^+ current in canine atrial myocytes. *Circ Res.* 2003;93:744-751.

9. Deal KK, England SK, Tamkun MM. Molecular physiology of cardiac potassium channels. *Physiol Rev.* 1996;76:49-67.

10. Wang Z, Fermini B, Nattel S. Effects of flecainide, quinidine, and 4-aminopyridine on transient outward and ultrarapid delayed rectifier currents in human atrial myocytes. *J Pharmacol Exp Ther.* 1995;272:184-196.

11. Yue L, Feng J, Li GR, Nattel S. Characterization of an ultrarapid delayed rectifier potassium channel involved in canine atrial repolarization. *J Physiol.* 1996;496 (Pt 3):647-662.

12. Boyle WA, Muralidharan S, Maher GM, Nerbonne JM. Vascular actions of 'caged' phenylephrine analogs depend on the structure and site of attachment of the 2-nitrobenzyl group. *J Photochem Photobiol B.* 1997;41:233-244.

13. Boyle WA, Nerbonne JM. A novel type of depolarization-activated K^+ current in isolated adult rat atrial myocytes. *Am J Physiol.* 1991;260:H1236-H1247.

14. Wang Z, Fermini B, Nattel S. Delayed rectifier outward current and repolarization in human atrial myocytes. *Circ Res.* 1993;73:276-285.

15. Wang Z, Fermini B, Nattel S. Rapid and slow components of delayed rectifier current in human atrial myocytes. *Cardiovasc Res.* 1994;28:1540-1546.

16. Wang Z, Fermini B, Nattel S. Sustained depolarization-induced outward current in human atrial myocytes. Evidence for a novel delayed rectifier K^+ current similar to Kv1.5 cloned channel currents. *Circ Res.* 1993;73:1061-1076.

17. Horie M, Hayashi S, Kawai C. Two types of delayed rectifying K^+ channels in atrial cells of guinea pig heart. *Jpn J Physiol.* 1990;40:479-490.

18. Sanguinetti MC, Jurkiewicz NK. Delayed rectifier outward K^+ current is composed of two currents in guinea pig atrial cells. *Am J Physiol.* 1991;260:H393-H399.

19. Sanguinetti MC, Jurkiewicz NK. Role of external Ca^{2+} and K^+ in gating of cardiac delayed rectifier K^+ currents. *Pflugers Arch.* 1992;420:180-186.

20. Li GR, Feng J, Yue L, Carrier M, Nattel S. Evidence for two components of delayed rectifier K^+ current in human ventricular myocytes. *Circ Res.* 1996;78:689-696.

21. Varro A, Nanasi PP, Lathrop DA. Potassium currents in isolated human atrial and ventricular cardiocytes. *Acta Physiol Scand.* 1993;149:133-142.

22. Liu DW, Antzelevitch C. Characteristics of the delayed rectifier current (I_{Kr} and I_{Ks}) in canine ventricular epicardial, midmyocardial, and endocardial myocytes. A weaker I_{Ks} contributes to the longer action potential of the M cell. *Circ Res.* 1995;76:351-365.

23. Volders PG, Sipido KR, Carmeliet E, Spatjens RL, Wellens HJ, Vos MA. Repolarizing K^+ currents I_{TO1} and I_{Ks} are larger in right than left canine ventricular midmyocardium. *Circulation.* 1999;99:206-210.

24. Yue L, Feng J, Li GR, Nattel S. Transient outward and delayed rectifier currents in canine atrium: properties and role of isolation methods. *Am J Physiol.* 1996;270:H2157-H2168.

25. Varro A, Balati B, Iost N, Takacs J, Virag L, Lathrop DA, Csaba L, Talosi L, Papp JG. The role of the delayed rectifier component I_{Ks} in dog

ventricular muscle and Purkinje fibre repolarization. *J Physiol.* 2000;523 Pt 1:67-81.

26. Veldkamp MW, van Ginneken AC, Bouman LN. Single delayed rectifier channels in the membrane of rabbit ventricular myocytes. *Circ Res.* 1993;72:865-878.

27. Salata JJ, Jurkiewicz NK, Jow B, Folander K, Guinosso PJ, Jr., Raynor B, Swanson R, Fermini B. I_K of rabbit ventricle is composed of two currents: evidence for I_{Ks}. *Am J Physiol.* 1996;271:H2477-H2489.

28. Brahmajothi MV, Morales MJ, Reimer KA, Strauss HC. Regional localization of ERG, the channel protein responsible for the rapid component of the delayed rectifier, K^+ current in the ferret heart. *Circ Res.* 1997;81:128-135.

29. Brahmajothi MV, Morales MJ, Rasmusson RL, Campbell DL, Strauss HC. Heterogeneity in K^+ channel transcript expression detected in isolated ferret cardiac myocytes. *Pacing Clin Electrophysiol.* 1997;20:388-396.

30. Follmer CH, Colatsky TJ. Block of delayed rectifier potassium current, I_K, by flecainide and E-4031 in cat ventricular myocytes. *Circulation.* 1990;82:289-293.

31. Veldkamp MW. Is the slowly activating component of the delayed rectifier current, I_{Ks}, absent from undiseased human ventricular myocardium? *Cardiovasc Res.* 1998;40:433-435.

32. Wang L, Feng ZP, Kondo CS, Sheldon RS, Duff HJ. Developmental changes in the delayed rectifier K^+ channels in mouse heart. *Circ Res.* 1996;79:79-85.

33. Dukes ID, Morad M. Tedisamil inactivates transient outward K^+ current in rat ventricular myocytes. *Am J Physiol.* 1989;257:H1746-H1749.

34. Tseng-Crank JC, Tseng GN, Schwartz A, Tanouye MA. Molecular cloning and functional expression of a potassium channel cDNA isolated from a rat cardiac library. *FEBS Lett.* 1990;268:63-68.

35. Xu H, Guo W, Nerbonne JM. Four kinetically distinct depolarization-activated K^+ currents in adult mouse ventricular myocytes. *J Gen Physiol.* 1999;113:661-678.

36. Tseng GN. $I_{(Kr)}$: the hERG channel. *J Mol Cell Cardiol.* 2001;33:835-849.

37. Sanguinetti MC, Jurkiewicz NK. Two components of cardiac delayed rectifier K^+ current. Differential sensitivity to block by class III antiarrhythmic agents. *J Gen Physiol.* 1990;96:195-215.

38. Carmeliet E. Voltage- and time-dependent block of the delayed K^+ current in cardiac myocytes by dofetilide. *J Pharmacol Exp Ther*. 1992;262:809-817.

39. Delpon E, Valenzuela C, Perez O, Casis O, Tamargo J. Propafenone preferentially blocks the rapidly activating component of delayed rectifier K^+ current in guinea pig ventricular myocytes. Voltage-independent and time-dependent block of the slowly activating component. *Circ Res*. 1995;76:223-235.

40. Carmeliet E. Use-dependent block and use-dependent unblock of the delayed rectifier K^+ current by almokalant in rabbit ventricular myocytes. *Circ Res*. 1993;73:857-868.

41. Wang DW, Kiyosue T, Sato T, Arita M. Comparison of the effects of class I anti-arrhythmic drugs, cibenzoline, mexiletine and flecainide, on the delayed rectifier K^+ current of guinea-pig ventricular myocytes. *J Mol Cell Cardiol*. 1996;28:893-903.

42. Mitcheson JS, Hancox JC. Modulation by mexiletine of action potentials, L-type Ca current and delayed rectifier K current recorded from isolated rabbit atrioventricular nodal myocytes. *Pflugers Arch*. 1997;434:855-858.

43. Rampe D, Roy ML, Dennis A, Brown AM. A mechanism for the proarrhythmic effects of cisapride (Propulsid): high affinity blockade of the human cardiac potassium channel HERG. *FEBS Lett*. 1997;417:28-32.

44. Salata JJ, Jurkiewicz NK, Wallace AA, Stupienski RF, III, Guinosso PJ, Jr., Lynch JJ, Jr. Cardiac electrophysiological actions of the histamine H1-receptor antagonists astemizole and terfenadine compared with chlorpheniramine and pyrilamine. *Circ Res*. 1995;76:110-119.

45. Suessbrich H, Waldegger S, Lang F, Busch AE. Blockade of HERG channels expressed in Xenopus oocytes by the histamine receptor antagonists terfenadine and astemizole. *FEBS Lett*. 1996;385:77-80.

46. Zhou Z, Gong Q, Epstein ML, January CT. HERG channel dysfunction in human long QT syndrome. Intracellular transport and functional defects. *J Biol Chem*. 1998;273:21061-21066.

47. Sanguinetti MC, Zou A. Molecular physiology of cardiac delayed rectifier K^+ channels. *Heart Vessels*. 1997;Suppl 12:170-172.

48. Kurokawa J, Abriel H, Kass RS. Molecular basis of the delayed rectifier current $I_{(ks)}$in heart. *J Mol Cell Cardiol*. 2001;33:873-882.

49. Silva J, Rudy Y. Subunit interaction determines I_{Ks} participation in cardiac repolarization and repolarization reserve. *Circulation*. 2005;112:1384-1391.

50. Jost N, Virag L, Bitay M, Takacs J, Lengyel C, Biliczki P, Nagy Z, Bogats G, Lathrop DA, Papp JG, Varro A. Restricting excessive cardiac action potential and QT prolongation: a vital role for I_{Ks} in human ventricular muscle. *Circulation*. 2005;112:1392-1399.

51. Busch AE, Suessbrich H, Waldegger S, Sailer E, Greger R, Lang H, Lang F, Gibson KJ, Maylie JG. Inhibition of I_{Ks} in guinea pig cardiac myocytes and guinea pig IsK channels by the chromanol 293B. *Pflugers Arch*. 1996;432:1094-1096.

52. Gogelein H, Bruggemann A, Gerlach U, Brendel J, Busch AE. Inhibition of I_{Ks} channels by HMR 1556. *Naunyn Schmiedebergs Arch Pharmacol*. 2000;362:480-488.

53. Shimizu W, Antzelevitch C. Cellular basis for the ECG features of the LQT1 form of the long-QT syndrome: effects of beta-adrenergic agonists and antagonists and sodium channel blockers on transmural dispersion of repolarization and torsade de pointes. *Circulation*. 1998;98:2314-2322.

54. Geelen P, Drolet B, Lessard E, Gilbert P, O'Hara GE, Turgeon J. Concomitant Block of the Rapid (I(Kr)) and Slow (I(Ks)) Components of the Delayed Rectifier Potassium Current is Associated With Additional Drug Effects on Lengthening of Cardiac Repolarization. *J Cardiovasc Pharmacol Ther*. 1999;4:143-150.

55. Cheng J, Kamiya K, Liu W, Tsuji Y, Toyama J, Kodama I. Heterogeneous distribution of the two components of delayed rectifier K^+ current: a potential mechanism of the proarrhythmic effects of methanesulfonanilideclass III agents. *Cardiovasc Res*. 1999;43:135-147.

56. Warmke JW, Ganetzky B. A family of potassium channel genes related to eag in Drosophila and mammals. *Proc Natl Acad Sci U S A*. 1994;91:3438-3442.

57. Sanguinetti MC, Jiang C, Curran ME, Keating MT. A mechanistic link between an inherited and an acquired cardiac arrhythmia: HERG encodes the I_{Kr} potassium channel. *Cell*. 1995;81:299-307.

58. Trudeau MC, Warmke JW, Ganetzky B, Robertson GA. HERG, a human inward rectifier in the voltage-gated potassium channel family. *Science*. 1995;269:92-95.

59. Roden DM, George AL, Jr. Structure and function of cardiac sodium and potassium channels. *Am J Physiol*. 1997;273:H511-H525.

60. Guy HR, Durell SR. Structural models of Na^+, Ca^{2+}, and K^+ channels. *Soc Gen Physiol Ser*. 1995;50:1-16.

61. Kukuljan M, Labarca P, Latorre R. Molecular determinants of ion conduction and inactivation in K^+ channels. *Am J Physiol.* 1995;268:C535-C556.

62. Splawski I, Shen J, Timothy KW, Vincent GM, Lehmann MH, Keating MT. Genomic structure of three long QT syndrome genes: KVLQT1, HERG, and KCNE1. *Genomics.* 1998;51:86-97.

63. Itoh T, Tanaka T, Nagai R, Kamiya T, Sawayama T, Nakayama T, Tomoike H, Sakurada H, Yazaki Y, Nakamura Y. Genomic organization and mutational analysis of HERG, a gene responsible for familial long QT syndrome. *Hum Genet.* 1998;102:435-439.

64. McDonald TV, Yu Z, Ming Z, Palma E, Meyers MB, Wang KW, Goldstein SA, Fishman GI. A minK-HERG complex regulates the cardiac potassium current $I_{(Kr)}$. *Nature.* 1997;388:289-292.

65. Abbott GW, Sesti F, Splawski I, Buck ME, Lehmann MH, Timothy KW, Keating MT, Goldstein SA. MiRP1 forms I_{Kr} potassium channels with HERG and is associated with cardiac arrhythmia. *Cell.* 1999;97:175-187.

66. Ohyama H, Kajita H, Omori K, Takumi T, Hiramoto N, Iwasaka T, Matsuda H. Inhibition of cardiac delayed rectifier K^+ currents by an antisense oligodeoxynucleotide against IsK (minK) and over-expression of IsK mutant D77N in neonatal mouse hearts. *Pflugers Arch.* 2001;442:329-335.

67. Sesti F, Abbott GW, Wei J, Murray KT, Sa_{ks}ena S, Schwartz PJ, Priori SG, Roden DM, George AL, Jr., Goldstein SA. A common polymorphism associated with antibiotic-induced cardiac arrhythmia. *Proc Natl Acad Sci U S A.* 2000;97:10613-10618.

68. Weerapura M, Nattel S, Chartier D, Caballero R, Hebert TE. A comparison of currents carried by HERG, with and without coexpression of MiRP1, and the native rapid delayed rectifier current. Is MiRP1 the missing link? *J Physiol.* 2002;540:15-27.

69. Zhang M, Jiang M, Tseng GN. minK-related peptide 1 associates with Kv4.2 and modulates its gating function: potential role as beta subunit of cardiac transient outward channel? *Circ Res.* 2001;88:1012-1019.

70. Splawski I, Shen J, Timothy KW, Lehmann MH, Priori S, Robinson JL, Moss AJ, Schwartz PJ, Towbin JA, Vincent GM, Keating MT. Spectrum of mutations in long-QT syndrome genes. KVLQT1, HERG, SCN5A, KCNE1, and KCNE2. *Circulation.* 2000;102:1178-1185.

71. Sanguinetti MC, Curran ME, Zou A, Shen J, Spector PS, Atkinson DL, Keating MT. Coassembly of K(V)LQT1 and minK (IsK) proteins to form cardiac $I_{(Ks)}$ potassium channel. *Nature*. 1996;384:80-83.

72. Wang Q, Curran ME, Splawski I, Burn TC, Millholland JM, VanRaay TJ, Shen J, Timothy KW, Vincent GM, de Jager T, Schwartz PJ, Toubin JA, Moss AJ, Atkinson DL, Landes GM, Connors TD, Keating MT. Positional cloning of a novel potassium channel gene: KVLQT1 mutations cause cardiac arrhythmias. *Nat Genet*. 1996;12:17-23.

73. Romey G, Attali B, Chouabe C, Abitbol I, Guillemare E, Barhanin J, Lazdunski M. Molecular mechanism and functional significance of the MinK control of the KvLQT1 channel activity. *J Biol Chem*. 1997;272:16713-16716.

74. Suessbrich H, Busch AE. The I_{Ks} channel: coassembly of IsK (minK) and KvLQT1 proteins. *Rev Physiol Biochem Pharmacol*. 1999;137:191-226.

75. Barhanin J, Lesage F, Guillemare E, Fink M, Lazdunski M, Romey G. K(V)LQT1 and lsK (minK) proteins associate to form the $I_{(Ks)}$ cardiac potassium current. *Nature*. 1996;384:78-80.

76. Yang WP, Levesque PC, Little WA, Conder ML, Shalaby FY, Blanar MA. KvLQT1, a voltage-gated potassium channel responsible for human cardiac arrhythmias. *Proc Natl Acad Sci U S A*. 1997;94:4017-4021.

77. Bianchi L, Shen Z, Dennis AT, Priori SG, Napolitano C, Ronchetti E, Bryskin R, Schwartz PJ, Brown AM. Cellular dysfunction of LQT5-minK mutants: abnormalities of I_{Ks}, I_{Kr} and trafficking in long QT syndrome. *Hum Mol Genet*. 1999;8:1499-1507.

78. Russell MW, Dick M, Collins FS, Brody LC. KVLQT1 mutations in three families with familial or sporadic long QT syndrome. *Hum Mol Genet*. 1996;5:1319-1324.

79. Splawski I, Tristani-Firouzi M, Lehmann MH, Sanguinetti MC, Keating MT. Mutations in the hminK gene cause long QT syndrome and suppress I_{Ks} function. *Nat Genet*. 1997;17:338-340.

80. London B, Trudeau MC, Newton KP, Beyer AK, Copeland NG, Gilbert DJ, Jenkins NA, Satler CA, Robertson GA. Two isoforms of the mouse ether-a-go-go-related gene coassemble to form channels with properties similar to the rapidly activating component of the cardiac delayed rectifier K^+ current. *Circ Res*. 1997;81:870-878.

81. Lees-Miller JP, Kondo C, Wang L, Duff HJ. Electrophysiological characterization of an alternatively processed ERG K^+ channel in mouse and human hearts. *Circ Res*. 1997;81:719-726.

82. Polvani S, Masi A, Pillozzi S, Gragnani L, Crociani O, Olivotto M, Becchetti A, Wanke E, Arcangeli A. Developmentally regulated expression of the mouse homologues of the potassium channel encoding genes m-erg1, m-erg2 and m-erg3. *Gene Expr Patterns*. 2003;3:767-776.

83. Jones EM, Roti Roti EC, Wang J, Delfosse SA, Robertson GA. Cardiac I_{Kr} channels minimally comprise hERG 1a and 1b subunits. *J Biol Chem*. 2004;279:44690-44694.

84. Robertson GA, Jones EM, Wang J. Gating and assembly of heteromeric hERG1a/1b channels underlying $I_{(Kr)}$ in the heart. *Novartis Found Symp*. 2005;266:4-15.

85. Pond AL, Scheve BK, Benedict AT, Petrecca K, Van Wagoner DR, Shrier A, Nerbonne JM. Expression of distinct ERG proteins in rat, mouse, and human heart. Relation to functional $I_{(Kr)}$ channels. *J Biol Chem*. 2000;275:5997-6006.

86. Lees-Miller JP, Guo J, Somers JR, Roach DE, Sheldon RS, Rancourt DE, Duff HJ. Selective knockout of mouse ERG1 B potassium channel eliminates $I_{(Kr)}$ in adult ventricular myocytes and elicits episodes of abrupt sinus bradycardia. *Mol Cell Biol*. 2003;23:1856-1862.

87. Demolombe S, Baro I, Pereon Y, Bliek J, Mohammad-Panah R, Pollard H, Morid S, Mannens M, Wilde A, Barhanin J, Charpentier F, Escande D. A dominant negative isoform of the long QT syndrome 1 gene product. *J Biol Chem*. 1998;273:6837-6843.

88. Pereon Y, Demolombe S, Baro I, Drouin E, Charpentier F, Escande D. Differential expression of KvLQT1 isoforms across the human ventricular wall. *Am J Physiol*. 2000;278:H1908-H1915.

89. Lande G, Demolombe S, Bammert A, Moorman A, Charpentier F, Escande D. Transgenic mice overexpressing human KvLQT1 dominant-negative isoform. Part II: Pharmacological profile. *Cardiovasc Res*. 2001;50:328-334.

90. Demolombe S, Lande G, Charpentier F, van Roon MA, van den Hoff MJ, Toumaniantz G, Baro I, Guihard G, Le Berre N, Corbier A, de Bakker J, Opthof T, Wilde A, Moorman AF, Escande D. Transgenic mice overexpressing human KvLQT1 dominant-negative isoform. Part I: Phenotypic characterisation. *Cardiovasc Res*. 2001;50:314-327.

91. Neyroud N, Richard P, Vignier N, Donger C, Denjoy I, Demay L, Shkolnikova M, Pesce R, Chevalier P, Hainque B, Coumel P, Schwartz K, Guicheney P. Genomic organization of the KCNQ1 K^+ channel gene and identification of C-terminal mutations in the long-QT syndrome. *Circ Res*. 1999;84:290-297.

92. Bryant SM, Wan X, Shipsey SJ, Hart G. Regional differences in the delayed rectifier current (I_{Kr} and I_{Ks}) contribute to the differences in action potential duration in basal left ventricular myocytes in guinea-pig. *Cardiovasc Res.* 1998;40:322-331.

93. Main MC, Bryant SM, Hart G. Regional differences in action potential characteristics and membrane currents of guinea-pig left ventricular myocytes. *Exp Physiol.* 1998;83:747-761.

94. Xu X, Rials SJ, Wu Y, Salata JJ, Liu T, Bharucha DB, Marinchak RA, Kowey PR. Left ventricular hypertrophy decreases slowly but not rapidly activating delayed rectifier potassium currents of epicardial and endocardial myocytes in rabbits. *Circulation.* 2001;103:1585-1590.

95. Li D, Zhang L, Kneller J, Nattel S. Potential ionic mechanism for repolarization differences between canine right and left atrium. *Circ Res.* 2001;88:1168-1175.

96. Volders PG, Sipido KR, Vos MA, Spatjens RL, Leunissen JD, Carmeliet E, Wellens HJ. Downregulation of delayed rectifier K(+) currents in dogs with chronic complete atrioventricular block and acquired torsades de pointes. *Circulation.* 1999;100:2455-2461.

97. Ramakers C, Vos MA, Doevendans PA, Schoenmakers M, Wu YS, Scicchitano S, Iodice A, Thomas GP, Antzelevitch C, Dumaine R. Coordinated down-regulation of KCNQ1 and KCNE1 expression contributes to reduction of I(Ks) in canine hypertrophied hearts. *Cardiovasc Res.* 2003;57:486-496.

98. Szentadrassy N, Banyasz T, Biro T, Szabo G, Toth BI, Magyar J, Lazar J, Varro A, Kovacs L, Nanasi PP. Apico-basal inhomogeneity in distribution of ion channels in canine and human ventricular myocardium. *Cardiovasc Res.* 2005;65:851-860.

99. Szabo G, Szentandrassy N, Biro T, Toth BI, Czifra G, Magyar J, Banyasz T, Varro A, Kovacs L, Nanasi PP. Asymmetrical distribution of ion channels in canine and human left-ventricular wall: epicardium versus midmyocardium. *Pflugers Arch.* 2005;450:307-316.

100. Verduyn SC, Vos MA, van der ZJ, Kulcsar A, Wellens HJ. Further observations to elucidate the role of interventricular dispersion of repolarization and early afterdepolarizations in the genesis of acquired torsade de pointes arrhythmias: a comparison between almokalant and d-sotalol using the dog as its own control. *J Am Coll Cardiol.* 1997;30:1575-1584.

101. Verduyn SC, Vos MA, van der ZJ, van der Hulst FF, Wellens HJ. Role of interventricular dispersion of repolarization in acquired torsade-de-pointes arrhythmias: reversal by magnesium. *Cardiovasc Res*. 1997;34:453-463.

102. Wang L, Duff HJ. Identification and characteristics of delayed rectifier K^+ current in fetal mouse ventricular myocytes. *Am J Physiol*. 1996;270:H2088-H2093.

103. Schwartz PJ, Periti M, Malliani A. The long Q-T syndrome. *Am Heart J*. 1975;89:378-390.

104. Zipes DP. Proarrhythmic effects of antiarrhythmic drugs. *Am J Cardiol*. 1987;59:26E-31E.

105. Romano C, Gemme G, Pongiglione R. [Rare cardiac arrythmias of the pediatric age. II. syncopal attacks due to paroxysmal ventricular fibrillation. (presentation of 1st case in Italian pediatric leterature)]. *Clin Pediatr (Bologna)*. 1963;45:656-683.

106. Ward OC. A new familial cardiac syndrome in children. *J Ir Med Assoc*. 1964;54:103-106.

107. Jervell A, Lange-Nielsen F. Congenital deaf-mutism, functional heart disease with prolongation of the Q-T interval and sudden death. *Am Heart J*. 1957;54:59-68.

108. Curran ME, Splawski I, Timothy KW, Vincent GM, Green ED, Keating MT. A molecular basis for cardiac arrhythmia: HERG mutations cause long QT syndrome. *Cell*. 1995;80:795-803.

109. Singh BN. Current antiarrhythmic drugs: an overview of mechanisms of action and potential clinical utility. *J Cardiovasc Electrophysiol*. 1999;10:283-301.

110. Roy ML, Saal D, Perney T, Sontheimer H, Waxman SG, Kaczmarek LK. Manipulation of the delayed rectifier Kv1.5 potassium channel in glial cells by antisense oligodeoxynucleotides. *Glia*. 1996;18:177-184.

111. Dumaine R, Roy ML, Brown AM. Blockade of HERG and Kv1.5 by ketoconazole. *J Pharmacol Exp Ther*. 1998;286:727-735.

112. Yap YG, Camm AJ. Arrhythmogenic mechanisms of non-sedating antihistamines. *Clin Exp Allergy*. 1999;29 Suppl 3:174-181.

113. Yap YG, Camm AJ. The current cardiac safety situation with antihistamines. *Clin Exp Allergy*. 1999;29 Suppl 1:15-24.

114. Lai LP, Deng CL, Moss AJ, Kass RS, Liang CS. Polymorphism of the gene encoding a human minimal potassium ion channel (minK). *Gene*. 1994;151:339-340.

115. Yan GX, Antzelevitch C. Cellular basis for the normal T wave and the electrocardiographic manifestations of the long-QT syndrome. *Circulation*. 1998;98:1928-1936.

116. Schulze-Bahr E, Wedekind H, Haverkamp W, Borggrefe M, Assmann G, Breithardt G, Funke H. The LQT syndromes--current status of molecular mechanisms. *Z Kardiol*. 1999;88:245-254.

117. Yue L, Feng J, Gaspo R, Li GR, Wang Z, Nattel S. Ionic remodeling underlying action potential changes in a canine model of atrial fibrillation. *Circ Res*. 1997;81:512-525.

118. Lai LP, Su MJ, Lin JL, Lin FY, Tsai CH, Chen YS, Tseng YZ, Lien WP, Huang SK. Changes in the mRNA levels of delayed rectifier potassium channels in human atrial fibrillation. *Cardiology*. 1999;92:248-255.

119. Gaborit N, Steenman M, Lamirault G, Le Meur N, Le Bouter S, Lande G, Leger J, Charpentier F, Christ T, Dobrev D, Escande D, Nattel S, Demolombe S. Human atrial ion channel and transporter subunit gene-expression remodeling associated with valvular heart disease and atrial fibrillation. *Circulation*. 2005;112:471-481.

120. Brundel BJ, Van Gelder IC, Henning RH, Tuinenburg AE, Wietses M, Grandjean JG, Wilde AA, Van Gilst WH, Crijns HJ. Alterations in potassium channel gene expression in atria of patients with persistent and paroxysmal atrial fibrillation: differential regulation of protein and mRNA levels for K^+ channels. *J Am Coll Cardiol*. 2001;37:926-932.

121. Sakatani T, Shirayama T, Yamamoto T, Mani H, Shiraishi H, Matsubara H. Cardiac hypertrophy diminished the effects of isoproterenol on delayed rectifier potassium current in rat heart. *J Physiol Sci*. 2006;56:173-181.

122. Tsuji Y, Opthof T, Yasui K, Inden Y, Takemura H, Niwa N, Lu Z, Lee JK, Honjo H, Kamiya K, Kodama I. Ionic mechanisms of acquired QT prolongation and torsades de pointes in rabbits with chronic complete atrioventricular block. *Circulation*. 2002;106:2012-2018.

123. Ahmmed GU, Dong PH, Song G, Ball NA, Xu Y, Walsh RA, Chiamvimonvat N. Changes in Ca(2+) cycling proteins underlie cardiac action potential prolongation in a pressure-overloaded guinea pig model with cardiac hypertrophy and failure. *Circ Res*. 2000;86:558-570.

124. Jiang M, Cabo C, Yao J, Boyden PA, Tseng G. Delayed rectifier K currents have reduced amplitudes and altered kinetics in myocytes from infarcted canine ventricle. *Cardiovasc Res*. 2000;48:34-43.

125. Shinmura K, Tani M, Hasegawa H, Ebihara Y, Nakamura Y. Effect of E4031, a class III antiarrhythmic drug, on ischemia- and reperfusion-induced arrhythmias in isolated rat hearts. *Jpn Heart J*. 1998;39:183-197.

126. Pinto JM, Boyden PA. Electrical remodeling in ischemia and infarction. *Cardiovasc Res*. 1999;42:284-297.

127. Wang J, Zhang Y, Wang H, Han H, Nattel S, Yang B, Wang Z. Potential mechanisms for the enhancement of HERG K^+ channel function by phospholipid metabolites. *Br J Pharmacol*. 2004;141:586-599.

128. Wang J, Wang H, Han H, Zhang Y, Yang B, Nattel S, Wang Z. Phospholipid metabolite 1-palmitoyl-lysophosphatidylcholine enhances human ether-a-go-go-related gene (HERG) $K(^+)$ channel function. *Circulation*. 2001;104:2645-2648.

129. Tsuji Y, Opthof T, Kamiya K, Yasui K, Liu W, Lu Z, Kodama I. Pacing-induced heart failure causes a reduction of delayed rectifier potassium currents along with decreases in calcium and transient outward currents in rabbit ventricle. *Cardiovasc Res*. 2000;48:300-309.

130. Li D, Melnyk P, Feng J, Wang Z, Petrecca K, Shrier A, Nattel S. Effects of experimental heart failure on atrial cellular and ionic electrophysiology. *Circulation*. 2000;101:2631-2638.

131. Li GR, Lau CP, Ducharme A, Tardif JC, Nattel S. Transmural action potential and ionic current remodeling in ventricles of failing canine hearts. *Am J Physiol*. 2002;283:H1031-H1041.

132. Lengyel C, Virag L, Biro T, Jost N, Magyar J, Biliczki P, Kocsis E, Skoumal R, Nanasi PP, Toth M, Kecskemeti V, Papp JG, Varro A. Diabetes mellitus attenuates the repolarization reserve in mammalian heart. *Cardiovasc Res*. 2007;73:512-520.

133. Zhang Y, Xiao J, Wang H, Luo X, Wang J, Villeneuve LR, Zhang H, Bai Y, Yang B, Wang Z. Restoring depressed HERG K^+ channel function as a mechanism for insulin treatment of abnormal QT prolongation and associated arrhythmias in diabetic rabbits. *Am J Physiol*. 2006;291:H1446-H1455.

134. Spencer JA, Misra RP. Expression of the serum response factor gene is regulated by serum response factor binding sites. *J Biol Chem*. 1996;271:16535-16543.

135. Ptashne M. Gene regulation by proteins acting nearby and at a distance. *Nature*. 1986;322:697-701.

136. Rosati B, McKinnon D. Regulation of ion channel expression. *Circ Res*. 2004;94:874-883.

137. Shi W, Wymore R, Yu H, Wu J, Wymore RT, Pan Z, Robinson RB, Dixon JE, McKinnon D, Cohen IS. Distribution and prevalence of hyperpolarization-activated cation channel (HCN) mRNA expression in cardiac tissues. *Circ Res*. 1999;85:e1-e6.

138. Bru-Mercier G, Deroubaix E, Capuano V, Ruchon Y, Rucker-Martin C, Coulombe A, Renaud JF. Expression of heart K^+ channels in adrenalectomized and catecholamine-depleted reserpine-treated rats. *J Mol Cell Cardiol*. 2003;35:153-163.

139. Duff HJ, Offord J, West J, Catterall WA. Class I and IV antiarrhythmic drugs and cytosolic calcium regulate mRNA encoding the sodium channel alpha subunit in rat cardiac muscle. *Mol Pharmacol*. 1992;42:570-574.

140. Xu M, Welling A, Paparisto S, Hofmann F, Klugbauer N. Enhanced expression of L-type Cav1.3 calcium channels in murine embryonic hearts from Cav1.2-deficient mice. *J Biol Chem*. 2003;278:40837-40841.

141. Zhou J, Kodirov S, Murata M, Buckett PD, Nerbonne JM, Koren G. Regional upregulation of Kv2.1-encoded current, IK,slow2, in Kv1DN mice is abolished by crossbreeding with Kv2DN mice. *Am J Physiol*. 2003;284:H491-H500.

142. Papadatos GA, Wallerstein PM, Head CE, Ratcliff R, Brady PA, Benndorf K, Saumarez RC, Trezise AE, Huang CL, Vandenberg JI, Colledge WH, Grace AA. Slowed conduction and ventricular tachycardia after targeted disruption of the cardiac sodium channel gene Scn5a. *Proc Natl Acad Sci U S A*. 2002;99:6210-6215.

143. Kuo HC, Cheng CF, Clark RB, Lin JJ, Lin JL, Hoshijima M, Nguyen-Tran VT, Gu Y, Ikeda Y, Chu PH, Ross J, Giles WR, Chien KR. A defect in the Kv channel-interacting protein 2 (KChIP2) gene leads to a complete loss of I(to) and confers susceptibility to ventricular tachycardia. *Cell*. 2001;107:801-813.

144. Kubo Y, Reuveny E, Slesinger PA, Jan YN, Jan LY. Primary structure and functional expression of a rat G-protein-coupled muscarinic potassium channel. *Nature*. 1993;364:802-806.

145. Dixon JE, McKinnon D. Quantitative analysis of potassium channel mRNA expression in atrial and ventricular muscle of rats. *Circ Res*. 1994;75:252-260.

146. Yue L, Melnyk P, Gaspo R, Wang Z, Nattel S. Molecular mechanisms underlying ionic remodeling in a dog model of atrial fibrillation. *Circ Res.* 1999;84:776-784.

147. Huang B, Qin D, Deng L, Boutjdir M, Sherif N. Reexpression of T-type Ca^{2+} channel gene and current in post-infarction remodeled rat left ventricle. *Cardiovasc Res.* 2000;46:442-449.

148. Rosati B, Pan Z, Lypen S, Wang HS, Cohen I, Dixon JE, McKinnon D. Regulation of KChIP2 potassium channel beta subunit gene expression underlies the gradient of transient outward current in canine and human ventricle. *J Physiol.* 2001;533:119-125.

149. Dobrev D, Graf E, Wettwer E, Himmel HM, Hala O, Doerfel C, Christ T, Schuler S, Ravens U. Molecular basis of downregulation of G-protein-coupled inward rectifying K(+) current I(K,ACh) in chronic human atrial fibrillation: decrease in GIRK4 mRNA correlates with reduced I(K,ACh) and muscarinic receptor-mediated shortening of action potentials. *Circulation.* 2001;104:2551-2557.

150. Kobayashi T, Yamada Y, Nagashima M, Seki S, Tsutsuura M, Ito Y, Sakuma I, Hamada H, Abe T, Tohse N. Contribution of KChIP2 to the developmental increase in transient outward current of rat cardiomyocytes. *J Mol Cell Cardiol.* 2003;35:1073-1082.

151. Le Bouter S, Demolombe S, Chambellan A, Bellocq C, Aimond F, Toumaniantz G, Lande G, Siavoshian S, Baro I, Pond AL, Nerbonne JM, Leger JJ, Escande D, Charpentier F. Microarray analysis reveals complex remodeling of cardiac ion channel expression with altered thyroid status: relation to cellular and integrated electrophysiology. *Circ Res.* 2003;92:234-242.

152. Fernandez-Velasco M, Goren N, Benito G, Blanco-Rivero J, Bosca L, Delgado C. Regional distribution of hyperpolarization-activated current (I_f) and hyperpolarization-activated cyclic nucleotide-gated channel mRNA expression in ventricular cells from control and hypertrophied rat hearts. *J Physiol.* 2003;553:395-405.

153. Heicklen-Klein A, McReynolds LJ, Evans T. Using the zebrafish model to study GATA transcription factors. *Semin Cell Dev Biol.* 2005;16:95-106.

154. Peterkin T, Gibson A, Loose M, Patient R. The roles of GATA-4, -5 and -6 in vertebrate heart development. *Semin Cell Dev Biol.* 2005;16:83-94.

155. Burch JB. Regulation of GATA gene expression during vertebrate development. *Semin Cell Dev Biol.* 2005;16:71-81.

156. Pikkarainen S, Tokola H, Kerkela R, Ruskoaho H. GATA transcription factors in the developing and adult heart. *Cardiovasc Res*. 2004;63:196-207.

157. Nemer G, Nemer M. Regulation of heart development and function through combinatorial interactions of transcription factors. *Ann Med*. 2001;33:604-610.

158. Molkentin JD. The zinc finger-containing transcription factors GATA-4, -5, and -6. Ubiquitously expressed regulators of tissue-specific gene expression. *J Biol Chem*. 2000;275:38949-38952.

159. Charron F, Nemer M. GATA transcription factors and cardiac development. *Semin Cell Dev Biol*. 1999;10:85-91.

160. Cripps RM, Black BL, Zhao B, Lien CL, Schulz RA, Olson EN. The myogenic regulatory gene Mef2 is a direct target for transcriptional activation by Twist during Drosophila myogenesis. *Genes Dev*. 1998;12:422-434.

161. Hatcher CJ, McDermott DA. Using the TBX5 transcription factor to grow and sculpt the heart. *Am J Med Genet A*. 2006;140:1414-1418.

162. Cripps RM, Olson EN. Twist is required for muscle template splitting during adult Drosophila myogenesis. *Dev Biol*. 1998;203:106-115.

163. Buckingham M, Meilhac S, Zaffran S. Building the mammalian heart from two sources of myocardial cells. *Nat Rev Genet*. 2005;6:826-835.

164. Srivastava D, Olson EN. A genetic blueprint for cardiac development. *Nature*. 2000;407:221-226.

165. Bruneau BG. Transcriptional regulation of vertebrate cardiac morphogenesis. *Circ Res*. 2002;90:509-519.

166. Schulz RA, Yutzey KE. Calcineurin signaling and NFAT activation in cardiovascular and skeletal muscle development. *Dev Biol*. 2004;266:1-16.

167. Jones WK, Brown M, Ren X, He S, McGuinness M. NF-kappaB as an integrator of diverse signaling pathways: the heart of myocardial signaling? *Cardiovasc Toxicol*. 2003;3:229-254.

168. Hilfiker-Kleiner D, Hilfiker A, Drexler H. Many good reasons to have STAT3 in the heart. *Pharmacol Ther*. 2005;107:131-137.

169. Hilfiker-Kleiner D, Limbourg A, Drexler H. STAT3-mediated activation of myocardial capillary growth. *Trends Cardiovasc Med*. 2005;15:152-157.

170. Jones WK, Brown M, Wilhide M, He S, Ren X. NF-kappaB in cardiovascular disease: diverse and specific effects of a "general" transcription factor? *Cardiovasc Toxicol.* 2005;5:183-202.

171. Stephanou A. Role of STAT-1 and STAT-3 in ischaemia/reperfusion injury. *J Cell Mol Med.* 2004;8:519-525.

172. Carlsen H, Alexander G, Austenaa LM, Ebihara K, Blomhoff R. Molecular imaging of the transcription factor NF-kappaB, a primary regulator of stress response. *Mutat Res.* 2004;551:199-211.

173. Nichols TC. NF-kappaB and reperfusion injury. *Drug News Perspect.* 2004;17:99-104.

174. Valen G. Signal transduction through nuclear factor kappa B in ischemia-reperfusion and heart failure. *Basic Res Cardiol.* 2004;99:1-7.

175. Harvey RP, Lai D, Elliott D, Biben C, Solloway M, Prall O, Stennard F, Schindeler A, Groves N, Lavulo L, Hyun C, Yeoh T, Costa M, Furtado M, Kirk E. Homeodomain factor Nkx2-5 in heart development and disease. *Cold Spring Harb Symp Quant Biol.* 2002;67:107-114.

176. Srivastava D, Gottlieb PD, Olson EN. Molecular mechanisms of ventricular hypoplasia. *Cold Spring Harb Symp Quant Biol.* 2002;67:121-125.

177. Wang D, Passier R, Liu ZP, Shin CH, Wang Z, Li S, Sutherland LB, Small E, Krieg PA, Olson EN. Regulation of cardiac growth and development by SRF and its cofactors. *Cold Spring Harb Symp Quant Biol.* 2002;67:97-105.

178. Ptashne M, Gann A. Transcription initiation: imposing specificity by localization. *Essays Biochem.* 2001;37:1-15.

179. Biggar SR, Crabtree GR. Cell signaling can direct either binary or graded transcriptional responses. *EMBO J.* 2001;20:3167-3176.

180. Hoppe UC, Marban E, Johns DC. Molecular dissection of cardiac repolarization by in vivo Kv4.3 gene transfer. *J Clin Invest.* 2000;105:1077-1084.

181. Antzelevitch C. The Brugada syndrome: ionic basis and arrhythmia mechanisms. *J Cardiovasc Electrophysiol.* 2001;12:268-272.

182. Viswanathan PC, Shaw RM, Rudy Y. Effects of I_{Kr} and I_{Ks} heterogeneity on action potential duration and its rate dependence: a simulation study. *Circulation.* 1999;99:2466-2474.

183. Pandit SV, Clark RB, Giles WR, Demir SS. A mathematical model of action potential heterogeneity in adult rat left ventricular myocytes. *Biophys J.* 2001;81:3029-3051.

184. Yang P, Kupershmidt S, Roden DM. Cloning and initial characterization of the human cardiac sodium channel (SCN5A) promoter. *Cardiovasc Res.* 2004;61:56-65.

185. Pang L, Koren G, Wang Z, Nattel S. Tissue-specific expression of two human Ca(v)1.2 isoforms under the control of distinct 5' flanking regulatory elements. *FEBS Lett.* 2003;546:349-354.

186. Mustapha Z, Pang L, Nattel S. Characterization of the cardiac KCNE1 gene promoter. *Cardiovasc Res.* 2007;73:82-91.

187. Lundquist AL, Turner CL, Ballester LY, George AL, Jr. Expression and transcriptional control of human KCNE genes. *Genomics.* 2006;87:119-128.

188. Kadonaga JT, Courey AJ, Ladika J, Tjian R. Distinct regions of Sp1 modulate DNA binding and transcriptional activation. *Science.* 1988;242:1566-1570.

189. Courey AJ, Tjian R. Analysis of Sp1 in vivo reveals multiple transcriptional domains, including a novel glutamine-rich activation motif. *Cell.* 1988;55:887-898.

190. Gidoni D, Dynan WS, Tjian R. Multiple specific contacts between a mammalian transcription factor and its cognate promoters. *Nature.* 1984;312:409-413.

191. Dynan WS, Tjian R. The promoter-specific transcription factor Sp1 binds to upstream sequences in the SV40 early promoter. *Cell.* 1983;35:79-87.

192. Jones KA, Yamamoto KR, Tjian R. Two distinct transcription factors bind to the HSV thymidine kinase promoter in vitro. *Cell.* 1985;42:559-572.

193. Brandeis M, Frank D, Keshet I, Siegfried Z, Mendelsohn M, Nemes A, Temper V, Razin A, Cedar H. Sp1 elements protect a CpG island from de novo methylation. *Nature.* 1994;371:435-438.

194. Macleod D, Charlton J, Mullins J, Bird AP. Sp1 sites in the mouse aprt gene promoter are required to prevent methylation of the CpG island. *Genes Dev.* 1994;8:2282-2292.

195. Ambros V. The functions of animal microRNAs. *Nature.* 2004;431:350-355.

196. Meister G, Tuschl T. Mechanisms of gene silencing by double-stranded RNA. *Nature.* 2004;431:343-349.

197. Bartel DP. MicroRNAs: genomics, biogenesis, mechanism, and function. *Cell*. 2004;116:281-297.

198. Liu J, Valencia-Sanchez MA, Hannon GJ, Parker R. MicroRNA-dependent localization of targeted mRNAs to mammalian P-bodies. *Nat Cell Biol*. 2005;7:719-723.

199. Sen GL, Blau HM. Argonaute 2/RISC resides in sites of mammalian mRNA decay known as cytoplasmic bodies. *Nat Cell Biol*. 2005;7:633-636.

200. Lee RC, Feinbaum RL, Ambros V. The C. elegans heterochronic gene lin-4 encodes small RNAs with antisense complementarity to lin-14. *Cell*. 1993;75:843-854.

201. Baulcombe D. RNA silencing in plants. *Nature*. 2004;431:356-363.

202. Chen JF, Mandel EM, Thomson JM, Wu Q, Callis TE, Hammond SM, Conlon FL, Wang DZ. The role of microRNA-1 and microRNA-133 in skeletal muscle proliferation and differentiation. *Nat Genet*. 2006;38:228-233.

203. Zhao Y, Samal E, Srivastava D. Serum response factor regulates a muscle-specific microRNA that targets Hand2 during cardiogenesis. *Nature*. 2005;436:214-220.

HYPOTHESIS

The 5'UTRs and 3'UTRs of *HERG1* and *KCNQ1* genes contain important sequence elements as the binding sites for transcription factors and *miR-1/miR-133*, and interactions between these sites and transcription factors and *miR-1/miR-133* determine the expression patterns and regional distributions of *HERG1* and *KCNQ1* genes and underlie the disparity between mRNA and protein expression of these genes.

OBJECTIVES

The overall objectives of this study were to explore the molecular mechanisms for transcriptional and post-transcriptional regulation of expression of *HERG1* and *KCNQ1* genes and to shed light on the molecular mechanisms underlying the regional heterogeneous distributions of I_{Kr} and I_{Ks} and its potential implication to arrhythmogenesis. The ultimate goal of this study is trying to develop an efficient and practical approach to precisely control the arrhythmogenic genes *HERG1* and *KCNQ1* by gene interfering. To achieve this goal, the following specific studies will be carried out:

1) To identify the transcription start sites in 5'UTRs of *HERG1a*, *HERG1b*, *KCNQ1a* and *KCNQ1b*, and to clone and characterize their promoters as well as identify the critical transactivators .

2) To characterize the 3'UTRs of *HERG1*, *KCNQ1*and *KCNE1* genes, and to evaluate their candidature as targets for post-transcriptional repression by the muscle-specific microRNAs, *miR-1* and *miR-133*.

3) To define the heterogeneous expression patterns of HERG1, KCNQ1 and KCNE1 at both the mRNA and protein levels.

4) To elucidate the molecular determinants for, or the roles of transcription factors and *miR-1* and *miR-133* in, the regional heterogeneities of I_{Kr} and I_{Ks}.

PART II.ORIGINAL CONTRIBUTIONS

CHAPTER 1.Genomic structure, transcriptional control and tissue distribution of *HERG1* and *KCNQ1* genes

In this chapter, we carried out studies mainly aiming at identification of all *HERG1* and *KCNQ1* genes' promoter region. We performed a detailed analysis of the driving elements for each gene, and we finally targeted Sp1 as the essential transactivator for all *HERG1* and *KCNQ1* genes by the computational method. We also assessed the tissue distributions of all isoforms and measured relative inter-chamber expression of mRNA level for each gene.

This manuscript has been submitted to ***FEBS Letter*** for review in 2007.

Genomic structure, transcriptional control and tissue distribution of human *ERG1* and *KCNQ1* genes

Xiaobin Luo[a,b], Jiening Xiao[a], Huixian Lin [a],
Hongli Shan[c,d], Baofeng Yang[c,d], Zhiguo Wang[a,b,d]

[a]Research Center, Montreal Heart Institute, Montreal, PQ H1T 1C8, Canada

[b]Department of Medicine, University of Montreal, Montreal, PQ H3C 3J7, Canada

[c]Department of Pharmacology and [d]Institute of Cardiovascular Research, Harbin Medical University, Harbin, Heilongjiang 150086, P. R. China

Short Title: **Transcriptional control of *HERG1* and *KCNQ1* genes**

To whom correspondence should be addressed: Research Center, Montreal Heart Institute, 5000 Belanger East, Montreal, PQ H1T 1C8, Canada; Tel.: (514) 376-3330. Fax: (514) 376-4452. E-mail: [redacted]

1.1 Abstract

The long QT syndrome genes *HERG1* and *KCNQ1*, encoding K^+ channels critical to cardiac repolarization, are both comprised of two isoforms: *HERG1a* and *HERG1b*, and *KCNQ1a* and *KCNQ1b*, respectively. Expression of these genes is dynamic depending on differentiation status and disease states. Here we identified their core promoter regions and transcription start sites. We obtained the data pointing to the potential role of Sp1 in transactivating these genes. We compared expression profiling of these genes across a variety of human tissues and demonstrated unexpectedly widespread tissue distributions of all the transcripts. We further revealed that the mRNA levels of all *HERG1* and *KCNQ1* isoforms are asymmetrically distributed within the heart, being predominant in the right relative to the left chambers. Our study provides highly valuable knowledge of core elements related to transcriptional regulation and identifies targets for studies of genetic variants in diseases associated with the *HERG1* and *KCNQ1* genes.

Keywords: Potassium channels; Promoter; Transcription; *HERG1a; HERG1b; KCNQ1a; KCNQ1b*; Sp1

1.2 Introduction

To date, no less than eight long QT syndrome (LQTS) genes have been isolated, which when genetically defected (loss-of-function mutations) can lead to different forms of LQTS. Among these LQTS genes, KvLQT1 (KCNQ1 or Kv7.1) and human *either-a-go-go*-related gene (*HERG1* or *KCNH2*) are responsible for a majority (~85-90%) of cases of inherited LQTS. Moreover, HERG1 protein is also a pharmacological target for a majority of acquired LQTS as a result of drug blockade. *HERG1* encodes the pore-forming α-subunit of a K^+ channel with biophysical and pharmacological properties similar to those of rapid delayed rectifier K^+ current (I_{Kr}), a critical repolarizing current in cardiac cells [1]. In mammalian heart, two *HERG1* transcripts (we term the long isoform *HERG1a* and the short isoform *HERG1b*), encode proteins differing in their amino-terminal sequence and gating properties [2-6]. A recent study proposed that cardiac I_{Kr} channels are minimally composed of *HERG1a* and *HERG1b* α-subunits that co-assemble in the membrane [5]. On the other hand, KCNQ1 encodes the pore-forming α-subunit of the K^+ channel underlying slow delayed rectifier K^+ current (I_{Ks}), another critical repolarizing current in cardiomyocytes [7]. Intriguingly, *KCNQ1* also is composed of two isoforms differing in their N-termini: isoform 2, encoding translational start in the middle of membrane segment 1 [8-10]. When expressed in a heterologous context, the isoform 2 protein functions as a dominant negative isoform [8]. For convenience, here we designate the two isoforms *KCNQ1a* (long isoform or isoform 1) and *KCNQ1b* (short isoform or isoform 2).

Strikingly, expression of both *HERG1* and *KCNQ1* genes is dynamic depending on differentiation status and cell cycle of the cells, contributing importantly to the developmental evolution of myocardial action potential morphology. For example, I_{Kr} is the sole component of delayed rectifier K^+ current in fetal day 18 mouse ventricles, yet both I_{Kr} and I_{Ks} are observed on postnatal day 1. By day 3, I_{Ks} is the dominant component. With further development into adulthood, neither I_{Kr} nor I_{Ks} is observed [11,12]. With respect to canine heart, it was found that I_{Ks} is absent or minimal before age 4 weeks, at which time I_{Kr} is the major repolarizing current [12]. With progression toward adulthood, I_{Ks} appears and

increases in density while I_{Kr} density diminishes. Moreover, when the adult cardiac cells become dedifferentiated or cancerous, such as AT-1 and HL-1 (murine atrial tumor cell lines) cells, I_{Kr} regains its predominance among the expressed K^+ channels [13,14]. While in tissues other than heart and brain there is restricted *HERG1* expression under normal situations, tumor cells of various histological origins overexpress the *HERG1a* and *HERG1b* genes and their protein products [15-20]. It appears that expressions of *HERG1* and *KCNQ1* genes are tightly controlled by certain factors according to a defined genetic program related to morphogenesis during development. Understanding the transcriptional control of these genes is therefore necessary.

The objective of this study was two fold: (1) to elucidate the genomic structure and promoter regions of *HERG1* and *KCNQ1* genes and (2) to map the distribution of *HERG1* and *KCNQ1* transcripts in multiple human tissues and in various regions of the heart. Our study defined the transcription start sites and 5' flanking genomic sequences of each isoform and delineated critical genomic elements necessary for transcriptional control of the genes. Our data demonstrated tissue-dependent distributions of the transcripts and revealed regional differences of expressions of these isoforms within cardiac tissues. The findings shed light on the molecular mechanisms for transcriptional control of these genes and enable future work to determine factors responsible for tissue-specific expression.

1.3 Results

1.3.1 Identification of the transcription start sites of the *HERG1* and *KCNQ1* genes

The *HERG1* genes refer to two different variants that diverge at the N terminus, *HERG1a* (*HERG*) and *HERG1b*. As documented in our previous studies [21], *HERG1a* contains a single transcription start site (TSS, designated +1) located to 79 bp upstream from the translation start codon (ATG) of *HERG1a* 5'-UTR (Fig. 1A, GenBank accession DQ120124). For *HERG1b*, 5'RACE identified one major fragment of 403 bp upstream ATG, along with two minor fragments with sizes of 150 bp and 296 bp, respectively, in the 5'-UTR of *HERG1b* (**Supplemental Figure 1**).

Sequencing of these fragments indicated the 403-bp and 296-bp bands represent two separate TSSs of *HERG1b*. The potential TSSs of *HERG1b* described above were verified by RNase protection assay using RNA samples from human heart (**Supplemental Figure 1**). The major fragment of 400-bp length corresponding to the larger TSS obtained by 5'RACE was identified along with a weak band of around 300-bp size. These results defined two principal TSSs in *HERG1b*: the larger (the most upstream) TSS revealed by 5'RACE is likely the major form of *HERG1b* transcripts in human heart and the minor TSS represents a relatively rare form of *HERG1b* transcripts (Fig. 1B, GenBank accession DQ120125).

Similar to the *HERG1* genes, the *KCNQ1* genes are also composed of two isoforms, the long isoform *KCNQ1a* and the short isoform *KCNQ1b* that also differ in their N-termini. 5'RACE was used to obtain the 5'ends of *KCNQ1a* and *KCNQ1b* transcripts. For *KCNQ1a*, the nested primer (the second reverse primer) was designed from the very end of the N-terminus of *KCNQ1a* because this region is unique to *KCNQ1a* and is absent in *KCNQ1b*. The experiment using RNA samples from human heart yielded two discrete fragments. Sequence analysis suggests that the two fragments represent separate transcription start sites: TSS1 (designated +1) and TSS2 (position +12) which are located to 80 bp and 68 bp, respectively, upstream of the translation start codon (ATG) of *KCNQ1a* gene (Fig. 1C, Genbank accession EF010934). For *KCNQ1b*, 5'RACE identified a single discrete fragment of ~400 bp size. Sequencing analysis indicates that the fragment spans a portion of the first intron of *KCNQ1* genomic DNA and a portion of *KCNQ1b* N-terminus (Fig. 1D, Genbank accession EF010935). The TSS of *KCNQ1b* was defined to 274 bp upstream of the translation start codon (ATG) of *KCNQ1b*.

1.3.2 Genomic arrangement of the *HERG1* and *KCNQ1* genes and their promoter regions

Figure 2 provides a schematic view of genomic arrangement of *HERG* genes with *HERG1a*, *HERG1b*, *HERG2* and *HEEG3* aligned for comparisons. Based on the results described above, it is clear that *HERG1a* promoter is localized to the 5'-flanking region of the *HERG1a* gene and the *HERG1b* promoter falls within the intron 5 of the *HERG* genomic DNA. The genomic exon 6 corresponds to the N-

terminus of *HERG1b*, whereas *HERG1a* uses the genomic exon 6 as a part of its intron that spans genomic intron 5, exon 6 and intron 6. As such, *HERG1b* uses the downstream 403-bp region of the intron 5 as its 5'-UTR and the 250-bp region upstream the TSSs as its core promoter sequence.

Genomic analysis indicates that the promoter sequence of *KCNQ1a* falls into the 5'-flanking region of the *KCNQ1* gene. *KCNQ1b* uses a portion of intron 1 of the *KCNQ1* genomic DNA as its promoter region, and its TSS and translation start codon (ATG) plus the next two nucleotides both fall within the intron 1 region (Fig. 3).

1.3.3 Structural analysis of the 5'-flanking regions of the *HERG1* and *KCNQ1* genes

Computer analysis of 3000-bp 5'-flanking regions of *HERG1* and *KCNQ1* using the *MatInspector* program revealed that none of them contains canonical mammalian TATA box within 1 kb upstream of their TSSs. They also lack other known common promoter elements that are required for transcription initiation complex, including the initiator element, the downstream promoter element (DPE), or the TFIIB recognition element (BRE). Less common promoter elements such as the downstream core element (DCE) and the multiple start site element downstream (MED-1) are also missing. There is one putative CCAAT site in *HERG1a* 5'flanking region, which is absent in the *HERG1b* promoter sequence. *KCNQ1b* has five CCAAT boxes, but *KCNQ1a* has none. However, among these five CCAAT consensus sites, only one is located within the core promoter region (-33) and others are at least 2.3 kb away from the TSS.

Cis-elements for the heart-specific GATA4 as the potent transactivator in cardiac cells is absent in the 5'-flanking regions of the *HERG1* and *KCNQ1* genes. Consensus sites for other members of the GATA family were identified. The distal 5'-flanking region of *HERG1b* contains two putative GATA1 binding sites (-628 and -1431) and one GATA3 binding site (-1446). The *KCNQ1a* 5'-flanking region contains three GATA1 consensus sites located distal to its TSS1 (1.4 kb, 1.6 kb and 2.0 kb upstream). *KCNQ1b* contains two GATA1 sites with one at 50 bp and the other at 1.5 kb upstream its TSSs. The cardiac-specific homeobox Nkx2.5 was found in none of the genes. *Cis*-elements for other TFs important to cardiac development and function,

including serum responsive factor (SRF), Hand2 and MyoD, were found in the 5'-flanking regions of *HERG1* and *KCNQ1* genes (Table 1).

1.3.4 Characterization of the promoter regions of the *HERG1* and *KCNQ1* genes

To assess the functional role of the 5'-flanking regions of *HERG1* and *KCNQ1* in the transcriptional regulation of these genes, various lengths of putative promoter fragment-luciferase constructs were generated and tested for their ability to drive expression of the reporter gene in a rat ventricular cell line (H9c2) and a human embryonic kidney cell line (HEK293).

The core promoter of the *HERG1a* gene was defined to 487-bp which showed a maximum luciferase activity >8 folds the activity of the promoter-less vector (PGL3-basic) (Fig. 4A). For *HERG1b*, the +85/+191 fragment demonstrated small but statistically significant luciferase activities. This fragment is contained within the 5'-UTR of the TSS1 variant but is in the proximal promoter region of the TSS2 isoform. Significant luciferase activity was obtained with a longer fragment (-60/+191), indicating that the basal promoter activity is contained in the very proximal 5'-flanking region (*i.e.* the first 60 bp upstream of TSS1). The maximum activity was reported by -250/+191, -390/+191 and -595/+191 constructs, suggesting that -250/+191 fragment contains the core promoter sequence of *HERG1b* (Fig. 4B).

KCNQ1a promoter constructs had approximately 10–15 times the activity of the promoterless vector (pGL3 basic) and 50% of the promoter activity of the pGL3 construct that contains both the SV40 promoter and enhancer (pGL3 control, data not shown). The overall transcription activities of different *KCNQ1a* promoter constructs were similar in all three cell lines and consistently, the -329/+60 fragment elicited the maximum promoter activities (Fig. 5A). The core promoter of the *KCNQ1a* gene was thus defined to -329/+60. For *KCNQ1b*, though a statistically significant luciferase activity was seen with a -117/+71 fragment relative to promoter-free PGL3-vector, more robust activities were consistently observed with longer fragments (Fig. 5B). For example, in both H9c2 and HEK293 cells, luciferase activities increased by around 15-fold with the vector containing -1336/+71 fragment of the *KCNQ1b* promoter.

1.3.5 Multiple Sp1 cis-elements and CpG islands in *HERG1* and *KCNQ1a* core promoter regions

Of particular note is the high GC content of the core promoter regions of *HERG1a*, *HERG1b* and *KCNQ1a*. The high GC content confers three important features to these genes. First, *HERG1a*, *HERG1b* and *KCNQ1a* all contain multiple Sp1 consensus sequences within their core promoter regions: -224, -366, -380 and -428 loci for *HERG1a* (Table 2), +118, +54, +26, -17 and -116 loci for *HERG1b* (relative to TSS1 in Fig. 4D), and -61, -114, -134, -190, -259, -277, -295, -347, -407, and -460 for *KCNQ1a*. By comparison, though there are seven putative Sp1 binding sites within 3-kb length of *KCNQ1b* 5'flanking region, only one site is proximal to its TSS (at position -15) and the other six sites are around 1-kb distal to its TSS. Strikingly, the positions of Sp1 clusters correspond well to the fragments that demonstrated significant promoter activities, as shown in Fig. 4 and Fig. 5. For example, the -487/+4 fragment that contains a cluster of four Sp1 sites in *HERG1a* showed the maximum promoter activity, and similar situations were seen with *HERG1b* and *KCNQ1a*. For *KCNQ1b*, the minimal promoter activity corresponded roughly to the presence of a single Sp1 site proximal to the TSS and the greatest promoter activity was coincident with the -1336/+71 fragment containing a cluster of three Sp1 elements.

The second feature of a GC-rich promoter is often the presence of so-called CpG islands [22,23], clusters of GC dinucleotides near the TSS. Using the CpG Island Searcher (**http://www.cpgislands.com**) [24], we made prediction of CpG islands in the promoter regions (500 bp upstream TSSs) of *HERG1a*, *HERG1b* and *KCNQ1a* and we identified two CpG islands in *HERG1a* and *KCNQ1a* and three in *HERG1b* (Fig. 6).

Another important feature associated with Sp1-rich promoters is the presence of GAGA boxes around the Sp1 elements [25,26]. We identified a total of seven GAGA boxes within 3-kb 5'-flanking region of *KCNQ1b*, among which four are in a cluster within the -1336/+71 fragment. By comparison, there is no GAGA box in the *KCNQ1a* 5'-flanking region, and there is only one in each *HERG1a* and *HERG1b* promoter regions.

1.3.6 Expression and tissue distribution of *HERG1* and *KCNQ1* genes

Expression of *HERG1* and *KCNQ1* genes was assessed from two aspects. First, the relative abundance of transcripts was determined by TaqMan real-time RT-PCR with RNA samples extracted from various human tissues. We found that the heart was the organ expressing an incomparably high level *HERG1a*; the mRNA level of *HERG1a* was found to be >100 times higher in heart than in other tissues except for brain where *HERG1a* mRNA levels was some 30% of the heart level (Fig. 7A). *HERG1b* transcripts were found to be most abundant in pancreas and colon, then in heart, kidney and lung (Fig. 7A). Surprisingly, the heart was one of the organs that express the lowest level of *KCNQ1a* (Fig. 7B); similar to *HERG1b*, *KCNQ1a* demonstrated the most abundant expression in pancreas, colon, kidney and lung. *KCNQ1b* predominantly expressed in heart and pancreas (Fig. 7B).

Second, we compared the relative abundance of transcripts across the four chambers of the human heart: left ventricle (LV), right ventricle (RV), left atrium (LA) and right atrium (RA). The results in Fig. 7C and 7D revealed that the four genes have a similar pattern of expression with significant interventricular and interatrial gradients of mRNA concentrations: RV>LV and RA>LA. And the regional differences of the four mRNAs were within the same range. There were no atrial-ventricular differences of expression.

1.4 Discussion

K^+ channels are represented by an extremely large and varied superfamily of genes including pore-forming α-subunits and regulatory auxiliary β-subunits. Many of these channels undergo remodeling processes, mostly with alteration in gene expression, during pathogenesis and disease progression. A number of K^+ channels have been investigated on their genomic structures, with their promoter regions identified and characterized. However, a majority of these studies were conducted with rat and mouse genes and the findings may or may not be applicable to human genes considering large interspecies variations in the 5'-flanking regions of genes. Research on promoter elements of human K^+ channel pore-forming α-subunits has been sparse despite that a recent report that described the transcriptional control of

several human KCNE genes (KCNE1-5) encoding a family of single-transmembrane-domain K^+ channel β-subunits that modulate the properties of several K^+ channel α-subunits [27]. *HERG1* and *KCNQ1* genes encode K^+ channel α-subunits that critically determine repolarization rate and repolarization reserve in cardiac cells thereby the likelihood of arrhythmias. Expression levels of these genes define the functional capacity of their gene products, I_{Kr} and I_{Ks}, which manifests in the course of early development of heart and during pathogenesis with dramatically altered gene expression. Elucidation of the promoter elements and transcriptional control of these genes is therefore a necessary step towards understanding the functional adaptation and impairment during developmental stages and pathological processes associated with electrical remodeling.

1.4.1 Transcriptional control of *HERG1* and *KCNQ1* genes

HERG1a and *HERG1b* have been believed to be alternatively splice variants of the same gene, so are *KCNQ1a* and *KCNQ1b* [3,4]. The present study does not support this notion; instead, our data suggest that they all represent independent transcripts because they each have their own transcription start sites and their own promoter regions.

Regulation of transcription is a complex set of events controlled by DNA sequences positioned in proximity to the genes (promoters) and by elements acting at a distance (enhancers). Promoters and enhancers that activate polymerase II transcribed mRNA genes are formed by a combinatorial puzzle of short sequences recognized by sequence-specific regulators.

One common feature of the promoter regions of *HERG1* and *KCNQ1* genes is GC rich; there exist multiple Sp1 consensus binding sites in the proximal promoter regions (>5 sites) of *HERG1a*, *HERG1b* and *KCNQ1a* genes and in the 5'-flanking region of *KCNQ1b*. Sp1 is a widely distributed member of a multigene family of zinc-finger transcription factors that bind DNA in mammalian cells primarily via interaction with GC-box elements [28-31]. The binding of Sp1 to GC-boxes is often critical to achieving significant levels of transcription from TATA-less promoters and is intimately involved in the determination of the transcription start site(s). Our previous studies have confirmed the role of Sp1 as a transactivator of *HERG1a* [21].

For *KCNQ1b*, there is one putative Sp1 site and one CCAAT box within its core promoter region, and there six more Sp1 sites and 4 more CCAAT boxes distal to the TSS within 3-kb frame of the 5'-flanking region. Protein binding to CCAAT boxes can activate gene transcription [32-34]. It is possible that the Sp1 and CCAAT within the promoter region cooperate to transactivate *KCNQ1b* and the distal Sp1 and CCAAT sites act as enhancers of *KCNQ1b* transcription. Our data therefore suggest that *HERG1* and *KCNQ1* genes are controlled by Sp1 for their transcription activation. Alternatively, the cluster of GAGA boxes, which exist only in *KCNQ1b* but not in *KCNQ1a* and *HERG1a/HERG1b*, may play a role in a positively cooperative way to enhance the as it has been documented that the GAGA factor acts as transcriptional coactivator/potentiator of Sp1 [25].

Another property of *HERG1a*, *HERG1b* and *KCNQ1a* promoters is the presence of CpG islands (clusters of CpG dinucleotides) near their TSSs. CpG islands often reside in the promoter region of genes, and the methylation of CpGs in these regions is thought to affect the expression of their downstream genes [22,23]. Whether the CpG islands play a role in regulating the activities of *HERG1a*, *HERG1b* and *KCNQ1a* promoters is worthy of detailed studies considering that the expression levels of these genes can have great impact on cardiac repolarization thereby the likelihood of arrhythmias.

1.4.2 Expression profiles of *HERG1* and *KCNQ1* genes

Consistent with the general lack of *cis*-elements for cardiac-specific transcription factors in the core promoter regions of *HERG1a/HERG1b* and *KCNQ1a/KCNQ1b* genes, the transcripts demonstrated widespread distribution across of a variety of human tissues. This could be explained by presence of multiple sites for ubiquitous Sp1 or of CCAAT box. Prominently, the ion channel gene promoters that have been identified to date, regardless of animal species from which they are from, share some general structural features common to the housekeeping-type promoters. That is, the promoters lack consensus TATA boxes and are GC-rich with multiple putative Sp1 consensus elements. However, it is also evident that there are clear tissue preferences of expression for each of the isoforms. For example, most of the transcripts were

found abundantly expressed in pancreas, heart, colon and lung, but rarely in skeletal muscle, liver and breast. Intriguingly, among the four transcripts, *HERG1a* and *KCNQ1b* were predominantly expressed in heart. This is in line with the fact that they both contain five putative *cis*-elements for the cardiac-specific transcription factor Hand2, while *HERG1b* and *KCNQ1a* do not.

Our study revealed regional differences or inter-chamber gradients of expression of *HERG1* and *KCNQ1* genes. Strikingly, all four isoforms demonstrated the same interventricular and interatrial gradients: RV>LV and RA>LA. The finding provides an explanation for the known interventricular gradients of I_{Ks} and I_{Kr} currents and of cardiac repolarization as well [35,36]. It has been well documented that the current densities of I_{Ks} and I_{Kr} both are larger in RV than in LV and accordingly, action potential duration (APD) is generally shorter in RV than in LV. This difference may be of physiological importance against arrhythmogenesis under normal conditions. However, when exacerbated under abnormal or pathological conditions, the repolarization heterogeneity becomes a substrate or prerequisite for arrhythmias to occur and to sustain (such as *torsade de pointes*). Our previous studies revealed that Sp1 level is higher in RV than in LV [37]. This may account for the interventricular gradients of *HERG1* and *KCNQ1* subunits. Future studies are required to clarify whether the interventricular inhomogeneity of expressions of these genes contributes to arrhythmogenesis.

It should be noted that the roles of *HERG1b* and *KCNQ1b* in forming I_{Kr} and I_{Ks} and their exact relationships to *HERG1a* and *KCNQ1a*, respectively, are to be better defined. It has been claimed that the cardiac I_{Kr} channels minimally comprise HERG1a and HERG1b subunits, implying that HERG1b co-assemble with HERG1a to form the complete HERG channels [2,5]. Based on the available data, KCNQ1b is a negative dominant isoform that co-assembles with KCNQ1a to dampen the function of the latter [8-10]. Based on these available data, the present study would suggest that the same mechanisms of transactivation between *HERG1a* and *HERG1b* should produce a positively cooperative effect on I_{Kr} function, whereas the same mechanisms of transactivation between *KCNQ1a* and *KCNQ1b* should produce a negative feedback effect on I_{Ks} function, at the gene transcription level.

In summary, we have identified the core promoter regions and the transcription start sites of *HERG1a*, *HERG1b*, *KCNQ1a* and *KCNQ1b* genes. We compared relative expression patterns of these genes across a variety of human tissues and demonstrated unexpectedly widespread tissue distributions of all the transcripts in addition to heart where the genes were originally cloned. Our data further revealed that the mRNA levels of all *HERG1* and *KCNQ1* isoforms are asymmetrically distributed within the heart, being predominant in the right chambers relative to the left ones. This finding may help us understand the molecular mechanisms for arrhythmogenesis since heterogeneity of ion channel activities is an important substrate for arrhythmia to occur. Our study therefore provides highly valuable knowledge of core elements related to transcriptional regulation and identifies targets for studies of genetic variants in diseases associated with the *HERG1* and *KCNQ1* genes.

1.5 Materials and methods

1.5.1 Rapid amplification of cDNA ends (5'RACE)

The transcription start sites (TSSs) of *HERG1b*, *KCNQ1a* and *KCNQ1b* genes were determined with Ambion's RNA–Ready cDNA Human Heart RNA ligase-mediated 5'RACE kit, as previously described [21]. Human ventricular RNA sample was purchased from Clontech. The gene specific primers (GSP) were designed based on the human *HERG1b* sequence (Genbank accession: NM_172057) and the GSP1 was 5'-CTTCCGTCTCCTTCAGCAGG-3' and the GSP2 (nested) was 5'-ATGCAGGATGGTCCAGCGGT-3', corresponding to 597-616 bp and 491-510 bp, respectively. For *KCNQ1a* (GenBank accession: NM_000218), the primers used for 5'RACE were GSP1: 5'-AGGAAGACGGCGAAGTGGTA-3' and GSP2: 5'-CGCGTGCTGTAGATGGAGAC-3'. *For KCNQ1b* (GenBank accession: NM_181798.1), The GSP1 was ACGTACTCCGTCCCGAAGAA and GSP2 was CACGATGAGGTCGATGATGG.

1.5.2 RNase protection assay (RPA)

To determine the exact TSSs of the *HERG1* genes, we hybridized 30 μg of total RNA from human hearts (Clontech) with a human genomic antisense riboprobes in a

solution hybridization/RNase protection assay [21,38]. For *HERG1b*, a human genomic antisense riboprobe (1000 bp) corresponding to the down stream 900 bp of intron 5 and upper stream 100 bp of exon 6 of the *HERG1* genomic sequence (NM_172057) was used. The fragment was PCR synthesized and cloned to pGEMT easy vector for preparation of RNA probes. RNA probes were synthesized using *in vitro* transcription kits (Ambion). RNase protection assays (RPAs) were performed according to the HybSpeed™ RPA (Ambion) protocols. Yeast tRNA (20 μg) was used as a negative control to test for the presence of probe self-protection bands.

1.5.3 PCR amplification of putative promoter regions and construction of promoter-luciferase fusion plasmids

A series of fragments of varying length including the TSSs of *HERG1* and *KCNQ1* promoters were amplified with human genomic DNA the Homo Sapiens bacterial artificial chromosome (BAC) clone RP11-166D23 (accession No. AC011234) for *HERG1* and RP5-915F1 (accession No. AC124057) for *KCNQ1* genes as templates using specific primers and PCR Advantage and Advantage-GC genomic polymerase mixes (Clontech K-1905-Y). PCR products were subcloned into luciferase-containing PGL3-Basic (Promega) vector. The integrity and orientation of all constructs were confirmed by restriction endonuclease analysis and DNA sequencing.

1.5.4 Cell culture

The cell lines used in this study were all purchased from American Type Culture Collection (ATCC, Manassas, VA). H9c2 (rat ventricular cell line) and HEK293 (human embryonic kidney cell line) were cultured in Dulbecco's Modified Eagle Medium (DMEM).[17] SKBr3 (human breast cancer cell line) cells were maintained in McCoy's 5A Modified Medium and LNCaP (human prostate cancer cell line) in RPMI 1640 medium. The cultures were all supplemented with 10% fetal bovine serum and 100 μg/ml penicillin/streptomycin. The non-cardiac cell lines were used to serve as comparison for H9c2 cardiac cells. SKBr3 has been shown to express endogenous HERG1 proteins [17], and HEK293 and LNCaP do not express functional HERG1 proteins [39].

1.5.5 Transfection and luciferase assay

Cells (1 x 10^5/well) were transfected with 1 μg PGL3–target DNA (firefly luciferase vector) and 0.1 μg PRL-TK (TK-driven Renilla luciferase expression vector) with lipofectamine 2000 (Invitrogen). Following transfection (48 h), luciferase activities were measured with a dual luciferase reporter assay kit (Promega) on a luminometer (Lumat LB9507) [21,37].

1.5.6 Real-time RT-PCR

The mRNA samples from various human tissues were purchased from Ambion. TaqMan quantitative assay of transcripts was performed with real-time two-step reverse transcription PCR (GeneAmp 5700, PE Biosystems), involving an initial reverse transcription with random primers and subsequent PCR amplification of the targets [21,37]. Master RT reaction mix 50 μl (containing 10× reverse transcription buffer 10 μl, 25× dNTPs 4 μl, 10× random primers 10 μl, MultiScribe™ Reverse Transcriptase (50 U/μl) 5 μl, and nuclease-free H_2O 21 μl) and 50 μl of RNA sample (10 μg) were mixed into a PCR reaction tube. The reaction was carried out at 25°C for 10 min and 37°C for 120 min to obtain the first strand cDNAs. Master PCR reaction mix 23 μl (including 2× TaqMan universal PCR master mix 12.5 μl, 20× assay mix 0.63 μl, H_2O 9.9 μl) and 2 μl of the first strand cDNA sample were pipetted into 96-well plate and centrifuged at 2000 rpm for 2 min at 4°C. The amplification reaction was set as follow: 50°C for 2 min and 95°C for 10 min, followed by 15 s at 95°C and 1 min at 60°C for 40 cycles. Human GAPDH control reagents (Applied Biosystems) were used as internal controls. We used the comparative cycling method (ΔC) to quantify the level of target transcripts (GeneAmp 5700 sequence detection system). ΔC values were calculated as: $\Delta C = C_{\text{Target}} - C_{\text{GAPDH}}$ and $\Delta\Delta C = \Delta C_{\text{Drug}} - \Delta C_{\text{NC}}$, where C indicates the number of cycles for amplification of target transcripts (C_{Target}) or GAPDH (C_{GAPDH}), ΔC_{Drug} represents the ΔC obtained from RNA samples treated with drugs the ΔC from RNA samples without drug treatment. Finally, the amount of target transcription, normalized to an endogenous reference GAPDH and relative to control, was calculated by $2^{-\Delta\Delta C}$.

1.5.7 Data analysis

Group data are expressed as mean ± S.E. Statistical comparisons (performed using ANOVA followed by Dunnett's method) were carried out using Microsoft

Excel. A two-tailed $p<0.05$ was taken to indicate a statistically significant difference. Nonlinear least square curve fitting was performed with CLAMPFIT in pCLAMP 8.0 or GraphPad Prism. *Cis*-elements for transcription factor binding sites were analyzed with *MatInspector* V2.2.

1.6 Acknowledgements

The authors thank XiaoFan Yang for excellent technical support. This work was supported in part by the National Sciences and Engineering Research Council of Canada and Fonds de la Recherche de l'Institut de Cardiologie de Montreal, awarded to Dr. Z Wang. Dr. Z. Wang is a senior research scholar of the Fonds de Recherche en Sante de Quebec.

1.7 References

[1] Sanguinetti MC, Jiang C, Curran ME, Keating MT. A mechanistic link between an inherited and an acquired cardiac arrhythmia: *HERG* encodes the I_{Kr} potassium channel. *Cell.* 1995;81:299–307.

[2] London B, Trudeau MC, Newton KP, Beyer AK, Copeland NG, Gilbert DJ, Jenkins NA, Satler CA, Robertson GA. Two isoforms of the mouse *ether-a-go-go*-related gene coassemble to form channels with properties similar to the rapidly activating component of the cardiac delayed rectifier K^+ current. *Circ Res.* 1997;81:870–878.

[3] Lees-Miller JP, Kondo C, Wang L, Duff HJ. Electrophysiological characterization of an alternatively processed ERG K^+ channel in mouse and human hearts. *Circ Res.* 1997;81:719–726.

[4] Crociani O, Guasti L, Balzi M, Becchetti A, Wanke E, Olivotto M, Wymore RS, Arcangeli A. Cell cycle-dependent expression of HERG1 and HERG1B isoforms in tumor cells. *J Biol Chem.* 2003;278:2947–2955.

[5] Jones EM, Roti Roti EC, Wang J, Delfosse SA, Robertson GA. Cardiac I_{Kr} channels minimally comprise hERG 1a and 1b subunits. *J Biol Chem.* 2004;279:44690–44694.

[6] Robertson GA, Jones EM, Wang J. Gating and assembly of heteromeric hERG1a/1b channels underlying I_{Kr} in the heart. *Novartis Found Symp.* 2005;266:4–15.

[7] Sanguinetti MC, Curran ME, Zou A, Shen J, Spector PS, Atkinson DL, Keating MT. Coassembly of K_VLQT1 and minK (IsK) proteins to form cardiac I_{Ks} potassium channel. *Nature.* 1996;384:80–83.

[8] Demolombe S, Baro I, Pereon Y, Bliek J, Mohammad-Panah R, Pollard H, Morid S, Mannens M, Wilde A, Barhanin J, Charpentier F, and Escande D. A dominant negative isoform of the long QT syndrome 1 gene product. *J Biol Chem* 1998;273:6837–6843.

[9] Pereon Y, Demolombe S, Baro I, Drouin E, Charpentier F, and Escande D. Differential expression of KvLQT1 isoforms across the human ventricular wall. *Am J Physiol.* 2000;278:H1908–H1915.

[10] Demolombe S, Lande G, Charpentier F, van Roon MA, van den Hoff MJ, Toumaniantz G, Baro I, Guihard G, Le Berre N, Corbier A, de Bakker J, Opthof T, Wilde A, Moorman AF, Escande D. Transgenic mice overexpressing human KvLQT1 dominant-negative isoform. Part I: Phenotypic characterization. *Cardiovasc Res.* 2001;50:314–27.

[11] Wang L, Duff HJ. Identification and characteristics of delayed rectifier K^+ currents in fetal mouse ventricular myocytes. *Am J Physiol.* 1996;270:H2088–H2093.

[12] Wang L, Feng Z-P, Kondo CS, Sheldon RS, Duff HJ. Developmental changes in the delayed rectifier K^+ channels in mouse heart. *Circ Res.* 1996;79:79–85.

[13] Yang T, Snyders DJ, Roden DM. Rapid inactivation determines the rectification and $[K^+]_o$ dependence of the rapid component of the delayed rectifier K^+ current in cardiac cells. *Circ Res.* 1997;80:782–789.

[14] Claycomb WC, Lanson NA Jr, Stallworth BS, Egeland DB, Delcarpio JB, Bahinski A, Izzo N J Jr. HL-1 cells: a cardiac muscle cell line that contracts and retains phenotypic characteristics of the adult cardiomyocyte. *Proc Natl Acad Sci USA.* 1998;95:2979–2984.

[15] Arcangeli A, Rosati B, Cherubini A, Crociani O, Fontana L, Ziller C, Wanke E, Olivotto M. HERG- and IRK-like inward rectifier currents are sequentially expressed during neuronal development of neural crest cells and their derivatives. *Eur J Neurosci.* 1997;9:2596–2604.

[16] Bianchi L, Wible B, Arcangeli A, Taglialatela M, Morra F, Castaldo P, Crociani O, Rosati B, Faravelli L, Olivotto M, Wanke E. HERG encodes a K^+ current highly conserved in tumors of different histogenesis: a selective advantage for cancer cells? *Cancer Res.* 1998;58:815–822.

[17] Wang H, Zhang Y, Cao L, Han H, Wang J, Yang B, Nattel S, Wang Z. HERG K^+ channel: A regulator of tumor cell apoptosis and proliferation. *Cancer Res.* 2002;62:4843–4848.

[18] Wang Z. Roles of K^+ channels in regulating tumor cell proliferation and apoptosis. *Pflügers Arch.* 2004;448:274–286.

[19] Arcangeli A. Expression and role of hERG channels in cancer cells. *Novartis Found Symp.* 2005;266:225–232.

[20] Conti M. Targeting K^+ channels for cancer therapy. *J Exp Ther Oncol.* 2004;4:161–166.

[21] Lin H, Xiao J, Luo X, Xu C, Gao H, Wang H, Yang B, Wang Z. Overexpression HERG K^+ channel gene mediates cell-growth signals on activation of oncoproteins Sp1 and NF-κB and inactivation of tumor suppressor Nkx3.1. *J Cell Physiol.* 2007;(in press).

[22] Teodoridis JM, Strathdee G, Brown R. Epigenetic silencing mediated by CpG island methylation: potential as a therapeutic target and as a biomarker. *Drug Resistance Updates* 2004;7:267–278.

[23] Yamashitaa R, Suzukic Y, Suganoc S, Nakai K. Genome-wide analysis reveals strong correlation between CpG islands with nearby transcription start sites of genes and their tissue specificity. *Gene* 2005;350:129–136.

[24] Takai D, Jones PA. Comprehensive analysis of CpG islands in human chromosomes 21 and 22. *Proc Natl Acad Sci USA.* 2002;99:3740–3745.

[25] Bevilacqua A, Fiorenza MT, Mangia F. A developmentally regulated GAGA box-binding factor and Sp1 are required for transcription of the hsp70.1 gene

at the onset of mouse zygotic genome activation. *Development* 2000;127:1541–1551.

[26] Wyse BD, Linas SL, Thekkumkara TJ. Functional role of a novel cis-acting element (GAGA box) in human type-1 angiotensin II receptor gene transcription. *J Mol Endocrinol.* 2000;25:97–108.

[27] Lundquist AL, Turner CL, Ballester LY, George Jr AL. Expression and transcriptional control of human KCNE genes. *Genomics*. 2006;87:119–128.

[28] Black AR, Black JD, Azizkhan-Clifford J. Sp1 and kruppel-like factor family of transcription factors in cell growth regulation and cancer. *J Cell Physiol.* 2001;188:143–160.

[29] Samson SL, Wong NC. Role of Sp1 in insulin regulation of gene expression. *J Mol Endocrinol.* 2002;29:265–279.

[30] Pugh BF, Tjian R. Mechanism of transcriptional activation by Sp1: evidence for coactivators. *Cell.* 1990;61:1187–1197.

[31] Kadonaga JT, Courey AJ, Ladika J, Tjian R. Distinct regions of Sp1 modulate DNA binding and transcriptional activation. *Science.* 1988;242:1566–1570.

[32] Morgan WD, Williams GT, Morimoto RI, Greene J, Kingston RE, Tjian R. Two transcriptional activators, CCAAT-box-binding transcription factor and heat shock transcription factor, interact with a human hsp70 gene promoter. *Mol Cell Biol.* 1987;7:1129–1138.

[33] Yagi H, Kato T, Nagata T, Habu T, Nozaki M, Matsushiro A, Nishimune Y, Morita T. Regulation of the mouse histone H2A.X gene promoter by the transcription factor E2F and CCAAT binding protein. *J Biol Chem.* 1995;270:18759–18765.

[34] Jump DB, Badin MV, Thelen A. The CCAAT box binding factor, NF-Y, is required for thyroid hormone regulation of rat liver S14 gene transcription. *J Biol Chem.* 1997;272:27778–27786.

[35] Volders PG, Sipido KR, Carmeliet E, Spatjens RL, Wellens HJ, Vos MA. Repolarizing K^+ currents I_{TO1} and I_{Ks} are larger in right than left canine ventricular midmyocardium. *Circulation* 1999;99:206–210.

[36] Ramakers C, Vos MA, Doevendans PA, Schoenmakers M, Wu YS, Scicchitano S, Iodice A, Thomas GP, Antzelevitch C, Dumaine R. Coordinated down-regulation of KCNQ1 and KCNE1 expression contributes to reduction of I_{Ks} in canine hypertrophied hearts. *Cardiovasc Res.* 2003;57:486–496.

[37] Luo X, Lin H, Lu Y, Li B, Xiao J, Yang B, Wang Z. Transcriptional activation by stimulating protein 1 and post-transcriptional repression by muscle-specific microRNAs of I_{Ks}-encoding genes and potential implications in regional heterogeneity of their expressions. *J Cell Physiol.* 2007 Aug;212(2):358-67.

[38] Yue L, Wang Z, Rindt H, Nattel S. Molecular evidence for a role of Shaw (Kv3) potassium channel subunits in potassium currents of dog atrium. *J Physiol.* 2000;527:467–478.

[39] Wang Z. Roles of K^+ channels in regulating tumor cell proliferation and apoptosis. *Pflügers Arch.* 2004;448:274–286.

1.8 Figures and Figure Legends

Figure 1. Identification of transcription start sites of *HERG1* and *KCNQ1* genes. Shown are the 5'-flanking regions containing the core promoter sequences of the *HERG1a* (**A**, Genbank accession No.: DQ120124), *HERG1b* (**B**, Genbank accession No.: DQ120125), *KCNQ1a* (**C**, Genbank accession No.: EF010934), and *KCNQ1b* (**D**, Genbank accession No.: EF010935) genes. Transcription start sites (TSSs) are indicated by backward arrows and designated position +1. The consensus binding sequences for Sp1 transcription factor (TF) or other TFs are underlined and the core sequences of the Sp1 *cis*-elements or other elements are bold. For convenience, the positions of consensus sites are indicated by the numbers within the brackets, which were counted by the first nucleotides of the consensus core sequences relative to TSS (+1).

Figure 2. Genomic structure of *HERG* gene subfamily. (**A**) The genomic arrangements of *HERG* gene subfamily members including *HERG1a*, *HERG1b*, *HERG2* and *HERG3* are aligned against the *HERG* genomic DNA. The first seven exons and introns in the *HERG* genomic DNA are labeled by arrows and numbers. (**B**) Schematic illustration of the relationships between the promoter regions (dashed lines) of *HERG1a* and *HERG1b* and the *HERG* genomic DNA.

Figure 3. Genomic structure of *KCNQ1* gene subfamily. Schematic illustration of the genomic arrangements of *KCNQ1* gene subfamily members *KCNQ1a* and *KCNQ1b* are aligned against the *KCNQ1* genomic DNA, showing the relationships between the promoter regions (dashed lines) of *KCNQ1a* and *KCNQ1b* and the *KCNQ* genomic DNA. Note that the TSS (transcription start site) and exon 1 of *KCNQ1b* falls into the intron 1 of *KCNQ1a*.

Figure 4. Analysis of the *HERG1a* (**A**) and *HERG1b* (**B**) promoter activities in various cell lines including H9c2 rat ventricular cells, LNCaP human prostate cancer cells, and HEK293 human embryonic kidney cells. A schematic representation of the 5' deletion constructs of the *HERG1a* or

HERG1b promoter region is shown in the left panels. Nucleotides of fusion plasmids are numbered with respect to the TSS (+1) identified by 5'RACE. Firefly luciferase expression levels were divided by co-expressed Renilla luciferase activity and expressed as relative activity divided by the promoter-less construct (PGL3-Basic). The experiments were performed in duplicate for each experiment and the number (n) of experiments is indicated by the values within the brackets.

Figure 5. Analysis of the *KCNQ1a* (**A**) and *KCNQ1b* (**B**) promoter activities in H9c2 rat ventricular cell line and HEK293 human kidney embryonic cell line. A schematic representation of the 5' deletion constructs of the *KCNQ1a* or *KCNQ1b* promoter region is shown in the left panels. Nucleotides of fusion plasmids are numbered with respect to the TSS (+1) identified by 5'RACE. Firefly luciferase expression levels were divided by co-expressed Renilla luciferase activity and expressed as relative activity divided by the promoter-less construct (PGL3-Basic). The experiments were performed in duplicate for each experiment and the number (n) of experiments is indicated by the values within the brackets.

Figure 6. CpG islands of *HERG1* and *KCNQ1* genes predicted using the CpG Island Searcher (**http://www.cpgislands.com**) [24]. The criteria for inclusion as CpG islands were %GC=55, observed CpG/ expected CpG (obsCpG/expCpG)=0.65, nucleotide length=200 bp. Xxx. For *HERG1a*, CpG island 1: %GC=67.3, obsCpG/expCpG=0.655, length=150; CpG island 2: %GC=74.4, obsCpG/expCpG=0.878, length=907. For *HERG1b*, CpG island 1: %GC=67.6, obsCpG/expCpG=0.924, length=855; CpG island 2: %GC=60.4, obsCpG/expCpG=0.652, length=268; CpG island 3: %GC=78.2, obsCpG/expCpG=0.654, length=238. For *KCNQ1a*, CpG island 1: %GC=59.7, obsCpG/expCpG=0.708, length=647; CpG island 2: %GC=74.2, obsCpG/expCpG=0.796, length=399. Note there are no CpG islands in 5'-flanking region of *KCNQ1b* gene.

Figure 7. Distribution of *HERG1* and *KCNQ1* transcripts in human tissues and regional differences of expression in the heart. (**A**) and (**B**) Relative

levels of *HERG1a/HERG1b* and *KCNQ1a/KCNQ1b* mRNAs, respectively, in various tissues indicated, showing the tissue distribution of the transcripts. The concentrations of mRNAs were determined by quantitative real-time RT-PCR. The data were normalized to the value in skeletal muscle. The mRNA levels in heart represent averaged concentrations of four different chambers: left ventricle (LV), right ventricle (RV), left atrium (LA) and right atrium (RA). (**C**) and (**D**) Relative levels of *HERG1a/HERG1b* and *KCNQ1a/KCNQ1b* mRNAs, respectively, in four different chambers of the heart, showing the regional difference of expression in the heart. *$p<0.05$ *vs.* LV or LA; +$p<0.05$ *vs.* *HERG1a* or *KCNQ1a.*

Figure 1

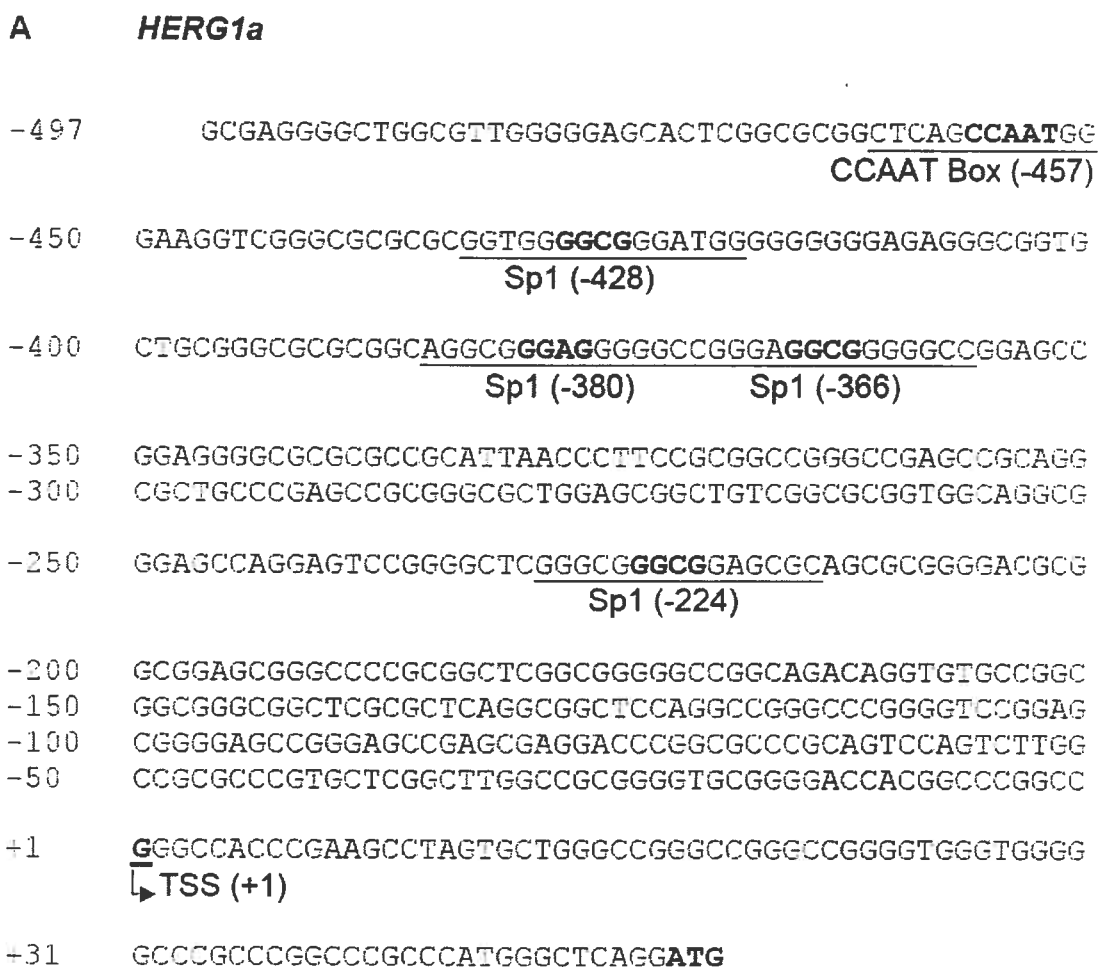
A
HERG1a
-497
GCGAGGGGCTGGCGTTGGGGGAGCACTCGGCGCGGCTCAGCCAATGG
CCAAT Box (-457)
-450
GAAGGTCGGGCGCGCGCGGTGGGGCGGATGGGGGGGGGAGAGGGCGGTG
Sp1 (-428)
-400
CTGCGGGCGCGCGGCAGGCGGGAGGGGGCCGGGAGGCGGGGGCCGGAGCC
Sp1 (-380)
Sp1 (-366)
-350
GGAGGGGCGCGCGCCGCATTAACCCTTCCGCGGCCGGGCCGAGCCGCAGG
-300
CGCTGCCCGAGCCGCGGGCGCTGGAGCGGCTGTCGGCGCGGTGGCAGGCG
-250
GGAGCCAGGAGTCCGGGGCTCGGGCGGGCGGAGCGCAGCGCGGGGACGCG
Sp1 (-224)
-200
GCGGAGCGGGCCCCGCGGCTCGGCGGGGGCCGGCAGACAGGTGTGCCGGC
-150
GGCGGGCGGCTCGCGCTCAGGCGGCTCCAGGCCGGGCCCGGGGTCCGGAG
-100
CGGGGAGCCGGGAGCCGAGCGAGGACCCGGCGCCCGCAGTCCAGTCTTGG
-50
CCGCGCCCGTGCTCGGCTTGGCCGCGGGGTGCGGGGACCACGGCCCGGCC
+1
GGGCCACCCGAAGCCTAGTGCTGGGCCGGGCCGGGCCGGGGTGGGTGGGG
TSS (+1)
+31
GCCCGCCCGGCCCGCCCATGGGCTCAGGATG

B ***HERG1b***

-300 CCACCTGAGCCCCTGGCATCTGCCCTGCTCCTGTGCCCGCTGCATGTGCC
-250 CGTGAGTTGCGGTGGGTCTGTGCATGTGCGCCTGTATGTGTCGGCAGGCG
-200 TGTGTGTTCCTGCCAGTCACTAGCAGTCTCTCCATCTCTGGGTGTCTCTG

-150 TCTGACTCTGGCTGGCTCAGCACTGGACCGGCTG**GGCG**GGGGTGTCAGGG
Sp1 (-116)

-100 AGACCATTAATCTGCGGTGACAGGCCCGGCTGCTGGCGGAGGGGGAGGGG

-50 CTCAGGCTGCGGGAGCGCCGCTGCAGGAGCCTG**GGCG**GGCTGCGGGGGAG
Sp1 (-17)

+1 **G**GGGCCGCTGGCTGGGCACCGGCGG**GGCG**GGGGAGCCTAGTGTGGCGGGG
TSS1 (+1) Sp1 (+26)

+51 TGGG**GGTG**GGGACCTGGTAGAAGGAGGGGCCGGCTGGAGGAGCTGAGGTT
Sp1 (+54)

+101 CCGAGT**G**CGGCCGCTGCTGGGCTGGCG**GGCG**GGCAGAGCACGGCACCCTG
TSS2 (+107) Sp1 (+118)

+151 GCAGCAGGGCCCACGCCACGGGGCCATGGGCAGCTCGAGCCAGGCAGGCT
+201 GCTGCCCACGCTTACTGCCAGGGTGACCCCAGCCCTGGGGCCCAGCCACA
+251 ACCACCCTGGCTTCATGCCAGGGGCTGCTCTGGTTGCCAGTCGGCCAGCC
+301 TCGGGGGTGCAGCCTGGGCTGGGACTGCTGCTGGGGTGCAGGTGAGGCAG
+351 TGGCCGGGCCCTCAGGCCCCAGGGCAGGCAGGCTGCAGGGAGCCAAGTCC

+401 TCC**ATG**

C ***KCNQ1a***

-538 AGGCAGAGCAGGCGGGCATCAGAAGTGGGGGCCAAGCAGGTGGGTGAGGG

-488 CAGGGCAGGAGCAAGCAGGGGAGATGCAGACGG**GGCG**GGGCCAAGCAGGT
Sp1 (-460)

-438 GGGTGAGGGCGGGGCCAAGCAGGTGGGCGGGGAGGG**GGCG**GGGCCAGGCG
Sp1 (-407)

-388 GGGTAAATGCACACTGGAACGGGGCCAAACAGGTGGGCGAGGAGGG**GGCG**
Sp1 (-347)

-338 GGGCCAAGCGGGATAGATGACACGAGCGGGGCTAAGCAGGTGGGCTC**GGG**
Sp1 (-295)

-288 **CG**GGGGGTGGGGGTGGG**GGCG**GGGGCGCAGGCGGG**GGCG**GGGGCGCGGACA
Sp1 (-277) Sp1 (-259)

-238 GGCCAAGCCAGGGGGTGAGGCGGAGGCAGGGCCAGGCCGGTCCGTGGGGA

-188 GAG**GGCG**GGCCAAGCCGGTGGGCGCGGGCAGGGACGCCCTGTGCGCGCCG
Sp1 (-190)

-138 GACCGGCGGG**GGCG**GGGCGTGCAGGCGGG**GGCG**GGGCACGCCGTCCCATG
Sp1 (-134) Sp1 (-114)

-88 GGACCGGCCCTCGGCCACTGCCCCCTCCGGCCC**CGCC**CCGAGCGCCCGGG
Sp1 (-61)

-38 CTGGGCCGGCAGCGGCCCCCCGCGGCGGGGCTGGCAGC**A**GTGGCTGCCC**G**
TSS1 (+1) TSS2

+13 CACTGCGCCCGGGCGCTCGCCTTCGCTGCAGCTCCCGGTGCCGCCGCTCG

+63 GGCCGGCCCCCCGGCAGGCCCTCCTCGTT**ATG**

D ***KCNQ1b***

-1336 GAGTCCTTGCTT
-1324 GCAGTGCCCATGGGCAGCAGAGGTGTCCGGAGATGCAACAGGGCCCAGAC

-1274 CCCTACCAGCCTGTGGCCCAGCTGG**GGGC**AGGACTCCG**GGGC**AGGGTGAG
Sp1 (-1249) Sp1 (-1236)

-1224 TCCCTGCGTGACCTGATTCTCTGTGGGCAGGCCGGGCAGGGTGGCTGCAG

-1174 **GGC**GGCGGAGCCTGTGCTGCTGGCCTGCATTTCTCTGGCTGGACAGATAC
Sp1 (-1175)

-1124 TGCGCCCATATCCCTGGTCTTTCAAAGGGCTCTGTGGCTGGTGGAGGGCA
-1074 GCAATGCCCCAAGGGAGGAGCAGGTGCCCAAGCCCCCAGGTGGCCCTGCG
-1024 GGTACAGGTACTTGTTTACTCTGTGGCATCAGTCCTGCTTCCCAGCTCAA

-974 GGCCCTGGCCTCCACAGGCCTCCTCCCTCC**CTCCCTCCCTCCCTCC**TTCC
GAGA Boxes (-928~-944)

-924 CTTTTTTCCTGTGGCTCCAAGGCCCACAGTAGAAAGGCTCCAGTCTGTGT
-874 TCGGTGTCCGACCTGGTGATGGGTCAGGTGTGATCAGGTGTGTGGGGCTC

-824 GGTCTGCATGTGCAGGGCTGTTTGAAGGCCTGT**GGGG**CCATCTGATGCCC
Ap2 (-191)

-174 CCCTTTTCTTCAGCCTTGGAGAGGATGGCTTCTCAGGCCGCCTCGCAGCA
-124 GATTTGTAGTCTGGTTGCTGTCGTTCCTGAAATAGCCTCTGAAGCTCTGT

-74 CCGGGAAGGGAACCTTGAGTGTGGAGGAGATAAGCCTGCTG**ACTGG**GTGA
CCAAT Box (-33)

-24 GCCGGCCGG**GGCG**GGGGTGGCCCC**T**CTTCCCTTCCTCCCCTGCAGCTTCC
Sp1 (-15) TSS (+1)

-27 ATGGCCT**GGGG**CTGTGAGAGGCCCGGGAAGGCACTGTCTTTGCGCCTGCA
Ap2 (+34)

-77 CATGTGTGTGTCTGGAGTGTAGGATGGCACTGGTGCCGGGCCTGGATTTA

-127 **CTCA**GCCCAGATCACGGCTGCTTTTGTTTACGTGGCCCCTGCTCTCAGTC
Ap1 (+127)

-177 ACAACTCCAGGTTTCTGGCTCTCGGGAATTTGAGGCCTGTGGCTGCTGTG

-237 GACCCTGGGAAAGAGCCTGTGCTTCCTGAGCCAGTGCGGGGCCTGGC**ATG**

Figure 2

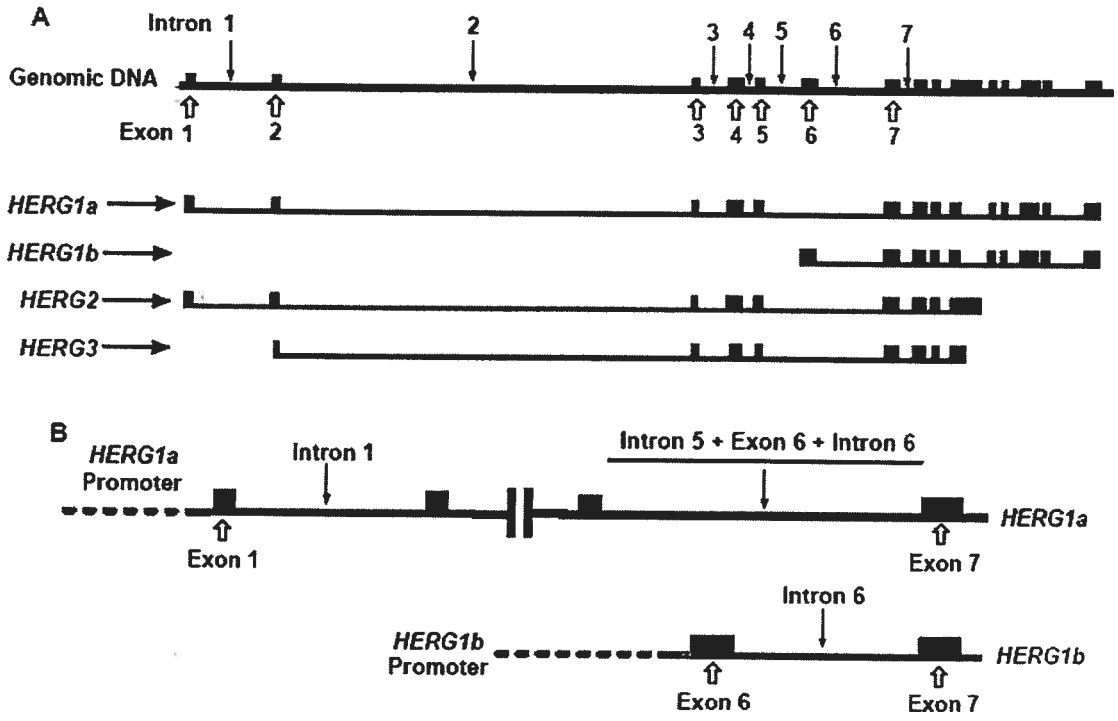
A
Intron 1
2
3 4 5 6 7
Genomic DNA
Exon 1 2 3 4 5 6 7
HERG1a
HERG1b
HERG2
HERG3
B
HERG1a Promoter
Intron 1
Intron 5 + Exon 6 + Intron 6
HERG1a
Exon 1
Exon 7
Intron 6
HERG1b Promoter
HERG1b
Exon 6
Exon 7

Figure 3

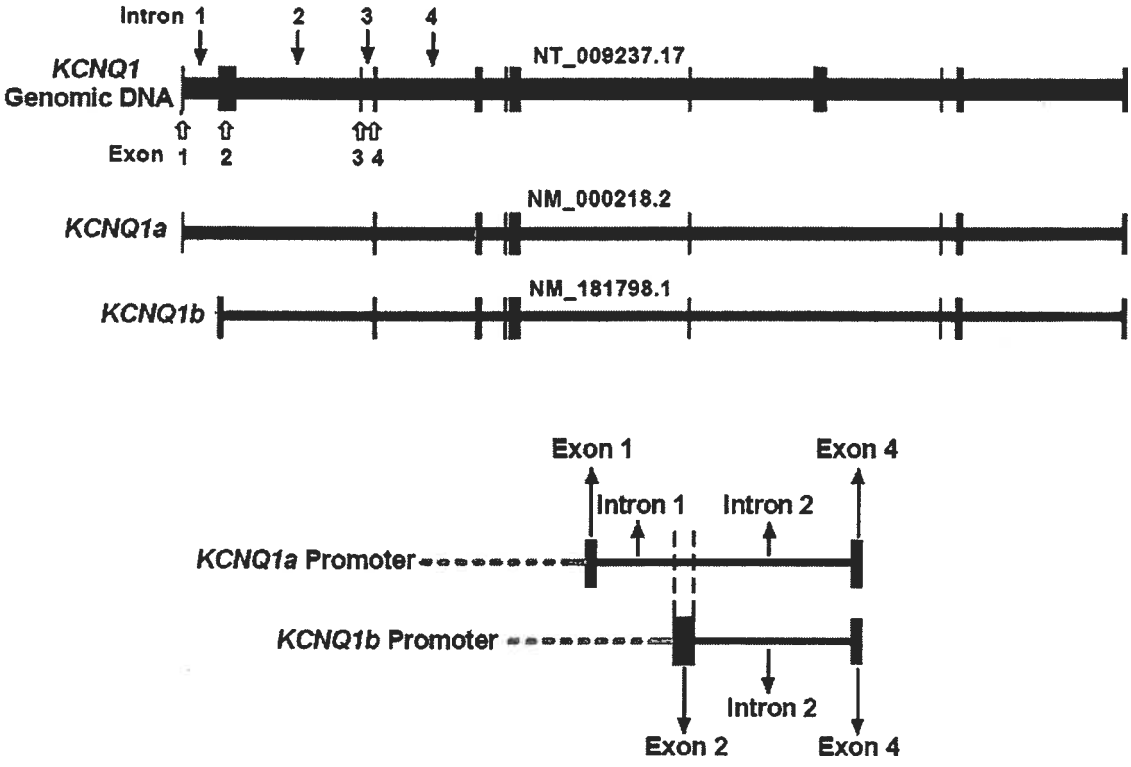
Intron 1
2
3
4
KCNQ1
Genomic DNA
NT_009237.17
Exon 1 2 3 4
KCNQ1a
NM_000218.2
KCNQ1b
NM_181798.1
Exon 1
Exon 4
Intron 1
Intron 2
KCNQ1a Promoter
KCNQ1b Promoter
Intron 2
Exon 2
Exon 4

Figure 4

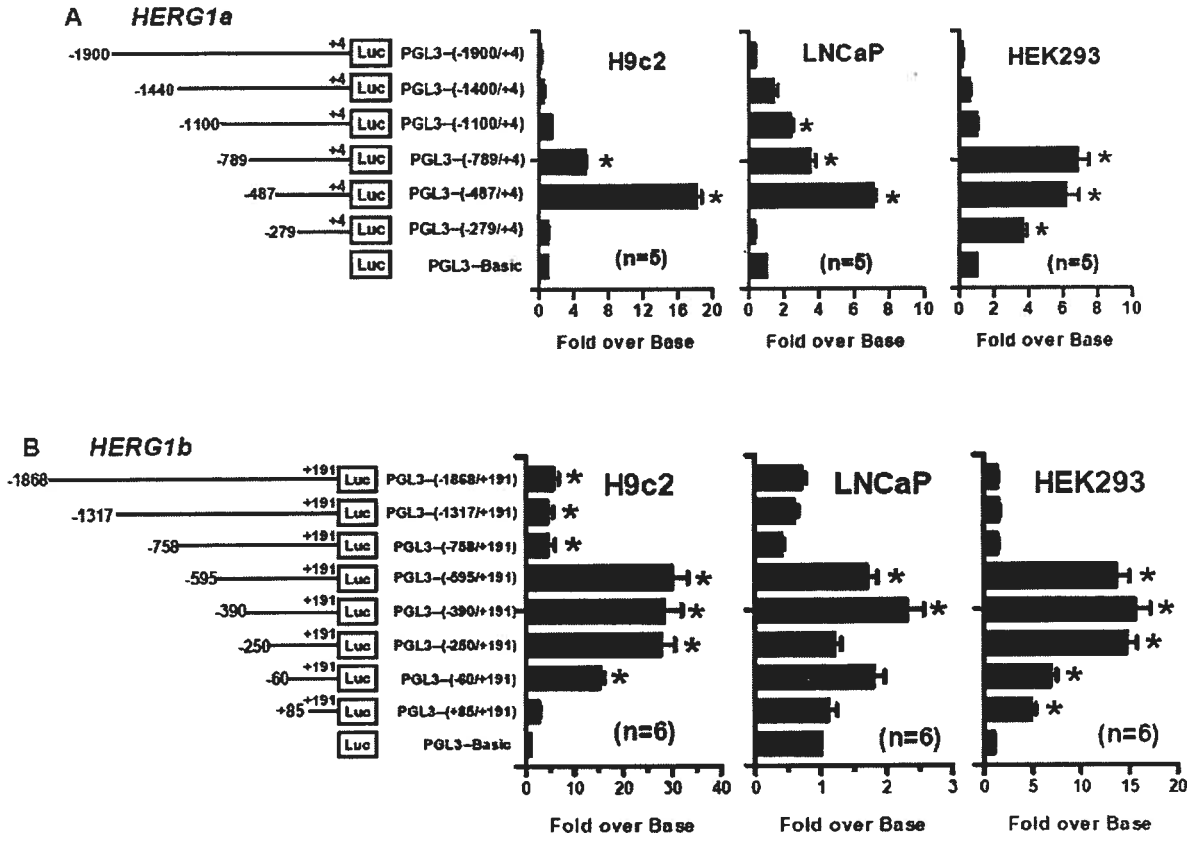
A HERG1a
-1900 +4 Luc PGL3-(-1900/+4)
-1440 +4 Luc PGL3-(-1440/+4)
-1100 +4 Luc PGL3-(-1100/+4)
-789 +4 Luc PGL3-(-789/+4)
-487 +4 Luc PGL3-(-487/+4)
-279 +4 Luc PGL3-(-279/+4)
Luc PGL3-Basic
H9c2
LNCaP
HEK293
(n=5)
(n=5)
(n=5)
0 4 8 12 16 20
0 2 4 6 8 10
0 2 4 6 8 10
Fold over Base
Fold over Base
Fold over Base
B HERG1b
-1868 +191 Luc PGL3-(-1868/+191)
-1317 +191 Luc PGL3-(-1317/+191)
-758 +191 Luc PGL3-(-758/+191)
-595 +191 Luc PGL3-(-595/+191)
-390 +191 Luc PGL3-(-390/+191)
-250 +191 Luc PGL3-(-250/+191)
-60 +191 Luc PGL3-(-60/+191)
+85 +191 Luc PGL3-(+85/+191)
Luc PGL3-Basic
H9c2
LNCaP
HEK293
(n=6)
(n=6)
(n=6)
0 10 20 30 40
0 1 2 3
0 5 10 15 20
Fold over Base
Fold over Base
Fold over Base

Figure 5

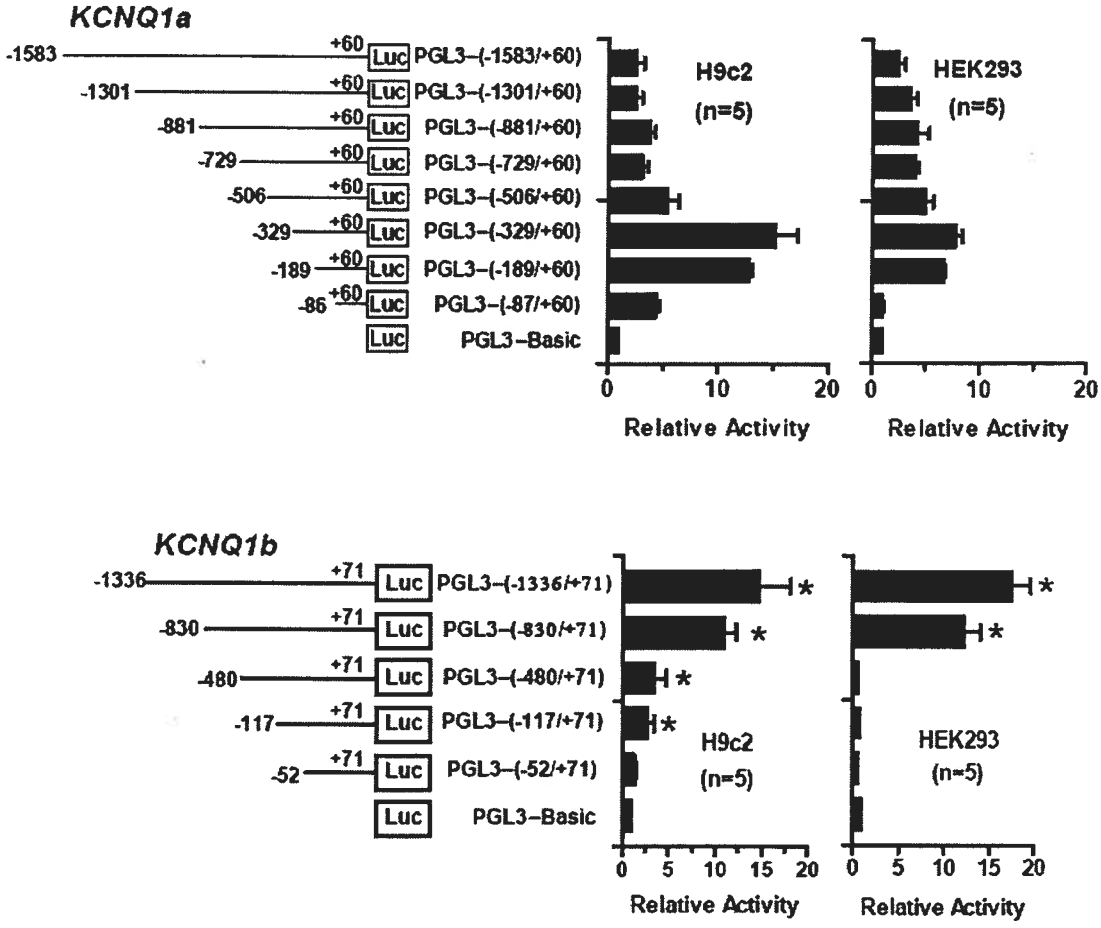
KCNQ1a
-1583
+60
Luc
PGL3–(-1583/+60)
-1301
PGL3–(-1301/+60)
-881
PGL3–(-881/+60)
-729
PGL3–(-729/+60)
-506
PGL3–(-506/+60)
-329
PGL3–(-329/+60)
-189
PGL3–(-189/+60)
-86
PGL3–(-87/+60)
PGL3–Basic
H9c2
(n=5)
HEK293
(n=5)
0
10
20
Relative Activity
KCNQ1b
-1336
+71
PGL3–(-1336/+71)
-830
PGL3–(-830/+71)
-480
PGL3–(-480/+71)
-117
PGL3–(-117/+71)
-52
PGL3–(-52/+71)
PGL3–Basic
*
H9c2
(n=5)
HEK293
(n=5)
0
5
10
15
20
Relative Activity

Figure 6

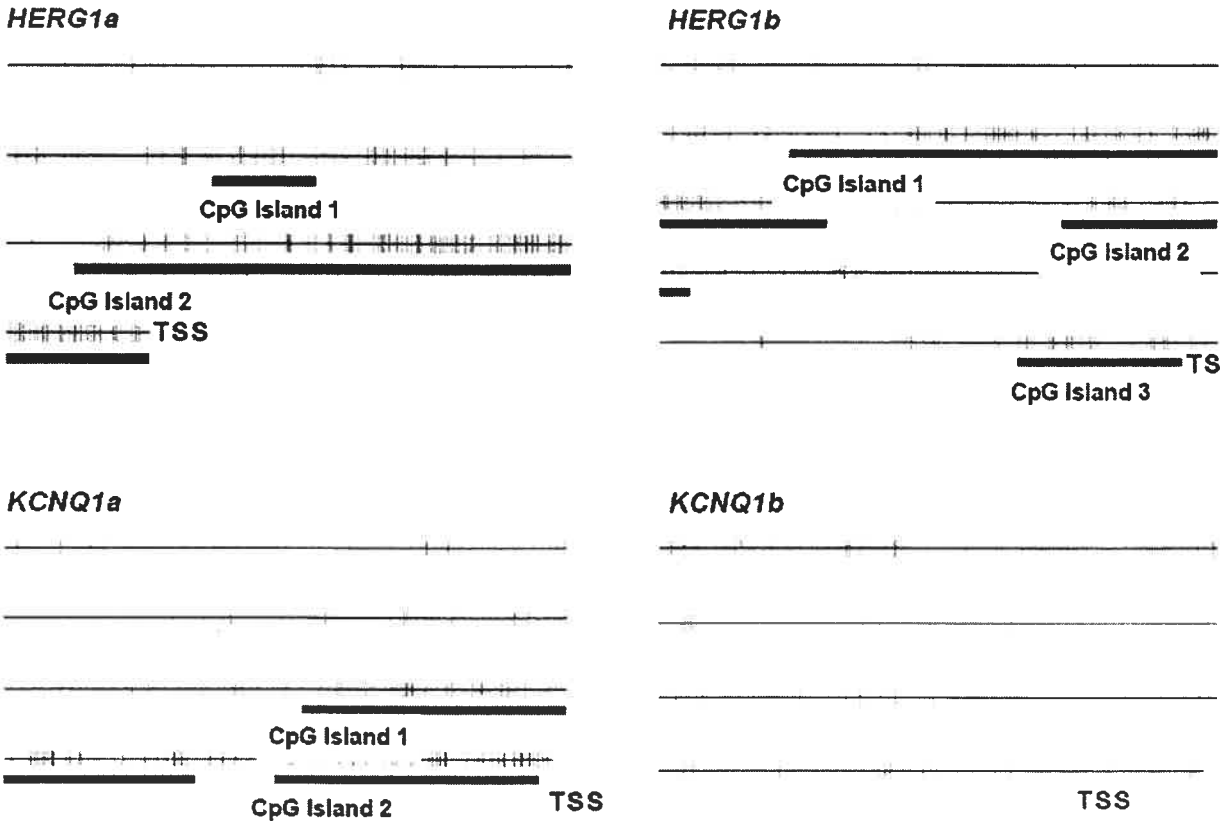
HERG1a
CpG Island 1
CpG Island 2
TSS
HERG1b
CpG Island 1
CpG Island 2
TS
CpG Island 3
KCNQ1a
CpG Island 1
CpG Island 2
TSS
KCNQ1b
TSS

Figure 7

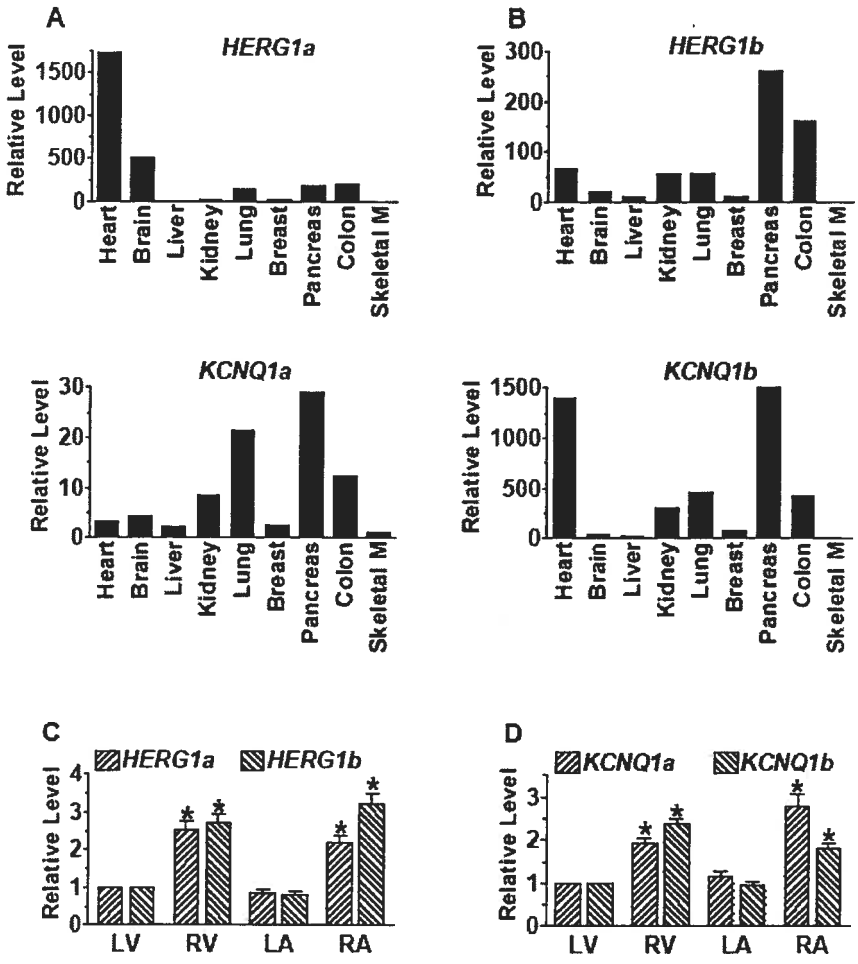
A
HERG1a
Relative Level
1500
1000
500
0
Heart
Brain
Liver
Kidney
Lung
Breast
Pancreas
Colon
Skeletal M
B
HERG1b
Relative Level
300
200
100
0
Heart
Brain
Liver
Kidney
Lung
Breast
Pancreas
Colon
Skeletal M
KCNQ1a
Relative Level
30
20
10
0
Heart
Brain
Liver
Kidney
Lung
Breast
Pancreas
Colon
Skeletal M
KCNQ1b
Relative Level
1500
1000
500
0
Heart
Brain
Liver
Kidney
Lung
Breast
Pancreas
Colon
Skeletal M
C
HERG1a
HERG1b
Relative Level
4
3
2
1
0
LV
RV
LA
RA
D
KCNQ1a
KCNQ1b
Relative Level
3
2
1
0
LV
RV
LA
RA

Table 1. Number of consensus binding sites for cardiac-specific or -related transcription factors within a 3-kb frame of the 5'-flanking regions of *HERG1* and *KCNQ1* genes

5'-Flanking Region	Hand2	SRF	MyoD	GATA4	Mef2	Nkx2.5
HERG1a	5	4	3	0	0	0
HERG1b	0	5	3	0	0	0
KCNQ1a	0	0	5	0	0	0
KCNQ1b	5	8	5	0	0	0

Table 2. **Number of consensus binding sites for stimulating protein 1 (Sp1) and CCAAT boxes within the core promoter regions and CpG islands within a 3-kb frame upstream the translational start sites (TSSs) of *HERG1* and *KCNQ1* genes**

5'-Flanking Region (3 kb)	Sp1	CpG	GAGA	CCAAT
HERG1a	12	2	1	1
HERG1b	6	3	1	0
KCNQ1a	19	2	0	0
KCNQ1b	7	0	7	5

CHAPTER 2. Transcriptional Activation by Stimulating Protein 1 and Post-Transcriptional Repression by Muscle-Specific MicroRNAs of I_{Ks}-Encoding Genes and Potential Implications in Regional Heterogeneity of Their Expressions

In this chapter, we verified the role of Sp1 in the transactivation of *KCNQ1* and *KCNE1* genes by several methods. We also experimentally established and verified the repression effect of *miR-1* and *miR-133* on KCNQ1 and KCNE1. Moreover, the expression distribution of KCNQ1, KCNE1, Sp1 and *miR-1/miR-133* were examined in different regions of the heart.

This work has been published in the ***Journal of Cellular Physiology*** (2007) Aug;212(2):358-67.

Transcriptional Activation by Stimulating Protein 1 and Post-Transcriptional Repression by Muscle-Specific MicroRNAs of I_{Ks}-Encoding Genes and Potential Implications in Regional Heterogeneity of Their Expressions

Xiaobin Luo*[†], Huixian Lin*, Baoxin Li[‡], Jiening Xiao*, Yanjie Lu[‡], Baofeng Yang[‡], and Zhiguo Wang*[†§]

*Research Center, Montreal Heart Institute, Montreal, PQ H1T 1C8 Canada; [†]Department of Medicine, University of Montreal, Montreal, PQ H3C 3J7 Canada; [‡]Department of Pharmacology (State-Province key lab of China), Harbin Medical University, Harbin, Heilongjiang 150086, P.R. China; and [§]Institute of Cardiovascular Research, Harbin Medical University, Harbin, Heilongjiang 150086, P.R. China

Running Title: Expression Regulation of I_{Ks}-Encoding Genes

Key Words: KCNQ1, KCNE1, miRNAs, *miR-1*, *miR-133*, promoters, Sp1

Correspondence to: Dr. Zhiguo Wang, Research Center, Montreal Heart Institute, 5000 Belanger East, Montreal, PQ H1T 1C8, Canada; Tel.: (514) 376-3330. Fax: (514) 376-1335. E-mail: [redacted] Dr. Baofeng Yang, Harbin Medical University, Heilongjiang 150086, P. R. China; Tel.: +86 (451) 8667-9473; E-mail: [redacted]

2.1 Abstract

In cardiac cells, KCNQ1 assembles with KCNE1 and forms a channel complex constituting the slow delayed rectifier current I_{Ks}. Expression of KCNQ1 and KCNE1 are regionally heterogeneous and changes with pathological states of the heart. The aims of this study were to decipher the molecular mechanisms for transcriptional and post-transcriptional regulation expression of *KCNQ1* and *KCNE1* genes and to shed light on the molecular mechanisms for their spatial heterogeneity of distribution. We cloned the 5'-flanking region and identified the transcription start sites of the *KCNQ1* gene. We characterized the core promoters of *KCNQ1* and *KCNE1* and revealed the simulating protein (Sp1) as a common transactivator of *KCNQ1* and *KCNE1* by interacting with the Sp1 *cis*-acting elements in the core promoter regions of these genes. We also characterized the 3' untranslated regions (3'UTRs) of the genes and experimentally established *KCNQ1* and *KCNE1* as targets for repression by the muscle-specific microRNAs *miR-133* and *miR-1*, respectively. We demonstrated spatial heterogeneity of KCNQ1 and KCNE1 distributions at three axes (interventricular, transmural and apical-basal) and disparity between mRNA and protein expressions of these genes. We also found characteristic regional differences of expressions of Sp1 and *miR-1/miR-133* in the heart. Our study unraveled a novel aspect of the cellular function of miRNAs and suggests that the I_{Ks}-encoding genes *KCNQ1* and *KCNE1* expressions are dynamically balanced by transcription factor regulation and miRNA repression. The heterogeneities of Sp1 and *miR-1/miR-133* offer an explanation for the well-recognized regional differences and disparity between mRNA and protein expressions of KCNQ1 and KCNE1.

2.2 Introduction

The voltage-gated KCNQ1 (KvLQT1, Kv7.1) K^+ channels are expressed in a variety of tissues throughout the body and regulate key physiological functions. In cardiac myocytes, the KCNQ1 subunit assembles with the KCNE1 β-subunit (minK) and forms a channel complex constituting the slow delayed rectifier current I_{Ks} (Barhanin et al., 1996; Sanguinetti et al., 1996). Mutations in *KCNQ1* or *KCNE1* can result in dysfunction of I_{Ks} and abnormality of cardiac repolarization, which is

responsible for a majority of inherited long QT syndrome. While the exact role of I_{Ks} in cardiac repolarization is still incompletely understood, it is clear that it can importantly affect cardiac action potential duration (APD) and arrhythmogenesis through two mechanisms. First, I_{Ks} acts as a powerful repolarization reserve or safety factor to restrict excessive cardiac APD and QT prolongation caused by other factors. Removal of this safety factor by I_{Ks} blockade facilitates LQTS (Roden and Yang, 2005; Jost et al., 2005). Second, distribution of I_{Ks} in the heart follows important spatial patterns in at least four different axes: (1) transmural heterogeneity with epicardium (Epi) ≥ endocardium (Endo) > midmyocardium (Mid) (Liu et al., 1995; Gintant, 1995; Szabo et al., 2005), (2) interventricular gradient with right ventricle (RV) > left ventricle (LV) (Volders et al., 1999; Ramakers et al., 2003), transseptal gradient with RV septum > LV septum (Ramakers et al., 2005), and apex-base difference with apical area > basal area (Szentadrassy et al., 2005). These intrinsic spatial patterns of distribution are important in maintaining the sequential excitations (depolarization and repolarization) of cardiac muscles, and disruption of the patterns and/or exaggeration of the regional heterogeneity can create substrates for arrhythmogenesis. Many pathological conditions can change the function and relative distribution of I_{Ks} by altering expression of its encoding genes (Ramakers et al., 2003; Tsuji et al., 2006; Volders et al., 1999; Tsuji et al., 2002; Akar and Tomaselli, 2005). Decreases in I_{Ks} density have been observed consistently in failing hearts of both animal models and patients. KCNQ1 and KCNE1 mRNA and protein levels were downregulated in both bradypaced and tachypaced rabbits. In chronic AV block, I_{Ks} is reduced likely due to transcriptional downregulation of KCNQ1 and KCNE1. Evidently, expression regulation of KCNQ1 and KCNE1 plays a critical role in defining the physiological function of I_{Ks}.

Expression of a gene is fine-tuned by its promoter sequence containing varying *cis*-acting elements in the 5'-flanking region for transcription factors to work. In order to understand such processes, it is necessary to identify and characterize the promoter region of a gene. In addition to transcriptional regulation, expression of a gene is further fine-tuned by post-transcriptional regulation. Recent discovery of microRNA-1 (miRNAs) has revolutionized our understanding of the mechanisms that

regulate gene expression. MiRNAs are endogenous ~22-nt non-coding RNAs that anneal to inexactly complementary sequences in the 3'UTRs of target mRNAs of protein-coding genes to specify translational repression or/and mRNA cleavage (Ambros, 2004; Meister and Tuschl, 2004; Alvarez-Garcia and Miska, 2005). Among >300 miRNAs identified thus far, *miR-1* and *miR-133* are known to specifically express in adult cardiac and skeletal muscle tissues. A recent study proposed a model in which *miR-1* and *miR-133* regulate myogenesis by controlling distinct aspects of the differentiation process; *miR-1* promotes myogenic differentiation *miR-133* enhances myoblast proliferation (Chen et al., 2006). *MiR-1* and *miR-133* are expressed in a chamber-specific manner during cardiogenesis and are activated during the period of differentiation (Chen et al., 2006; Zhao et al., 2005). Increasing expression of *miR-1* and *miR-133* has been found in neonatal hearts, and substantially higher levels are maintained in adult cardiac tissues (Chen et al., 2006). Whether these miRNAs are involved in regulation of ion channel expression remained unknown.

This study was designed to decipher the transcriptional and post-transcriptional regulations of I_{Ks}-encoding genes KCNQ1 and KCNE1, and to shed light on the molecular mechanisms for the spatial heterogeneity of the channels. To this end, we performed detailed analysis of the core promoter regions and the 3'UTRs of the genes for their putative binding elements for transcription factors and miRNAs. We then experimentally tested the roles of the key elements in mediating the transcriptional activation and post-transcriptional repression of KCNQ1 and KCNE1. Finally, we also compared the spatial distribution patterns of KCNQ1/KCNE1 with those of Sp1 and *miR-1*/*miR-133* at both mRNA and protein levels, in a hope to find a link between them.

2.3 Materials and Methods

2.3.1 Rapid amplification of cDNA ends (5'RACE)

The transcription start sites (TSSs) of *KCNQ1* were determined with Ambion's RNA–Ready cDNA Human Heart RNA ligase-mediated 5'RACE kit, as previously described (Pang et al., 2003). Human RNA sample was purchased from

Clontech. The gene specific primers were designed based on the human KCNQ1 cDNA (GenBank accession NM_000218).

2.3.2 Construction of promoter-luciferase fusion plasmids

A series of fragments of varying length were amplified using human genomic DNA the Homo sapiens bacterial artificial chromosome (BAC) clone RP5-915F1 (accession No. AC124057) as a template and PCR Advantage and Advantage-GC genomic polymerase mixes (Clontech K-1905-Y). PCR products were subcloned into luciferase-containing PGL3-Basic (Promega) vector. The integrity and orientation of all constructs were confirmed by restriction endonuclease analysis and DNA sequencing.

2.3.3 Synthesis of miRNAs and anti-miRNA antisense inhibitors

MiR-1 and *miR-133* and their respective mutant constructs were synthesized by Integrated DNA Technologies, Inc. (IDT). The sequences of the anti-*miR-1* and anti-*miR-133* antisense inhibitor oligonucleotides (AMO-1 and AMO-133, respectively) used in our studies are the exact antisense copies of their respective mature miRNA sequences and five nucleotides at both ends were locked (the ribose ring is constrained by a methylene bridge between the 2'-*O*- and the 4'-C atoms).

2.3.4 Mutagenesis

Deletion mutations and base-substitution mutations were created by direct oligomers synthesis or by PCR-based methods (Pang et al., 2003). Mutations were made to the 5'-flanking regions of *KCNQ1* and *KCNE1*, and also to *miR-1* and *miR-133*.

2.3.5 Construction of chimeric miRNA-target site—luciferase reporter vectors

To construct reporter vectors bearing miRNA-target sites, we synthesized (by Invitrogen) fragments containing the exact target sites for *miR-1* and *miR-133* or the mutated target sites, the 3'UTRs of *KCNQ1* and *KCNE1* without or with mutations by PCR amplification. The sense and antisense strands of the oligonucleotides were annealed by adding 2 μg of each oligonucleotides to 46 μl of annealing solution (100 mmol/L K-acetate, 30 mmol/L HEPES-KOH, pH 7.4 and 2 mmol/L Mg-acetate) and incubated at 90°C for 5 min and then at 37°C for 1 h. The annealed oligonucleotides were inserted into the multiple cloning sites downstream the luciferase gene (HindIII

and SpeI sites) in the pMIR-REPORT™ luciferase miRNA expression reporter vector (Ambion, Inc.).

2.3.6 Cell culture

The cell lines used in this study were all purchased from American Type Culture Collection (ATCC, Manassas, VA). H9c2 (rat ventricular cell line) and HEK293 (human embryonic kidney cell line) were maintain in Dulbecco's Modified Eagle Medium (DMEM). The cultures were all supplemented with 10% fetal bovine serum and 100 μg/ml penicillin/streptomycin.

2.3.7 Transfection and luciferase assay

For promoter activity assays, 1 μg PGL3–target DNA (firefly luciferase vector) and 0.1 μg PRL-TK (TK-driven Renilla luciferase expression vector) were co-transfected with lipofectamine 2000 (Invitrogen), according to the manufacturer's instructions.[21] Following transfection (48 h), luciferase activities were measured with a dual luciferase reporter assay kit (Promega) on a luminometer (Lumat LB9507). The plasmid vector carrying stimulating protein 1 (Sp1; CMVp-Sp1) was a generous gift from Dr. Robert Tjian (University of California, Berkeley, CA) (Kadonaga et al., 1988; Pugh and Tjian, 1990). CMVp-Sp1 or Sp1-free CMVp vector was co-transfected with PGL3–target DNA and PRL-TK into H9c2 cells for studying promoter activities or they were transfected into HEK293 cells for studying native *KCNQ1* expression. For miRNA experiments, cells (1×10^5/well) were transfected with 1 μg *miR-1*, *miR-133* or other constructs (mutant miRNAs, AMO-1 or AMO-133), alone or together as to be specified, with lipofectamine 2000. For all experiments, transfection took place 24 h after starvation of cells in serum-free medium.

Drosophila *Schneider cells (SL2)*

SL2 cells were cultured at 25°C in Schneider's *Drosophila* medium (Gibco). Transfection was performed using Lipofectamine 2000. The DNA transfection mixture contained 250 ng reporter plasmid, varying amounts of pPac-Sp1 plasmid, and empty pPac0 vector (kind gifts from Dr. Robert Tjian, University of California) as control (Kadonaga et al., 1988; Pugh and Tjian, 1990). Cells were harvested 48 h after transfection for reporter analysis.

2.3.8 Real-time RT-PCR

For quantification of *KCNQ1*, *KCNE1* and *Sp1* transcripts, conventional real-time RT-PCR was carried out with total RNA samples extracted from HEK293 cells or human hearts 48 h after transfection, and treated with DNase I, as previously described (Pang et al., 2003; Zhang et al., 2006). The tissues were dissected from the Epi of basal area for comparison between LV and RV, from basal area of LV for comparison between Epi and Mid, and from Epi of LV for comparison between apex and basal. TaqMan quantitative assay of transcripts was performed with real-time two-step reverse transcription PCR (GeneAmp 5700, PE Biosystems), involving an initial reverse transcription with random primers and subsequent PCR amplification of the targets. Expression level of GAPDH was used as an internal control.

The *mir*Vana™ qRT-PCR miRNA Detection Kit (Ambion) is a quantitative reverse transcription-PCR (qRT-PCR) kit enabling sensitive, rapid quantification of miRNA expression from total RNA samples, and was used in conjunction with real-time PCR with SYBR Green I for quantification of the total *miR-133* (*miR-133a* + *miR-133b*) transcripts in our study, following the manufacturer's instructions. The total RNA samples were isolated with Ambion's *mir*Vana miRNA Isolation Kit. Reactions contained *mir*Vana qRT-PCR Primer sets specific for *miR-1* and *miR-133*, or 5S rRNA as a positive internal control. QRT-PCR was performed on a GeneAmp 5700 thermocycler for 40 cycles. We first determined the appropriate cycle threshold (Ct) using the automatic baseline determination feature. We then performed dissociation analysis (melt-curve) on the reactions to identify the characteristic peak associated with primer-dimers in order to separate from the single prominent peak representing the successful PCR amplification of *miR-133*. Fold variations in expression of *miR-133* between RNA samples were calculated after normalization to 5s rRNA. A total number of six human heart preparations were used in this study and they were all from patients without heart disease. Human tissues were obtained from the Second Affiliated Hospital of Harbin Medical University under the procedures approved by the Ethnic Committee for Use of Human Samples of the Harbin Medical University and from the Réseau de tissus pour études biologiques (RETEB) tissue bank under the procedures approved by the Human Research Ethics Committee of the

Montreal Heart Institute.

2.3.9 Western blot

The protein samples were extracted from human heart preparations as described above for RNA isolation and from HEK293 cells for immunoblotting analysis of the KCNQ1, KCNE1 and Sp1 proteins, with the procedures essentially the same as described in detail elsewhere (Zhang et al., 2006; Wang et al., 2001). For KCNQ1 and KCNE1, membrane protein samples were extracted, and for Sp1, cytosolic protein samples were used. The protein content was determined with Bio-Rad Protein Assay Kit (Bio-Rad, Mississauga, ON, Canada) using bovine serum albumin as the standard. Protein sample (~30 μg) was fractionated by SDS-PAGE (7.5%-10% polyacrylamide gels) and transferred to PVDF membrane (Millipore, Bedford, MA). The sample was incubated overnight at 4°C with the primary antibodies in 1:50~1:200. Affinity purified goat polyclonal anti-KCNQ1 antibody, anti-KCNE1 antibody and rabbit polyclonal anti-Sp1 antibody were all purchased from Santa Cruz and used as the primary antibodies. Inhibitory peptide for each antibody (Santa Cruz) was used to test the antibody specificity. Next day, the membrane was washed in TTBS three times (10 min/each) and incubated for 2 h with the HRP-conjugated donkey anti-goat IgG (H+L) (1:600, Santa Cruz) in the blocking buffer. Bound antibodies were detected using the chemiluminescent substrate (Western Blot Chemiluminescence Reagent Plus, NEN Life Science Products, Boston, USA). GAPDH was used as an internal control for equal input of protein samples, using anti-GAPDH antibody from RDI (Flanders, NJ). Western blot bands were quantified using QuantityOne software by measuring the band intensity (Area x OD) for each group and normalizing to GAPDH. The final results are expressed as fold changes by normalizing the data to the control values.

2.3.10 Drug treatment

In experiments involving mithramycin (Sigma Chemicals), the drug was applied to the culture medium 12 h after transfection of PGL3–target DNA was performed, in serum- and antibiotics-free medium to starve and synchronize cells. The cells were further incubated for 24 h before harvested for measuring luciferase activities in cell lines or for extracting total RNA and protein samples.

2.3.11 Data analysis

Group data are expressed as mean ± S.E. Statistical comparisons (performed using ANOVA followed by Dunnett's method) were carried out using Microsoft Excel. A two-tailed $p<0.05$ was taken to indicate a statistically significant difference. *Cis*-elements for transcription factor binding sites were analyzed with *MatInspector* V2.2.

2.4 Results

2.4.1 Transcription start sites of *KCNQ1*

5'RACE techniques were used to obtain the 5'ends of *KCNQ1* transcripts. The experiment using RNA samples from human heart yielded two discrete fragments. Sequence analysis suggests that the two fragments represent separate transcription start sites: TSS1 (designated +1) and TSS2 (position +12) which are located 12-nt apart at 80 bp and 68 bp (GenBank accession No. EF010934), respectively, upstream from the translation start codon (ATG) of *KCNQ1* (GenBank accession No. MN_000218) (Fig. 1). The transcription start sites of *KCNE1* have been previously reported (Lundquist et al., 2006).

Promoter regions *of KCNQ1* and *KCNE1*

Computer analysis using the *MatInspector* program of 3000-bp 5'-flanking region of *KCNQ1* revealed that it contains one TATA box located 1.4 kb upstream of TSS1, which is unlikely to be the transcription initiation element because it is too distal to the TSSs. The 5'-flanking region of *KCNQ1* also lacks other known common promoter elements that are required for transcription initiation complex, including the initiator element, the downstream promoter element (DPE), or the TFIIB recognition element (BRE). Less common promoter elements such as the downstream core element (DCE) and the multiple start site element downstream (MED-1) are also missing. Three GATA1 consensus sites located distal to TSS1 (1.4 kb, 1.6 kb and 2.0 kb upstream) were identified, but the heart-specific GATA4 as the potent transactivator in cardiac cells is absent in the *KCNQ1* 5'-flanking region. Of particular note is the high GC content of the proximal promoter region of *KCNQ1*

containing multiple Sp1 consensus sequences located to -61, -114, -134, -190, -259, -277, -295, -347, -407, and -460 (Fig. 1).

The functional role of the 5'-flanking region in the regulation of transcription of the *KCNQ1* gene was assessed by its ability to drive expression of the luciferase reporter gene. Varying lengths of putative promoter fragment-luciferase constructs were generated and tested for their ability to drive expression of the reporter gene in a rat ventricular cell line (H9c2), a human lung cancer cell line (A549), and a human embryonic kidney cell line (HEK293), to map the promoter activity in the *KCNQ1* 5'-flanking region. H9c2 and HEK293 were used for most parts of our study because the former is a cardiac cell line (Shi et al., 2002) that express significant *miR-1/miR-133* but minimal endogenous KCNQ1 and KCNE1 and the latter is a human cell line that expresses endogenous KCNQ1 and KCNE1 lacking of *miR-1/miR-133* (Zheng et al., 2006; Vallon et al., 2001). *KCNQ1* promoter constructs had approximately 10–15 times the activity of the promoterless vector (pGL3 basic) and 50% of the promoter activity of the pGL3 construct that contains both the SV40 promoter and enhancer (pGL3 control, data not shown). The overall transcription activities of different *KCNQ1* promoter constructs were similar in all three cell lines and consistently, the -329/+60 fragment elicited the maximum promoter activities (Fig. 2). The core promoter of the *KCNQ1* gene was thus defined to -329/+60.

Two different isoforms of *KCNE1* were identified, designated *KCNE1a* and *KCNE1b*, of which *KCNE1a* is more prominently expressed in the heart (Lundquist et al., 2006). The protein-encoding regions and the 3' untranslated regions (3'UTRs) of the two isoforms are identical. The core promoter region of *KCNE1a* was mapped to -244 bp upstream of the TSS and it shares some similarities with that of *KCNQ1*, with a cluster of five putative Sp1 *cis*-elements (-50, -97, -133, -145, and -198), without other known transactivator elements. The core promoter of *KCNE1b* (-921/+70) also contains several putative Sp1 binding sites. Thus, only KCNE1a was used for luciferase activity measurements and KCNE1 (including both KCNE1a and KCNE1b) was used for all other experiments.

2.4.2 Sp1 as a transcription activator of *KCNQ1* and *KCNE1a*

Apparently, a common feature of the *KCNQ1* and *KCNE1* core promoters is the presence of multiple Sp1 consensus binding sites. Sp1 is a widely distributed member of a multigene family of zinc-finger transcription factors that binds DNA in mammalian cells primarily via interaction with GC-box elements. The binding of Sp1 to GC-boxes is often critical to achieving significant levels of transcription from TATA-less promoters and is intimately involved in the determination of TSS (Kadonaga et al., 1988; Pugh and Tjian, 1990; Black et al., 2001; Courey and Tjian, 1998).

To investigate the role of Sp1 in the transcription of *KCNQ1* and *KCNE1a* genes, we first assessed the effects of Sp1 inhibitor mithramycin (Pugh and Tjian, 1990; Courey and Tjian, 1998) on the luciferase activities driven by the core promoters of these genes in H9c2 cells and endogenous expressions of these genes at mRNA and protein levels in HEK293 cells. As depicted in Figure 3A and 3B, mithramycin produced considerable reduction of the promoter activities and of expression levels of native *KCNQ1* and *KCNE1a* transcripts and proteins.

We then evaluated the effects of Sp1 overexpression on *KCNQ1* and *KCNE1a* expression by co-transfection of CMVp-Sp1 vectors with *KCNQ1* or *KCNE1a*-carrying PGL-3 vectors in H9c2 cells to study the promoter activities and by transfection of CMVp-Sp1 into HEK293 cells to study endogenous mRNA levels of *KCNQ1* and *KCNE1* genes. Sp1 overexpression strikingly enhanced the promoter activities and native transcript levels, as compared with transfection of Sp1-null CMVp vectors (Fig. 3C).

We reasoned if Sp1 is indeed important for the promoter activities of *KCNQ1* and *KCNE1a*, then in a Sp1-null environment, such as the SL2 cells (Bond et al., 2004), the core promoter fragments should lose their ability to elicit luciferase activities unless exogenous Sp1 is supplied. This notion was verified by our experiments using SL2 cells. The luciferase reporter activity was undetectable with any one of the core promoter fragments in absence of exogenous Sp1 cDNA, whereas in the SL2 cells co-transfected with Sp1 cDNA, it was readily detectable (Fig. 3D).

Furthermore, a series of truncation mutations and site-directed mutations were made to determine the relative importance of the Sp1 *cis*-elements in the core

promoter region of *KCNQ1*. The truncation mutations were designed as such that each fragment contains a certain numbers of Sp1 *cis*-elements. For instance, the -87/+60 fragment contains only the first Sp1 site (-61), the -189/+60 fragment contains a group of Sp1 sites (-114/-134/-190) in addition to the first Sp1 site. As shown in Figure 2, the fragment containing only the first Sp1 *cis*-elements demonstrated as much as ~30% of the maximum reporter activities conferred by -329/+60 fragment in H9c2 cardiac cells, but nearly null HEK293 kidney cells, indicating the first Sp1 *cis*-element accounting for initiation of promoter activity and being required for maintaining the minimal transcriptional activity of *KCNQ1* in cardiomyocytes. When the fragment was lengthened to include the subsequent three Sp1 *cis*-elements (-114/-134/-190) to form the -189/+60 fragment, the reporter activity robustly increased to ~85% of the maximum activity conferred by -329/+60 fragment that contains another cluster of Sp1 sites further upstream of the TSS. The result indicates that the Sp1 *cis*-elements located at -60, -114, -134 and -190 are the most critical sites defining the core promoter region of *KCNQ1*.

2.4.3 *MiR-133* as a post-transcriptional repressor of *KCNQ1*

Neither *KCNQ1* nor *KCNE1* genes are listed as candidate targets for *miR-1* and *miR-133* according to the prediction by TargetScan hosted by Wellcome Trust Sanger Institute (Griffiths-Jones, 2004). However, by detailed analysis of the 3'UTR of *KCNQ1*, we identified four putative binding sites for *miR-133* based solely on complementarity, each of them containing six nucleotides exactly matching the 2-7 nucleotides from the 5'-end of *miR-133* (Fig. 4A and 4B). No sites with more than five complementary nucleotides to *miR-1* were found in the 3'UTR of *KCNQ1*.

Perturbation of miRNA expression, including overexpression and silencing, is a powerful approach to study miRNA function (Cheng et al., 2005; Chan et al., 2005; Krutzfeldt et al., 2005). Transient overexpression of miRNAs in cell-based assays can be achieved by transfection of double-stranded RNA molecules that mimic the Dicer cleavage product. Moreover, the anti-miRNA antisense inhibitor oligonucleotides (AMOs) specifically and stoichiometrically bind, and efficiently and irreversibly silence, their target miRNAs, by competitive binding to miRNAs, and by degrading them as well with unknown mechanisms. To verify that *KCNQ1* is indeed the cognate

targets of *miR-133* for post-transcriptional repression, we took the following approaches. We first inserted the 3'UTR of *KCNQ1* into the 3'UTR of a luciferase reporter plasmid containing a constitutively active promoter in order to determine the effects of *miR-133* on reporter expression. Co-transfection of the chimeric luciferase-*KCNQ1* 3'UTR vector with *miR-133* (Fig. 4C) into HEK293 cells that express minimal *miR-1/miR-133* consistently demonstrated smaller luciferase activities relative to transfection of the chimeric plasmid alone or co-transfection with the mutant *miR-133* failed to produce any effects. Co-application of *miR-133* with AMO-133 eliminated the silencing effect on luciferase reporter activities. A mutated *miR-133* failed to elicit any effects.

As a second step, we used *miR-1* and *miR-133* standards in which the complementary sequences of *miR-1* and *miR-133* were cloned downstream of luciferase gene in the pMIR-REPORT plasmid (Chen et al., 2006; Cheng et al., 2005). With these constructs, we were able to confirm the uptake and activities of transfected miRNAs. Our experiments demonstrated that co-transfection of *miR-133* into HEK293 cells nearly abolished the luciferase activities seen with transfection of the plasmid containing *miR-133* standards alone. The luciferase expression was unaffected if *miR-1* was co-transfected with *miR-133* standards (Fig. 4D).

To see if *KCNQ1* repression by *miR-133* reported by luciferase assays has functional implications, we determined the effects of *miR-133* on endogenous expression of KCNQ1 at protein levels by Western blot with HEK293 membrane protein samples. Our data showed that transfection of *miR-133* at 10 nM remarkably reduced KCNQ1 protein level, and as a negative control the mutant *miR-133* did not cause any appreciable changes (Fig. 4EC). Co-application of *miR-133* with its antisense (AMO-133) nearly abolished the effects, verifying the specificity of the *miR-133* action. Transfection of *miR-1* (100 nM) failed to affect KCNQ1 protein level, validating base-pairing as a major criterion for miRNA targeting. Moreover, transfection of AMO-133 alone significantly increased KCNQ1 protein level, presumably by removing the inhibitory effect of endogenous *miR-133*. By comparison, *miR-133* produced marginal reduction of KCNQ1 mRNA level (Fig. 4F), indicating that *miR-133* does not affect KCNQ1 mRNA stability.

2.4.4 *MiR-1* as a post-transcriptional repressor of *KCNE1*

By comparison, the 3'UTR of *KCNE1* (*KCNE1a* and *KCNE1b* have the same 3'UTR) contains three putative *miR-1* binding sites with each carrying at least seven consecutive complementary nucleotides to the 5'-end of *miR-1*, but it does not contain *miR-133* target sites (Fig. 5A). Similar approaches to those described for *KCNQ1* were applied to *KCNE1*. Our experiments demonstrated that *KCNE1* is critically regulated by *miR-1*, but not by *miR-133*; *miR-1* (10 nM) produced some 79% abrogation of the luciferase activity reported by the vectors carrying the 3'UTR of *KCNE1* and 70% reduction of KCNE1 protein level (Fig. 5C and 5E). Notably, transfection of AMO-1 alone significantly increased KCNE1 protein level (Fig. 5E). The KCNE1 mRNA was unaffected by miR-1 (Fig. 5F).

We then verified the transfection and effect of *miR-1* using the *miR-1* standard as described above. Co-transfection of *miR-1* into HEK293 cells nearly abolished the luciferase activities seen with transfection of the plasmid containing the *miR-1* standard alone. The luciferase expression was unaffected if *miR-133* was co-transfected with the *miR-1* standard (Fig. 5D).

The mechanism of actions of AMOs was verified by real-time RT-PCR quantification of *miR-1* and *miR-133* in H9c2 cells that express endogenous *miR-1/miR-133*, since AMOs have been shown to degrade their target miRNAs through some unknown mechanisms. As shown in Figure 5G, AMO-1 specifically reduced the endogenous *miR-1* level when applied alone or the total *miR-1* levels when co-transfected with exogenous *miR-1*, without notable effects on *miR-133* levels. *Vice versa*, AMO-133 specifically decreased *miR-133* level without altering *miR-1*.

2.4.5 Sp1 and *miR-1/miR-133* and their roles in regional heterogeneity of *KCNQ1* and *KCNE1* expressions

As already described in Introduction, I_{Ks} along with its underlying channel proteins KCNQ1 and KCNE1 demonstrates important spatial heterogeneity of distribution. This regional inhomogeneity exists along at least three axes including transmural difference (Epi>Mid), interventricular gradient (RV>LV) and apex-base asymmetry (Apex>Base). In order to investigate if Sp1 and *miR-1/miR-133* contribute

to the spatial heterogeneity of I_{Ks} in human heart, we first quantified the I_{Ks}-encoding genes KCNQ1 and KCNE1 at both protein and mRNA levels. Western blot analysis revealed that KCNQ1 protein level was predominant in RV *vs.* LV (1.7:1), in Epi *vs.* Mid (1.6:1) and in Apex *vs.* Base (2.2:1). Similarly, the protein level of KCNE1 was also found RV>LV (2:1) and Apex>Base (1.5:1); however, it was more pronounced in Mid than in Epi (1.4:1), opposite to the distribution of KCNQ1 channels. (Fig. 6, upper). Real-time RT-PCR quantification of *KCNQ1* and *KCNE1* transcripts showed that the mRNA levels of both *KCNQ1* and *KCNE1* were higher in RV than in LV (Fig. 6, lower). By comparison, we found no such a regional difference of KCNQ1 and KCNE1 in mRNA levels between Epi and Mid and between Apex and Base.

We subsequently quantified the expression of Sp1 using the same mRNA and protein samples as for KCNQ1/KCNE1. The anti-Sp1 Western blot showed a Sp1 protein doublet at 110 kDa and 95 kDa positions (Bond et al., 2004). Notably, both the major (95 kDa) and the minor (110 kD) bands were significantly higher in their densities with RV than with LV samples (2.2:1). The abundance of Sp1 transcripts was in good agreement with the interventricular gradients of *KCNQ1* and *KCNE1* transcripts, being RV>LV with a ratio of approximately 2.4:1 (Fig. 7A). However, no significant differences of Sp1 transcripts and proteins were observed in the transmural and apical-basal axes (Fig. 7A).

Strikingly, the regional distribution profiles of *miR-1* and *miR-133* were converse to those of Sp1 transcripts. Neither *miR-1* nor *miR-133* showed any appreciable interventricular differences. However, the transmural and apical-basal gradients were consistently seen. For *miR-1*, the levels were Epi>Mid (1.4:1) and Base>Apex (1.5:1) (Fig. 7B), and for *miR-133*, the levels were Mid>Epi (2.8:1) and Base>Apex (2.5:1) (Fig. 7C).

2.5 Discussion

The aims of this study were to explore the molecular mechanisms for transcriptional and post-transcriptional regulation of expression of *KCNQ1* and *KCNE1* genes and to shed light on the molecular mechanisms of spatially heterogeneous expressions of these genes. We identified the simulating protein (Sp1)

as an important transactivator of *KCNQ1* and *KCNE1* by interacting with the Sp1 *cis*-acting elements in the core promoter regions of these genes. We also experimentally established KCNQ1 and KCNE1 as targets for repression by the muscle-specific miRNAs *miR-133* and *miR-1*, respectively, which unraveled a novel aspect of the cellular function of miRNAs. We demonstrated, for the first time, that expressions of Sp1 and *miR-1/miR-133* in the heart are spatially heterogeneous, and these heterogeneities may contribute to the well-recognized regional differences of distribution of KCNQ1 and KCNE1.

Having generated a tremendous amount of excitement about miRNAs in many areas of biology, research over the past five years has put miRNAs at centre stage. Indeed, miRNA-mediated gene regulation is now considered a fundamental layer of genetic programs that operates at the post-transcriptional level. However, in spite of our ability to identify miRNAs, regulatory targets have not been established or even confidently predicted for any of the vertebrate miRNAs, which has hampered progress toward elucidating the functions of miRNAs. Our current understanding of the functions of miRNAs primarily relies on their tissue-specific or developmental stage-specific expression patterns as well as their evolutionary conservation, and is thus largely limited to biogenesis and oncogenesis. Target finding and function discovery are two major challenges to researchers in miRNA research. Based on computational predictions, neither KCNQ1 nor KCNE1 were considered targets for *miR-1/miR-133*, despite that they both have substantial complementarity to the miRNAs, likely due to unfavorable free energy status. However, by detailed analysis of the 3'UTR of *KCNQ1*, we identified four putative binding sites for *miR-133* (Fig. 4A). Similarly, the 3'UTR of *KCNE1* was found containing three putative *miR-1* binding sites (Fig. 5A). These multiple sites may cooperate with one another to confer significant effects of the miRNAs. Our experimental data convincingly demonstrated that the expression levels of KCNQ1 and KCNE1 are importantly regulated by *miR-133* and *miR-1*, respectively. Consistent with the principle of action of miRNAs, *miR-133* and *miR-1* decreased KCNQ1 and KCNE1 protein level without significantly affecting their mRNA levels. It is not clear at this time what pathophysiological implications of this post-transcriptional repression are. One might

speculate that the miRNAs can act to limit excessive expression of KCNQ1 and KCNE1 genes, if any. As to be discussed below, our study also revealed for the first time that distribution of the miRNAs in adult human hearts is heterogeneous and this heterogeneity may contribute to regional asymmetry of many proteins.

Since the beginning of the last decade, when Day, McComb, and Campbell (Day et al., 1990) introduced the concept of QT dispersion as a potential marker of arrhythmogenicity risk and hence of cardiovascular morbi–mortality, various electrocardiographic ventricular repolarization parameters have been tested as prognostic factors in several conditions such as coronary heart disease, heart failure, cardiomyopathies, as well as in population-based studies. QT dispersion mainly reflects regional dispersion of ventricular repolarization or APD. Under normal physiological conditions, these regional differences are genetically programmed with a certain pattern with APD gradient from long to short following the sequence of activation of myocardial mass during an excitation, which constitutes an intrinsic protection mechanism against arrhythmias which could be induced due to radial and retrograde excitation propagation. Under pathological situations, the spatial heterogeneity is abnormally increased and the intrinsic pattern of spatial heterogeneity may also be broken. These changes render the heart a loss of the intrinsic antiarrhythmic mechanism and a vulnerability to arrhythmogenesis. For example, enlarged interventricular differences have been shown to cause acquired LQTS (Verduyn et al., 1997a and 1997b). The spatial heterogeneity of cardiac repolarization is largely due to diversity and varying densities of repolarizing K^+ currents. The well-recognized regional heterogeneity of I_{Ks} is one of the important factors determining the spatial dispersion of electrical activities (Liu et al., 1995). In this study, we qualitatively reproduced the results reported in previous published studies: (1) KCNQ1 and KCNE1 distribute with significant interventricular gradients (RV>LV) at both mRNA and protein levels (Ramakers et al., 2003), (2) The protein levels of both KCNQ1 and KCNE1 are higher in apical than in basal area (Szentadrassy et al., 2005), despite that their mRNA levels are not significantly different, and (3) KCNQ1 protein level is greater in Epi than in Mid (Szabo et al., 2005), whereas that of KCNE1 is the opposite, and there is not transmural difference

in mRNA levels of KCNQ1 and KCNE1 (Pereon et al., 2000). Clearly, in addition to the regional difference of KCNQ1 and KCNE1 expressions, there is also a consistent discrepancy between the protein and mRNA expressions of these genes. Intriguingly, the distribution patterns of Sp1 and *miR-1/miR-133* seem to provide a reasonable explanation for the observations and this can be sorted out as following. First, the interventricular difference of Sp1, which drives KCNQ1 and KCNE1 expressions, corresponds exactly to the interventricular differences of KCNQ1 and KCNE1, at both mRNA and protein levels. By comparison, *miR-1* and *miR-133* do not show any chamber-dependent difference. These suggest that the higher abundance of Sp1 in RV likely contributes to the higher abundance of KCNQ1 and KCNE1 in the same chamber. Second, there is no difference of Sp1 expression either across the LV wall or along the apical-basal axis, coincident with the uniformity of distributions of KCNQ1 and KCNE1 transcripts in these two axes. Most strikingly, the *miR-133* level was found much greater in Base than in Apex and in Mid than in Epi. Considering the fact that *miR-133* represses KCNQ1 proteins leaving its transcripts unaltered, it is not difficult to understand why KCNQ1 protein levels have the opposite patterns of transmural and apical-basal gradients to those of *miR-133* but KCNQ1 mRNA does not have transmural and apical-basal gradients. The same logic can be applied to *miR-1* and KCNE1; the characteristic regional distributions of *miR-1*, Base>Apex and Epi>Mid, can be one of the causal factors for the converse transmural and apical-basal gradients of KCNE1 protein levels. It seems reasonable to come to a conclusion that the combination and interplay of the characteristic spatial distributions of Sp1 and *miR-1/miR-133* account, at least partially, for the regional heterogeneity of I_{Ks}-encoding genes and the disparity between protein and mRNA expressions of these genes. It should be mentioned, however, that our data are only supportive, but not confirmative, to this notion. Further studies using *in vivo* genetic engineering of Sp1 and *miR-1/miR-133* are absolutely needed to fully establish the link.

2.6 Acknowledgments

*The authors thank XiaoFan Yang for excellent technical support. This work was supported in part by the Fonds de la Recherche de l'Institut de Cardiologie de Montreal, awarded to Dr. Z Wang. Dr. Z. Wang is a senior research scholar of the Fonds de Recherche en Sante de Quebec.

2.7 References

Akar FG, Tomaselli GF. 2005. Ion channels as novel therapeutic targets in heart failure. Ann Med 37:44–54.

Alvarez-Garcia I, Miska EA. 2005. MicroRNA functions in animal development and human disease. Development 132:4653–4662.

Ambros V. 2004. The functions of animal microRNAs. Nature 431:350–355.

Barhanin J, Lesage F, Guillemare E, Fink M, Lazdunski M, Romey G. 1996. K_VLQT1 and lsK (minK) proteins associate to form the I_{Ks} cardiac potassium current. Nature 384:78–80.

Black AR, Black JD, Azizkhan-Clifford J. 2001. Sp1 and kruppel-like factor family of transcription factors in cell growth regulation and cancer. J Cell Physiol 188:143–160.

Bond GL, Hu W, Bond EE, Robins H, Lutzker SG, Arva NC, Bargonetti J, Bartel F, Taubert H, Wuerl P, Onel K, Yip L, Hwang SJ, Strong LC, Lozano G, Levine AJ. 2004. A single nucleotide polymorphism in the MDM2 promoter attenuates the p53 tumor suppressor pathway and accelerates tumor formation in humans. Cell 119:591–602.

Chan JA, Krichevsky AM, Kosik KS. 2005. MicroRNA-21 is an antiapoptotic factor in human glioblastoma cells. Cancer Res 65:6029–6033.

Chen JF, Mandel EM, Thomson JM, Wu Q, Callis TE, Hammond SM, Conlon FL, Wang DZ. 2006. The role of microRNA-1 and microRNA-133 in skeletal muscle proliferation and differentiation. Nat Genet 38:228–233.

Cheng AM, Byrom MW, Shelton J, Ford LP. 2005. Antisense inhibition of human miRNAs and indications for an involvement of miRNA in cell growth and apoptosis. Nucleic Acids Res 33:1290–1297.

Courey AJ, Tjian R. 1998. Analysis of Sp1 in vivo reveals multiple transcriptional domains, including a novel glutamine-rich activation motif. Cell 55:887–898.

Day CP. McComb JM, Campbell RWF. 1990. QT dispersion: an indication of arrhythmia risk in patients with long QT intervals. Br Heart J 63:342–344.

Gintant GA. 1995. Regional differences in I_K density in canine left ventricle: role of I_{Ks} in electrical heterogeneity. Am J Physiol 268:H604–H613.

Griffiths-Jones S. 2004. The miRNA Registry. Nucleic Acids Res 32:D109–D111.

Jost N, Virag L, Bitay M, Takacs J, Lengyel C, Biliczki P, Nagy Z, Bogats G, Lathrop DA, Papp JG, Varro A. 2005. Restricting excessive cardiac action potential and QT prolongation: a vital role for I_{Ks} in human ventricular muscle. Circulation 112:1392–1399.

Kadonaga JT, Courey AJ, Ladika J, Tjian R. 1988. Distinct regions of Sp1 modulate DNA binding and transcriptional activation. Science 242:1566–1570.

Krutzfeldt J, Rajewsky N, Braich R, Rajeev KG, Tuschl T, Manoharan M, Stoffel M. 2005. Silencing of microRNAs in vivo with 'antagomirs'. Nature 438:685–689.

Liu DW, Antzelevitch C. 1995. Characteristics of the delayed rectifier current (I_{Kr} and I_{Ks}) in canine ventricular epicardial, midmyocardial, and endocardial myocytes. A weaker I_{Ks} contributes to the longer action potential of the M cell. Circ Res 76:351–365.

Lundquist AL, Turner CL, Ballester LY, George Jr, AL. 2006. Expression and transcriptional control of human KCNE genes. Genomics 87:119–128.

Meister G, Tuschl T. 2004. Mechanisms of gene silencing by double-stranded RNA. Nature 431:343–349.

Pang L, Koren G, Wang Z, Nattel S. Tissue-specific expression of two human $Ca_v1.2$ isoforms under the control of distinct 5'-flanking regulatory elements. 2003. FEBS Lett 546:349–354.

Pereon Y, Demolombe S, Baro I, Drouin E, Charpentier F, Escande D. 2000. Differential expression of KvLQT1 isoforms across the human ventricular wall. Am J Physiol 278:H1908–H1915.

Pugh BF, Tjian R. 1990. Mechanism of transcriptional activation by Sp1: evidence for coactivators. Cell 61:1187–1197.

Ramakers C, Vos MA, Doevendans PA, Schoenmakers M, Wu YS, Scicchitano S, Iodice A, Thomas GP, Antzelevitch C, Dumaine R. 2003. Coordinated down-regulation of KCNQ1 and KCNE1 expression contributes to reduction of I_{Ks} in canine hypertrophied hearts. Cardiovasc Res 57:486–496.

Ramakers C, Stengl M, Spatjens RL, Moorman AF, Vos MA. 2005. Molecular and electrical characterization of the canine cardiac ventricular septum. J Mol Cell Cardiol 38:153–161.

Roden DM, Yang T. 2005. Protecting the heart against arrhythmias: potassium current physiology and repolarization reserve. Circulation 112:1376–1378.

Sanguinetti MC, Curran ME, Zou A, Shen J, Spector PS, Atkinson DL, Keating MT. 1996. Coassembly of K_VLQT1 and minK (IsK) proteins to form cardiac I_{Ks} potassium channel. Nature 384:80–83.

Shi H, Wang H, Han H, Xu D, Yang B, Nattel S, Wang Z. 2002. Ultrarapid delayed rectifier K^+ current in the myogenic H9c2 cells: biophysical property and molecular identify. Cell Physiol Biochem 12:215–226.

Szabo G, Szentandrassy N, Biro T, Toth BI, Czifra G, Magyar J, Banyasz T, Varro A, Kovacs L, Nanasi PP. 2005. Asymmetrical distribution of ion channels in canine and human left-ventricular wall: epicardium versus midmyocardium. Pflugers Arch 450:307–316.

Szentadrassy N, Banyasz T, Biro T, Szabo G, Toth BI, Magyar J, Lazar J, Varro A, Kovacs L, Nanasi PP. 2005. Apico–basal inhomogeneity in distribution of ion channels in canine and human ventricular myocardium. Cardiovasc Res 65:851–860.

Tsuji Y, Opthof T, Yasui K, Inden Y, Takemura H, Niwa N, Lu Z, Lee JK, Honjo H, Kamiya K, Kodama I. 2002. Ionic mechanisms of acquired QT prolongation and torsades de pointes in rabbits with chronic complete atrioventricular block. Circulation 106:2012–2018.

Tsuji Y, Zicha S, Qi XY, Kodama I, Nattel S. 2006. Potassium channel subunit remodeling in rabbits exposed to long-term bradycardia or tachycardia: discrete arrhythmogenic consequences related to differential delayed-rectifier changes. Circulation 113:345–55.

Vallon V, Grahammer F, Richter K, Bleich M, Lang F, Barhanin J, Volkl H, Warth R. 2001. Role of KCNE1-dependent K^+ fluxes in mouse proximal tubule. J Am Soc Nephrol 12:2003–2011.

Verduyn SC, Vos MA, van der Zande J, van der Hulst FF, Wellens HJ. 1997. Role of interventricular dispersion of repolarization in acquired torsade-de-pointes arrhythmias: reversal by magnesium. Cardiovasc Res 34:453–463.

Verduyn SC, Vos MA, van der Zande J, Kulcsar A, Wellens HJ. 1997. Further observations to elucidate the role of interventricular dispersion of repolarization and early afterdepolarizations in the genesis of acquired torsade de pointes arrhythmias: a comparison between almokalant and d-sotalol using the dog as its own control. J Am Coll Cardiol 30:1575–1584.

Volders PG, Sipido KR, Carmeliet E, Spatjens RL, Wellens HJ, Vos MA. 1999. Repolarizing K^+ currents I_{TO1} and I_{Ks} are larger in right than left canine ventricular midmyocardium. Circulation 99:206–210.

Volders PG, Sipido KR, Vos MA, Spatjens RL, Leunissen JD, Carmeliet E, Wellens HJ. 1999. Downregulation of delayed rectifier K^+ currents in dogs with chronic complete atrioventricular block and acquired torsades de pointes. Circulation 100:2455–2461.

Wang H, Han H, Zhang L, Shi H, Schram G, Nattel S, Wang Z. 2001. Expression of multiple subtypes of muscarinic receptors and cellular distribution in the human heart. Mol Pharmacol 59:1029–1036.

Zhang Y, Wang J, Bai Y, Zhang H, Yang B, Wang H, Wang Z. 2006. Restoring depressed HERG K^+ channel function as a mechanism for insulin treatment of the abnormal QT prolongation and the associated arrhythmias in diabetic rabbits. Am J Physiol 291:1446–1455.

ZhaoY, Samal E, Srivastava D. 2005. Serum response factor regulates a muscle-specific microRNA that targets Hand2 during cardiogenesis. Nature 436:214–220.

Zheng W, Verlander JW, Lynch IJ, Cash MN, Shao J, Stow LR, Cain BD, Weiner ID, Wall SM, Wingo CS. 2006. Cellular distribution of the potassium channel,

KCNQ1, in normal mouse kidney. Am J Physiol Renal Physiol [Epub ahead of print].

2.8 Figures and Figure Legends

Figure 1 The 5'-flanking regions containing the core promoter sequence and transcription start sites of the *KCNQ1*. Transcription start sites (TSSs) are indicated by backward arrows and designated position +1. The consensus binding sequences for Sp1 transcription factor are underlined and core sequences of the Sp1 *cis*-elements are bold. For convenience, the Sp1 consensus sites are numbered in order from TSS and the positions, relative to TSS, at the first nucleotide of the consensus core sequence are donated by the numbers in the brackets. The core promoter sequence *KCNE1a* is presented for comparison.

Figure 2 Analysis of the *KCNQ1* promoter activities in various cell lines. A schematic representation of the 5' deletion constructs of the *KCNQ1* promoter region is shown in up-left panels. Nucleotides of fusion plasmids are numbered with respect to the TSS (+1) identified by 5'RACE. Firefly luciferase expression levels were divided by co-expressed Renilla luciferase activity and expressed as relative activity divided by the promoter-less construct (PGL3-Basic). The experiments were performed in duplicate for each experiment and the number (n) of experiments is indicated in the brackets.

Figure 3 Role of stimulating protein 1 (Sp1) as a common driving factor for *KCNQ1* and *KCNE1a* transcriptions. (**A**) and (**B**) Effects of Sp1 inhibitor mithramycin (100 nM) on the activities of the core promoters (*KCNQ1*: -329/+60 and *KCNE1a*: -244/+257) and endogenous mRNA levels were evaluated in H9c2 cells. **p*<0.05 *vs.* PGL3-Basic (Base) or Control (Ctl); n=5 for each group. (**C**) Effects of Sp1 overexpression (+CMVp-Sp1) on *KCNQ1* and *KCNE1a* promoter (-329/+60 and -244/+257, respectively) activities and endogenous mRNA levels in HEK293 cells. +CMVp: co-transfection of Sp1-null CMVp vector and target DNA-PGL-3 vectors. **p*<0.05 +CMVp-Sp1 *vs.* +CMVp; n=6 for each group. (**D**) Reporter activities of the core promoter fragments of *KCNQ1* (-329/+60) and

KCNE1a (-244/+257) in Sp1-null *Drosophila* Schneider cells (SL2). Cells were transfected with Sp1-free plasmid (pPac) or with Sp1-carrying plasmid (pPac-Sp1). *p<0.05 pPac-Sp1 *vs.* pPac; n=4 for each group. The experiments were performed in duplicate for each experiment.

Figure 4 Post-transcriptional repression of KCNQ1 by the muscle-specific microRNA *miR-133*. (**A**) The complementarity (bold font) between *miR-133* and each of the four target sites in the 3'UTR of *KCNQ1*. (**B**) Sequences of *miR-133*, mutant *miR-133* and anti-*miR-133* antisense inhibitor oligonucleotides (AMO-133). Bold-face letters indicate the 'seed site' critical for miRNA::mRNA binding and interaction; lower-case letters indicate the base substitution mutations made to the sequences; italics in the AMO-133 indicate the locked nucleotides (the ribose ring is constrained by a methylene bridge between the 2'-*O*- and the 4'-C atoms, to confer a higher thermal stability, discriminative power and a longer half-life). (**C**) Luciferase reporter activities showing the interaction between *miR-133* and *KCNQ1*-3'UTR in HEK293 cells. *miR-133* (10 nM), mutant *miR-133* (100 nM, Mt-133), +AMO-133 (100 nM) or *miR-1* (10 nM). The "+" before the labels indicate co-transfection with miRNA. *p<0.05 *vs.* Ctl; +p<0.05 *vs.* *miR-133* (10 nM); n=6 for each group. (**D**) Luciferase reporter activities verifying the interactions of *miR-133* with its exact binding sequence (standard) in HEK293 cells. *p<0.05 *vs.* Ctl; n=8 for each group. (**E**) Western blot analysis of KCNQ1 protein level under various conditions with protein samples isolated from HEK293 cells. AP: antigenic peptide pretreatment. *p<0.05 *vs.* Ctl; +p<0.05 *vs.* *miR-133* (10 nM); n=5 for each group. (**F**) Real-time RT-PCR analysis of *KCNQ1* mRNA levels in HEK293 cells. *p<0.05 *vs.* Ctl; +p<0.05 *vs.* *miR-133* (10 nM); n=4 for each group.

Figure 5 Post-transcriptional repression of KCNE1 by the muscle-specific microRNA *miR-1*. (**A**) The complementarity (bold font) between *miR-1* and each of the four target sites in the 3'UTR of *KCNE1*. (**B**) Sequences of *miR-1*, mutant *miR-1* and anti-*miR-1* antisense inhibitor oligonucleotides

(AMO-1). Bold-face letters indicate the 'seed site' critical for miRNA::mRNA binding and interaction; lower-case letters indicate the base substitution mutations made to the sequences; italics in the AMO-1 indicate the locked nucleotides. (**C**) Luciferase reporter activities showing the interaction between *miR-1* and *KCNE1*-3'UTR in HEK293 cells. *miR-1* (10 nM), mutant *miR-1* (100 nM, Mt-1), AMO-1 (100 nM) or *miR-133* (10 nM). The "+" before the labels indicate co-transfection with miRNA. **p*<0.05 *vs*. Ctl; +*p*<0.05 *vs*. *miR-1* (10 nM); n=5 for each group. (**D**) Luciferase reporter activities verifying the interactions of *miR-1* with its exact binding sequence (standard) in HEK293 cells. **p*<0.05 *vs*. Ctl; n=8 for each group. (**E**) Western blot analysis of KCNE1 protein level (35 kDa) under various conditions with protein samples isolated from HEK293 cells. AP: antigenic peptide pretreatment. **p*<0.05 *vs*. Ctl; +*p*<0.05 *vs*. *miR-1* (10 nM); n=6 for each group. (**F**) Real-time RT-PCR analysis of *KCNE1* mRNA levels in HEK293 cells. **p*<0.05 *vs*. Ctl; +*p*<0.05 *vs*. *miR-1* (10 nM); n=4 for each group. (**G**) Real-time RT-PCR analysis of *miR-1* and *miR-133* levels in H9c2 cells. Transfection of AMO-1 (10 nM) and AMO-133 (10 nM) alone for studying the endogenous miRNAs or co-transfection with *miR-1* (10 nM) or *miR-133* (10 nM), as indicated by +AMO-1 or +AMO-133, for verifying the efficacy against the exogenous miRNAs. **p*<0.05 *vs*. Ctl; n=5 for each group.

Figure 6 Regional differences of expressions of *KCNQ1* (**A**) and *KCNE1* (**B**) at protein and mRNA levels, determined by Western blot and real-time-RT-PCR, in human hearts. Protein and RNA samples were isolated from left (LV) and right ventricular (RV) epicardium, epicardium (Epi) and midmyocardium (Mid) of left ventricular wall, and apical (Apex or Ax) and basal (Base or Bs) areas of left ventricular epicardium. **p*<0.05, Unpaired Student *t*-test; LV *vs*. RV, Epi *vs*. Mid, or Apex (Ax) *vs*. Base (Bs). The number of samples used for data analysis is indicated in the brackets.

Figure 7 Regional differences of expressions of Sp1 (**A**) and *miR-1* (**B**) and *miR-133* (**C**) genes in human hearts. *$p<0.05$, Unpaired Student *t*-test; LV *vs.* RV, Epi *vs.* Mid, or Apex (Ax) *vs.* Base (Bs). The number of samples used for data analysis is indicated in the brackets.

Figure 1

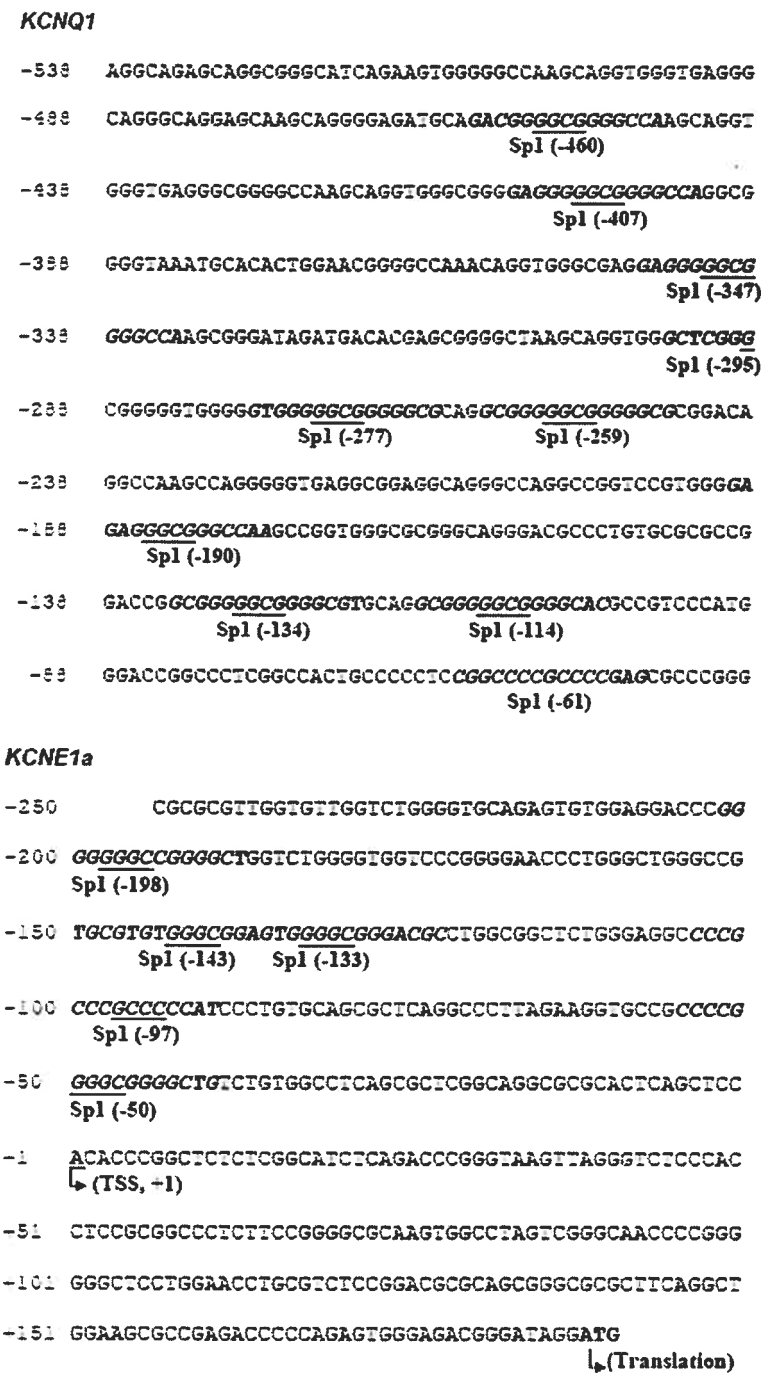
KCNQ1
-538 AGGCAGAGCAGGCGGGCATCAGAAGTGGGGGCCAAGCAGGTGGGTGAGGG
-488 CAGGGCAGGAGCAAGCAGGGGAGATGCAGACGGGGCGGGGCCAAGCAGGT
Sp1 (-460)
-438 GGGTGAGGGCGGGGCCAAGCAGGTGGGCGGGGAGGGGGCGGGGCCAGGCG
Sp1 (-407)
-388 GGGTAAATGCACACTGGAACGGGGCCAAACAGGTGGGCGAGGAGGGGGCG
Sp1 (-347)
-338 GGGCCAAGCGGGATAGATGACACGAGCGGGGCTAAGCAGGTGGGCTCGGG
Sp1 (-295)
-288 CGGGGGTGGGGGTGGGGGCGGGGGCGCAGGCGGGGGCGGGGGCGCGGACA
Sp1 (-277) Sp1 (-259)
-238 GGCCAAGCCAGGGGGTGAGGCGGAGGCAGGGCCAGGCCGGTCCGTGGGGA
-188 GAGGGCGGGCCAAGCCGGTGGGCGCGGGCAGGGACGCCCTGTGCGCGCCG
Sp1 (-190)
-138 GACCGGCGGGGGCGGGGCGTGCAGGCGGGGGCGGGGCACGCCGTCCCATG
Sp1 (-134) Sp1 (-114)
-88 GGACCGGCCCTCGGCCACTGCCCCCTCCGGCCCCGCCCCGAGCGCCCGGG
Sp1 (-61)
KCNE1a
-250 CGCGCGTTGGTGTTGGTCTGGGGTGCAGAGTGTGGAGGACCCGG
-200 GGGGGCCGGGGCTGGTCTGGGGTGGTCCCGGGGAACCCTGGGCTGGGCCG
Sp1 (-198)
-150 TGCGTGTGGGCGGAGTGGGGCGGGACGCCTGGCGGCTCTGGGAGGCCCCG
Sp1 (-143) Sp1 (-133)
-100 CCCGCCCCCATCCCTGTGCAGCGCTCAGGCCCTTAGAAGGTGCCGCCCCG
Sp1 (-97)
-50 GGGCGGGGCTGTCTGTGGCCTCAGCGCTCGGCAGGCGCGCACTCAGCTCC
Sp1 (-50)
-1 ACACCCGGCTCTCTCGGCATCTCAGACCCGGGTAAGTTAGGGTCTCCCAC
(TSS, +1)
-51 CTCCGCGGCCCTCTTCCGGGGCGCAAGTGGCCTAGTCGGGCAACCCCGGG
-101 GGGCTCCTGGAACCTGCGTCTCCGGACGCGCAGCGGGCGCGCTTCAGGCT
-151 GGAAGCGCCGAGACCCCCAGAGTGGGAGACGGGATAGGATG
(Translation)

Figure 2

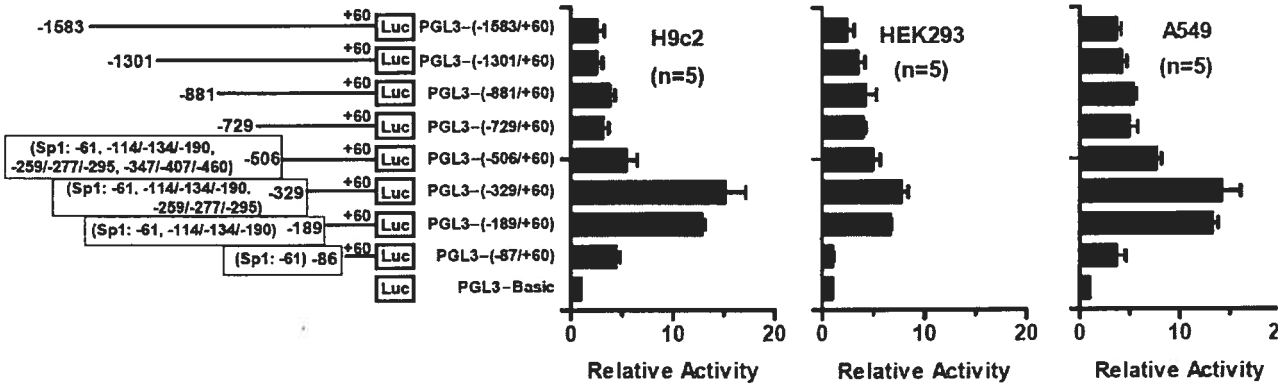
-1583
+60
Luc
PGL3–(-1583/+60)
-1301
PGL3–(-1301/+60)
-881
PGL3–(-881/+60)
-729
PGL3–(-729/+60)
(Sp1: -61, -114/-134/-190, -259/-277/-295, -347/-407/-460)
-506
PGL3–(-506/+60)
(Sp1: -61, -114/-134/-190, -259/-277/-295)
-329
PGL3–(-329/+60)
(Sp1: -61, -114/-134/-190)
-189
PGL3–(-189/+60)
(Sp1: -61)
-86
PGL3–(-87/+60)
PGL3–Basic
H9c2
(n=5)
HEK293
(n=5)
A549
(n=5)
0
10
20
Relative Activity

Figure 3

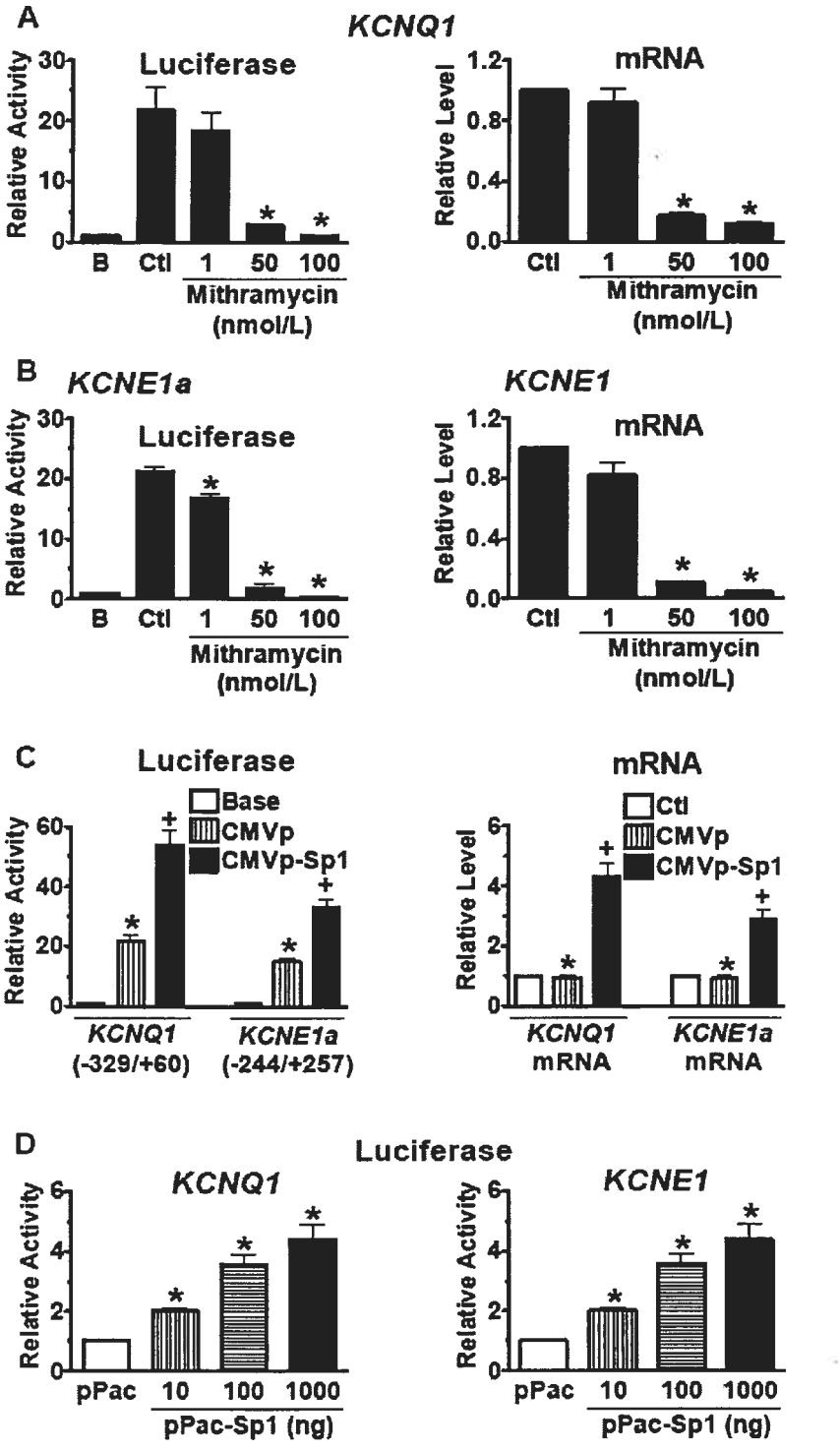
A
KCNQ1
Luciferase
Relative Activity
30
20
10
0
B Ctl 1 50 100
Mithramycin (nmol/L)
mRNA
Relative Level
1.2
0.8
0.4
0.0
Ctl 1 50 100
Mithramycin (nmol/L)
B
KCNE1a
KCNE1
Luciferase
mRNA
C
Luciferase
mRNA
Base
CMVp
CMVp-Sp1
Ctl
Relative Activity
60
40
20
0
Relative Level
6
4
2
0
KCNQ1 (-329/+60)
KCNE1a (-244/+257)
KCNQ1 mRNA
KCNE1a mRNA
D
Luciferase
KCNQ1
KCNE1
pPac 10 100 1000
pPac-Sp1 (ng)

Figure 4

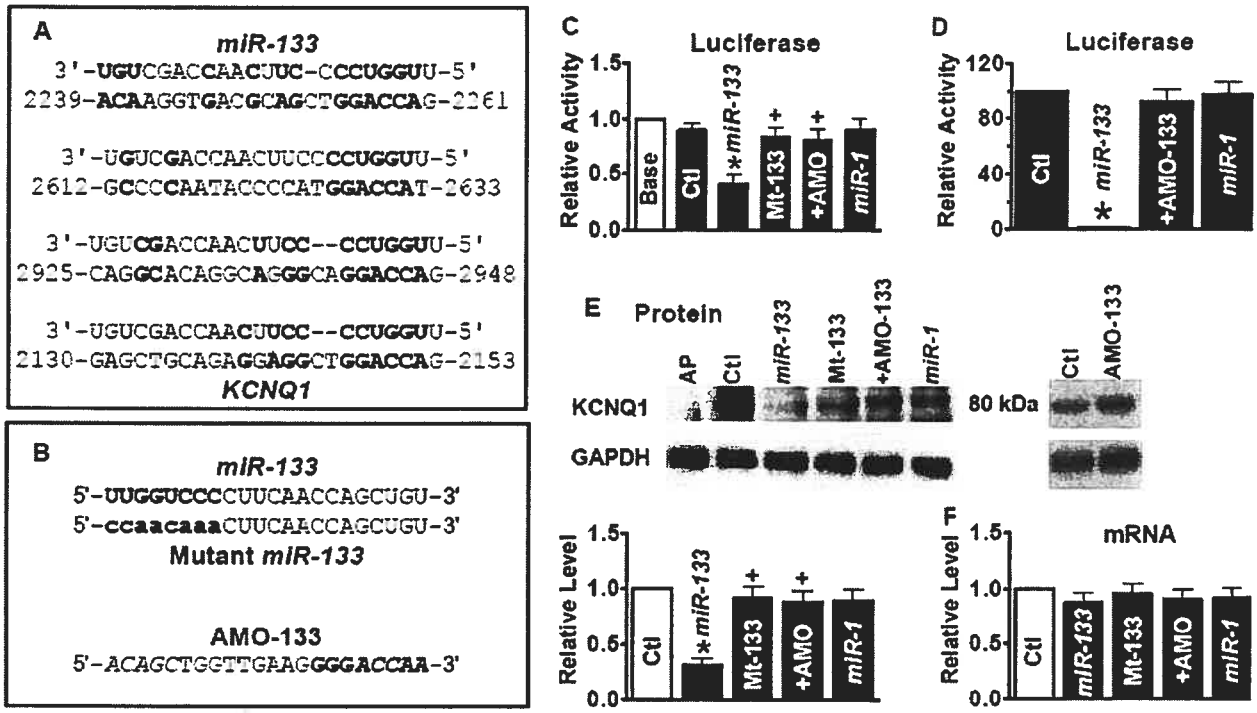
A
miR-133
3'-UGUCGACCAACUUC-CCCUGGUU-5'
2239-ACAAGGTGACGCAGCTGGACCAG-2261
3'-UGUCGACCAACUUCCCCUGGUU-5'
2612-GCCCCAATACCCCATGGACCAT-2633
3'-UGUCGACCAACUUCC--CCUGGUU-5'
2925-CAGGCACAGGCAGGGCAGGACCAG-2948
3'-UGUCGACCAACUUCC--CCUGGUU-5'
2130-GAGCTGCAGAGGAGGCTGGACCAG-2153
KCNQ1
B
miR-133
5'-UUGGUCCCCUUCAACCAGCUGU-3'
5'-ccaacaaaCUUCAACCAGCUGU-3'
Mutant miR-133
AMO-133
5'-ACAGCTGGTTGAAGGGACCAA-3'
C
Luciferase
Relative Activity
Base
Ctl
*miR-133
Mt-133
+AMO
miR-1
D
Luciferase
Relative Activity
Ctl
* miR-133
+AMO-133
miR-1
E
Protein
AP
Ctl
miR-133
Mt-133
+AMO-133
miR-1
KCNQ1
GAPDH
80 kDa
Ctl
AMO-133
Relative Level
mRNA
Ctl
*miR-133
Mt-133
+AMO
miR-1

Figure 5

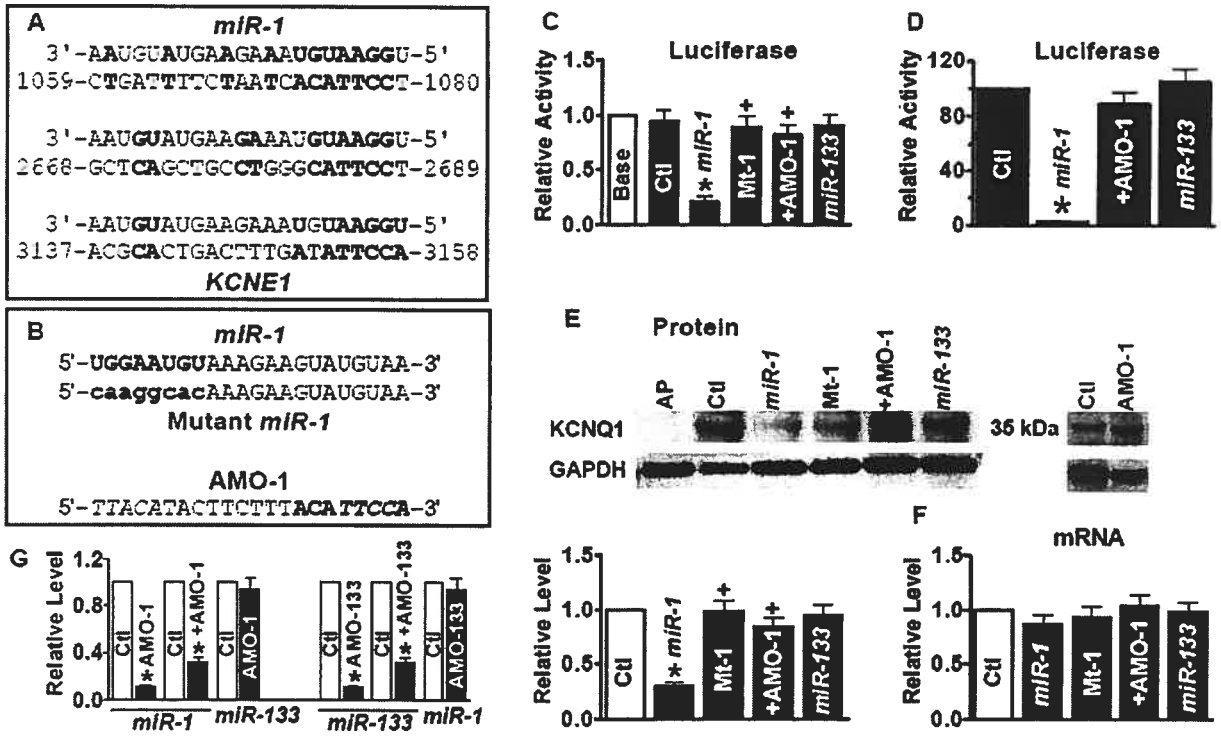
A
miR-1
3'-AAUGUAUGAAGAAAUGUAAGGU-5'
1059-CTGATTTCTAATCACATTCCT-1080
3'-AAUGUAUGAAGAAAUGUAAGGU-5'
2668-GCTCAGCTGCCTGGGCATTCCT-2689
3'-AAUGUAUGAAGAAAUGUAAGGU-5'
3137-ACGCACTGACTTTGATATTCCA-3158
KCNE1
B
miR-1
5'-UGGAAUGUAAAGAAGUAUGUAA-3'
5'-caaggcacAAAGAAGUAUGUAA-3'
Mutant miR-1
AMO-1
5'-TTACATACTTCTTTACATTCCA-3'
C
Luciferase
Relative Activity
Base
Ctl
* miR-1
Mt-1
+AMO-1
miR-133
D
Luciferase
Relative Activity
Ctl
* miR-1
+AMO-1
miR-133
E
Protein
AP
Ctl
miR-1
Mt-1
+AMO-1
miR-133
KCNQ1
GAPDH
35 kDa
Ctl
AMO-1
F
mRNA
Relative Level
Ctl
* miR-1
Mt-1
+AMO-1
miR-133
G
Relative Level
Ctl
* AMO-1
Ctl
* +AMO-1
Ctl
AMO-1
Ctl
* AMO-133
Ctl
* +AMO-133
Ctl
AMO-133
miR-1
miR-133
miR-133
miR-1

Figure 6

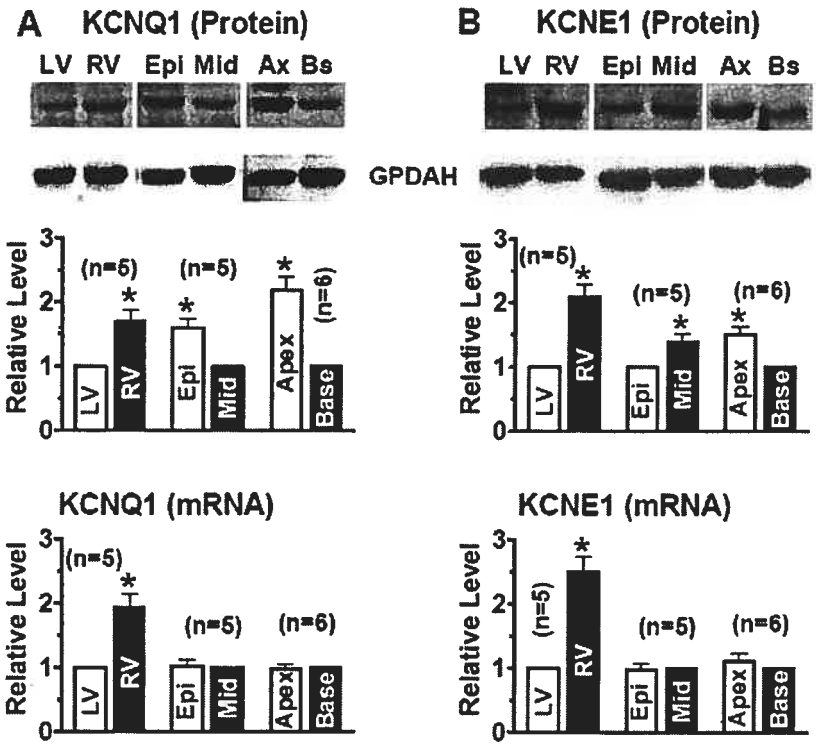
A KCNQ1 (Protein)
LV RV Epi Mid Ax Bs
GPDAH
B KCNE1 (Protein)
LV RV Epi Mid Ax Bs
Relative Level
(n=5)
(n=5)
(n=6)
LV
RV
Epi
Mid
Apex
Base
KCNQ1 (mRNA)
KCNE1 (mRNA)

Figure 7

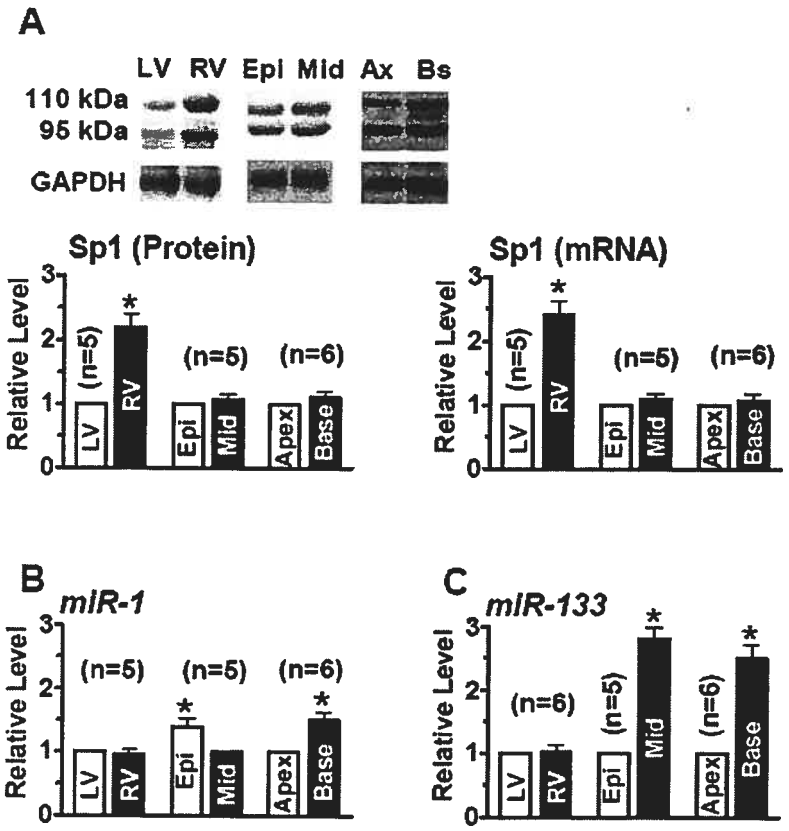
A
LV RV Epi Mid Ax Bs
110 kDa
95 kDa
GAPDH
Sp1 (Protein)
Relative Level
(n=5)
(n=5)
(n=6)
LV
RV
Epi
Mid
Apex
Base
Sp1 (mRNA)
B
miR-1
C
miR-133

Chapter 3. MicroRNA *miR-133* Represses HERG K^+ Channel Expression

In this chapter, we experimentally established the post-transcriptional repression of HERG1 by *miR-133*. We also examined the role of *miR-133* in determining the disparate expression of HERG1 on mRNA and protein levels under diabetic condition.

This work is published in the ***Journal of Biological Chemistry*** 2007; 282(17):12363-7.

MICRORNA *MIR-133* REPRESSES HERG K^+ CHANNEL EXPRESSION CONTRIBUTING TO QT PROLONGATION IN DIABETIC HEARTS*

Jiening Xiao,[†§¶] Xiaobin Luo,[†§¶] Huixian Lin,[†§¶] Ying Zhang,[‡¶] Yanjie Lu,[‡¶] Ning Wang,[‡¶]

Yiqiang Zhang,[†§] Baofeng Yang,[‡¶] and Zhiguo Wang,[†§¶]

[†]Research Center, Montreal Heart Institute, Montreal, PQ H1T 1C8 Canada;

[§]Department of Medicine, University of Montreal, Montreal, PQ H3C 3J7 Canada;

[‡]Department of Pharmacology (State-Province Key Laboratories of Biomedicine-Pharmaceutics) and [¶]Institute of Cardiovascular Research, Harbin Medical University, Harbin, Heilongjiang 150086, P.R. China

Running Title: Role of *microRNA-133* in diabetic QT prolongation

Address correspondence to: Dr. Zhiguo Wang, Research Center, Montreal Heart Institute, 5000 Belanger East, Montreal, PQ H1T 1C8, Canada; Tel.: (514) 376-3330. Fax: (514) 376-1335. E-mail: [redacted]. Prof. Baofeng Yang, Harbin Medical University, Heilongjiang 150086, P. R. China; Tel.: +86 (451) 8667-9473; E-[redacted]

3.1 Abstract

Discovery of microRNA (miRNA) has revolutionized our understanding of the mechanisms that regulate gene expression. However, the potential pathophysiological roles of the muscle-specific microRNA *miR-133* in adult hearts remained unexplored. We have previously found that the *ether-a-go-go* related gene (ERG), a long QT syndrome gene encoding a key K^+ channel (I_{Kr}) in cardiac cells, is severely depressed in its expression at the protein level but not at the mRNA level in diabetic subjects. The mechanisms underlying the disparate alterations of ERG protein and mRNA, however, remained unknown. We report here a remarkable overexpression of *miR-133* in hearts from a rabbit model of diabetes, and in parallel the expression of serum response factor (SRF), which is known to be a transactivator of *miR-133*, was also robustly increased. Delivery of exogenous *miR-133* into the rabbit myocytes and cell lines produced post-transcriptional repression of ERG, downregulating ERG protein level without altering its transcript level and caused substantial depression of I_{Kr}, an effect abrogated by the *miR-133* antisense inhibitor. The mutant *miR-133* failed to produce any effects. Functional inhibition or gene silencing of SRF downregulated *miR-133* expression and increased I_{Kr} density. Repression of ERG by *miR-133* likely underlies the differential changes of ERG protein and transcript thereby depression of I_{Kr}, and contributes to repolarization slowing thereby QT prolongation and the associated arrhythmias, in diabetic hearts. Our study provided the first evidence for the pathological role of *miR-133* in adult hearts, and thus expanded our understanding of the cellular function and pathophysiological roles of miRNAs.

3.2 Introduction

Abnormal QT interval prolongation is a prominent electrical disorder and has been proposed a predictor of mortality in patients with diabetes mellitus (DM), presumably because it is associated with an increased risk of sudden cardiac death consequent to lethal ventricular arrhythmias (1-8). Our recent study revealed that the

long QT syndrome gene, human *ether-a-go-go*-related gene (*HERG*) encoding the channel responsible for rapid delayed rectifier K^+ current (I_{Kr}), is significantly downregulated in its expression in diabetic hearts and this downregulation contributes critically to diabetic repolarization slowing and QT prolongation (9,10). Strikingly, HERG expressions at transcriptional and post-transcriptional levels diverge in diabetic hearts, with its protein levels being reduced by some 60% while the mRNA levels remaining essentially unaltered (10). These disparate changes indicate that HERG expression is impaired mainly at the post-transcriptional level; however, it remained unclear what are the determinants for the differential regulations of HERG expression at protein and transcript levels.

MicroRNAs (miRNAs) are endogenous ~22-nt non-coding RNAs that anneal to inexactly complementary sequences in the 3'UTRs of target mRNAs of protein-coding genes to regulate gene expression. The major characteristics of miRNA actions is to specify translational repression without affecting the levels of the targeted mRNA (11,12). Among >300 miRNAs identified thus far, *miR-1* and *miR-133* are known to specifically express in adult cardiac and skeletal muscle tissues (13,14). Recent studies revealed that *miR-1* and *miR-133* play critical roles in regulating myogenesis. Increasing expression of *miR-1* and *miR-133* has been found in neonatal hearts and substantially higher levels are maintained in adult cardiac tissues (14), suggesting that in addition to regulating myogenesis, they may also possess other cellular functions in adult cardiac cells. However, our current understanding of the function of these miRNAs is still limited to developmental regulation and their possible roles in other cellular processes have not yet been explored.

We proposed that the muscle-specific miRNAs *miR-1/miR-133* are able to repress HERG translation while keeping its mRNA unaffected and their levels are upregulated in diabetic hearts, which causes the disparate changes of HERG protein and mRNA levels. This study was designed to test this hypothesis.

3.3 Experimental Procedures

3.3.1 Preparation of Rabbit Model of Diabetes Mellitus (DM)

Male New Zealand white rabbits weighing 1.6~2.0 Kg (Charles River Canada Inc) were used and the procedures for development of alloxan-induced DM model were the same as previously described in detail (9,10). The QT measurements and simultaneously recorded RR intervals were used to derive heart rate corrected QT intervals. Incidences of ventricular tachycardia (VT) and ventricular fibrillation (VF) were determined. All procedures are in accordance with the guidelines set by the Animal Ethics Committee of the Montreal Heart Institute and of Harbin Medical University.

3.3.2 Isolation of Rabbit Ventricular Myocytes and Cell Culture

Myocytes were isolated from rabbit left ventricular endocardium via enzymatic digestion of the whole heart on a Langendorff apparatus with the procedures similar to previously described (9,10). The freshly isolated myocytes were stored either in the extracellular solution for patch-clamp recordings or in 199 Medium as detailed elsewhere (9,15).

3.3.3 Whole-Cell Patch-Clamp Recording

Patch-clamp recording of I_{Kr} currents has been described in detail elsewhere (9,10).

3.3.4 Synthesis of miRNAs and Anti-miRNA Antisense Inhibitors and Their Mutant Constructs

MiR-1 and *miR-133* and their respective mutant constructs were synthesized by Integrated DNA Technologies, Inc. (IDT) as detailed elsewhere (16) (also see **Supplementary Fig. 1**). The mutant miRNAs each had eight nucleotides mismatches at the 5'-end, which disrupts their binding to the target sites and thus turns the miRNAs into negative controls (11-14,16).

3.3.5 Construction of Chimeric miRNA-Target Site–Luciferase Reporter Vectors

To construct reporter vectors bearing miRNA-target sites, we synthesized (by Invitrogen) fragments containing the exact target sites for *miR-1* and *miR-133* or the

mutated target sites, *HERG* cDNA and inserted these fragments into the multiple cloning sites downstream the luciferase gene (HindIII and SpeI sites) in the pMIR-REPORT™ luciferase miRNA expression reporter vector (Ambion, Inc.), as detailed elsewhere (16).

3.3.6 Small Interference RNA (siRNA) Treatment

The Stealth™ siRNAs targeting SRF (sense: 5'GCAGAGGCAACUGACUUCAUUUGUG3' and antisense: 5'CACAAAUGAAGUCAGUUGCCUCUGC3'; 3096-3131) and a negative control siRNA (sense: 5'GCAACGGGUCAUUCAUUACUAGGUG3' and antisense: 5'CACCUAGUAAUGAAUGACCCGUUGC3'; 3096-3131) were synthesized by Invitrogen.

3.3.7 Cell Culture

SKBr3 (human breast cancer cell line) and HEK293 (human embryonic kidney cell line) were purchased from American Type Culture Collection (ATCC, Manassas, VA). The cells were cultured as previously described (17)

3.3.8 Transfection and Luciferase Assay

The transfection procedures for cell lines and rabbit cardiac myocytes in primary culture, and luciferase activity assays were the same as described in detail elsewhere (16,17). Before transfection, cells were starved to synchronize growth by incubating in serum- and antibiotics-free medium for 12 h.

3.3.9 Quantification of mRNA and miRNA Levels

The procedures for quantification of HERG and serum responsive factor (SRF) transcripts by conventional Taqman real-time RT-PCR were the same as previously described (16).

The *mir*Vana™ qRT-PCR miRNA Detection Kit (Ambion), a quantitative reverse transcription-PCR (qRT-PCR) kit was used in conjunction with real-time PCR with SYBR Green I for quantification of *miR-1* and *miR-133* (*miR-133a* + *miR-133b*) transcripts (16). The total RNA samples were isolated with Ambion's *mir*Vana miRNA Isolation Kit from SKBr3 cells, HEK293 cells, rabbit hearts and human hearts. Fold variations in expression of *miR-133* between RNA samples were calculated after normalization to 5s rRNA. Human tissues were obtained from the

Second Affiliated Hospital of Harbin Medical University under the procedures approved by the Ethnic Committee for Use of Human Samples of the Harbin Medical University and from the Réseau de tissus pour études biologiques (RETEB) tissue bank under the procedures approved by the Human Research Ethics Committee of the Montreal Heart Institute. The criteria for inclusion of the tissues in our study were the patients that did not have primary heart problems at the time of death.

3.3.10 Western Blot

The procedures for semi-quantification of ERG and SRF protein levels were the same as described in detail elsewhere (9,10,15-17). Membrane protein samples were extracted from left ventricular wall of rabbits and SKBr3 cells. The goat polyclonal antibodies against ERG and SRF were both purchased from Santa Cruz Biotechnology Inc.

3.3.11 Data Analysis

Group data are expressed as mean ± S.E. Statistical comparisons (performed using ANOVA followed by Dunnett's method) were carried out using Microsoft Excel. A two-tailed $p<0.05$ was taken to indicate a statistically significant difference.

3.4 Results

3.4.1 Overexpression of miR-1 and miR-133 and Downregulation of ERG Protein Level in Diabetic Hearts

Both *miR-1* and *miR-133* were expressed in rabbit hearts; however, *miR-133* was approximately 10 times more abundant than that of *miR-1*. The levels of both *miR-1* and *miR-133* were found some 2.2 folds and 3 folds higher, respectively, in the ventricular RNA samples from rabbits with DM than those from healthy control animals. Upregulation of the muscle-specific miRNAs was also observed in the ventricular samples from DM patients (Fig. 1).

We also reproduced the observations reported in our previous study (9,10), i.e., the protein level of the rabbit ERG (rbERG) was significantly lower in diabetic hearts than in healthy hearts despite that the transcript level remained unchanged. We further demonstrated the same disparity between HERG protein and mRNA

expression levels in the hearts from DM patients (Fig. 1). Note that the molecular masses of ERG in rabbit (155 kDa and 135 kDa) and human (140 kDa and 120 kDa) were somewhat different presumably due to different glycosylations in different species; the larger band represents the mature glycosylated form and the smaller band represents the non-glycosylated form of ERG protein (16). The size rbERG is consistent with our previous finding (9,10) and that of HERG is identical to the results reported by Jones *et al* (18).

3.4.2 Post-Transcriptional Repression of HERG Expression by miR-133

HERG and rbERG share 91% homology in their sequences. We identified multiple putative target sites for *miR-133* in rbERG and in HERG based on complementarity: at least six nucleotides exactly matching the 2-10 nucleotides from the 5'-end of *miR-133* (**Supplementary Fig. 1**). These sites may cooperate to confer the regulation by *miR-133*. Neither HERG nor rbERG contains any sites with more than five complementary nucleotides to *miR-1*.

To verify that HERG and rbERG are the cognate targets of *miR-133* for post-transcriptional repression, we first inserted *HERG* cDNA into the 3'UTR of a luciferase reporter plasmid containing a constitutively active promoter in order to determine the effects of *miR-133* on reporter expression. Co-transfection of *miR-133* and the chimeric luciferase-*HERG* vector into HEK293 cells consistently demonstrated smaller luciferase activities relative to transfection of the chimeric plasmid alone, but co-transfection of the mutant *miR-133* (M-*miR-133*) failed to produce any effects (Fig. 2A). HEK293 cells were used for luciferase reporter assays because these cells do not express endogenous ERG protein and *miR-1*/*miR-133* (**Supplementary Fig. 2**). Co-application of *miR-133* with its antisense inhibitor AMO-133 eliminated the silencing effect on luciferase reporter activities (16,19,20). As an additional negative control, application of *miR-1* failed to affect luciferase reporter activity.

The uptake and activities of transfected miRNAs was confirmed by using *miR-1* and *miR-133* standards in which the complementary sequences of *miR-1* and *miR-133* were cloned downstream of luciferase gene in the pMIR-REPORT plasmid (Fig. 2B).

We determined the effects of *miR-133* on endogenous expression of HERG at the protein level by Western blot with SKBr3 membrane protein samples. SKBr3 was used because it is a human cell line that expresses endogenous HERG (17) but does not express the muscle-specific *miR-1* or *miR-133* (**Supplementary Fig. 2**). Our data showed that transfection of *miR-133* reduced HERG protein level down to ~10% of control value, and as a negative control the mutant *miR-133* did not cause any appreciable changes (Fig. 2C). Co-application of AMO-133 nearly abolished the effects of *miR-133*, verifying the specificity of the *miR-133* action. Moreover, transfection of *miR-1* failed to affect HERG protein level. By comparison, *miR-133* produced virtually no effects on HERG mRNA level (Fig. 2D), indicating that *miR-133* does not affect HERG mRNA stability.

The functional significance of ERG regulation by *miR-133* was explored by whole-cell patch-clamp studies of I_{Kr} in isolated ventricular myocytes in primary culture. I_{Kr} density in the myocytes from DM hearts or in the myocytes from healthy control heart transfected with *miR-133* was severely diminished (Fig. 2E). The depression induced by DM was partially reversed by AMO-133 and that induced by exogenous *miR-133* was abolished by AMO-133. AMO-133 slightly enhanced I_{Kr} in control cells, presumably by eliminating the repressive effects of basal endogenous *miR-133*. As a negative control, *miR-1* failed to affect I_{Kr}.

3.4.3 Potential Role of Serum Responsive Factor (SRF) in miR-133 Overexpression

It has been shown that expression of *miR1/miR-133* is dependent upon binding of SRF to their promoter regions (13,14), an important transcriptional factor in cardiac cells (21-24). SRF protein level was found significantly increased in diabetic hearts relative to healthy hearts, and so was SRF transcript level (Fig. 3A). Incubation of the DM myocytes in primary culture with distamycin A, which has been shown to selectively inhibit binding of SRF to its *cis*-element (25), largely reversed the increases in *miR-1/miR-133* expression (Fig. 3B). This effect was further confirmed by silencing of SRF using the siRNA directed against SRF (SRF-siRNA) (Fig. 3C). Moreover, in cells isolated from DM rabbits, SRF-siRNA, but not the negative control siRNA, increased I_{Kr} density (Fig. 3D). The siRNA and distamycin

A both slightly increased I_{Kr} density in healthy control cells, presumably by inhibiting basal SRF. The efficiency of the SRF-siRNA in silencing SRF expression at mRNA level was verified (Fig. 3E). Unfortunately, the primary culture did not allow for sufficient quantity of protein samples for Western blot analysis of SRF protein levels or HERG protein levels.

3.5 Discussion

MiRNA-mediated gene regulation is now considered a fundamental layer of genetic programs that operates at the post-transcriptional level. However, in spite of our ability to identify miRNAs, regulatory targets have not been established or even confidently predicted for any of the vertebrate miRNAs, which has hampered progress toward elucidating the functions of miRNAs. Our current understanding of the functions of miRNAs primarily relies on their tissue-specific or developmental stage-specific expression patterns as well as their evolutionary conservation, and is thus largely limited to biogenesis and oncogenesis. Target finding and function discovery are two major challenges to researchers in miRNA research. The present study revealed the ability of a miRNA to regulate ion channel expression and the possible role in electrical remodeling in diabetic myocardium. It thus expanded our understanding of the cellular function and pathophysiological roles of miRNAs in a whole, reconsolidating the view that miRNAs likely have widespread functions in the cells.

Our study provides an explanation for the observed discrepancy between changes of HERG/rbERG expression at protein and mRNA levels. In our recent study on QT prolongation of diabetic hearts, we demonstrated that I_{Kr} density and ERG protein level were remarkably diminished, being the major factor for QT prolongation in diabetic rabbits, whilst ERG mRNA level was unaffected (9). Reduction of I_{Kr} due to expression repression of HERG by *miR-133* is expected to result in repolarization slowing thereby QT prolongation. In our recent study, we found that *miR-133* repressed KCNQ1 (16), a channel protein responsible for the slow delayed rectifier K^+ current (I_{Ks}) in cardiac cells. However, whether I_{Ks} has significant contribution to

diabetic QT prolongation is still an open question and our previous studies suggest a minimal role of I_{Ks} (9,10). Nonetheless, our study points to an important role of *miR-133* in abnormal QT prolongation in diabetes and maybe in other pathological conditions as well. Our data also indicate that the cardiac-specific *miR-1* is not responsible for the down-regulation of I_{Kr} in DM heart.

It is important to note here that the phenomenon of disparate changes of ERG expression at protein and mRNA levels have also been observed in failing heart and ischemic myocardium. For example, several studies found that I_{Kr} current density was significantly diminished in myocytes from failing hearts that is also electrophysiologically characterized by repolarization slowing and QT prolongation similar to diabetic hearts, despite that the mRNA level of HERG was barely altered under these conditions (24-29). Whether these disparate changes of ERG protein and mRNA in failing hearts and ischemic myocardium are consequent to upregulation of *miR-133* expression is worthy of detailed studies.

Our study also provides evidence for the potential role of SRF in *miR-133* overexpression in DM myocytes. The SRF-siRNA not only nullifies the increase in *miR-133* but also rescues depressed I_{Kr} in DM. Whether SRF inhibition or knockdown could have beneficial effects on diabetic QT prolongation merits future investigations.

3.6 References

1. Christensen, P.K., Gall, M.A., Major-Pedersen, A., Sato, A., Rossing, P., Breum, L., Pietersen, A., Kastrup, J., and Parving, H.H. (2000) *Scand. J. Clin. Lab. Invest.* **60,** 323–332.
2. Okin, P.M., Devereux, R.B., Lee, E.T., Galloway, J.M., and Howard, B.V. (2004) *Diabetes* **53,** 434–440.
3. Rossing, P., Breum, L., Major-Peteresen, A., Sato, A., Winding, H., Pietersen, A, Kastrup, J., and Parving, H.H. (2001) *Diabet. Med.* **18,** 199–205.
4. Veglio, M., Chinaglia, A., and Cavallo-Perin, P. (2004) *J. Endocrinol. Invest.* **27,** 175–181.
5. Rana, B.S., Lim, P.O., Naas, A.A.O., Ogston, S.A., Newton, R.W., Jung, R.T., Morris, A.D., and Struthers, A.D. (2005) *Heart* **91,** 44–50.
6. Sawicki, P.T., Dahne, R., Bender, R., and Berger, M. (1996) *Diabetologia* **39,** 77–81.
7. Veglio, M., Bruno, G., Borra, M., Macchia, G., Bargero, G., D'Errico, N., Pagano, G.F., and Cavallo-Perin, P. (2002) *J. Intern. Med.* **251,** 317–324.
8. Cardoso, C.R., Salles, G.F., and Deccache, W. (2003) *Stroke* **34,** 2187–2194.
9. Zhang, Y., Lin, H., Xiao, J., Bai, Y.L., Wang, J., Zhang, H., Yang, B., and Wang, Z. (2007) *Cell. Physiol. Biochem.* **19,** 225–238.
10. Zhang, Y., Wang, J., Bai, Y., Zhang, H., Yang, B., Wang, H., and Wang, Z. (2006) *Am. J. Physiol.* **291,** 1446–1455.
11. Ambros, V. (2004) *Nature* **431,** 350–355.
12. Brennecke, J., Stark, A., Russell, R.B., and Cohen, S.M. (2005) *PLoS Biol.* **3(e85),** 404–418.
13. Zhao, Y., Samal, E., and Srivastava, D. (2005) *Nature* **436,** 214–220.
14. Chen, J.F., Mandel, E.M., Thomson, J.M., Wu, Q., Callis, T.E., Hammond, S.M., Conlon, F.L., and Wang, D.Z. (2006) *Nat. Genet.* **38,** 228–233.
15. Wang, Z., Feng, J., Shi, H., Pond, A., Nerbonne, J.M., and Nattel, S. (1999) *Circ. Res.* **84,** 551–561.
16. Luo, X., Lin, H., Lu, Y., Li, B., Xiao, J., Yang, B., and Wang, Z. (2007) *J. Cell. Physiol.* (in press).

17. Wang, H., Zhang, Y., Cao, L., Han, H., Wang, J., Yang, B., Nattel, S., and Wang, Z. (2002) *Can. Res.* **62,** 4843–4848.

18. Jones, E.M., Roti, E.C., Wang, J., Delfosse, S.A., Robertson, G.A. (2004) *J. Biol. Chem.* **279,** 44690–44694.

19. Krutzfeldt, J., Rajewsky, N., Braich, R., Rajeev, K.G., Tuschl, T., Manoharan ,M., and Stoffel, M. (2005) *Nature* **438,** 685–689

20. Cheng, A.M., Byrom, M.W., Shelton. J., and Ford, L.P. (2005) *Nucleic Acids Res* **33,** 1290–1297.

21. Lu, X.G., Azhar, G., Liu, L., Tsou, H., and Wei, J.Y. (1998) *J. Gerontol. A. Biol. Sci. Med. Sci.* **53,** B3–B10.

22. Nelson, T.J., Balza Jr., R., Xiao, Q., and Misra, R.P. (2005) *J. Mol. Cell. Cardiol.* **39,** 479–489.

23. Zhang, X., Azhar, G., Chai, J., Sheridan, P., Nagano, K., Brown, T., Yang, J., Khrapko, K., Borras, A.M., Lawitts, J., Misra, R.P., and Wei. J.Y. (2001) *Am. J. Physiol.* **280,** H1782–H1792.

24. Spencer, J.A., and Misra, R.P. (1996) *J. Biol. Chem.* **271,** 16535–16543.

25. Taylor, A., Webster, K.A., Gustafson, T.A., and Kedes, L. (1997) *Mol. Cell. Biochem.* **169,** 61–72.

26. Choy, A-M, Kuperschmidt, S., Lang, C.C., Pierson, R.N., and Roden, D.M. (1996) *Circulation* **94,** 164.

27. Janse, M.J. (1994) *Cardiovasc. Res.* **61:** 208–217

28. Li, G.R., Lau, C.P., Ducharme, A., Tardif, J.C., and Nattel, S (2002) *Am. J. Physiol.* **283,** H1031–H1041.

29. Tsuji, Y., Opthof, T., Kamiya, K., Yasui, K., Liu, W., Lu, Z., Kodama, I. (2000) *Cardiovasc. Res.* **48,** 300–309.

3.7 Acknowledgements

*The authors thank XiaoFan Yang for excellent technical support and Marrie-Andrée Lupien for handling human tissues. This work was supported in part by the Canada Diabetes Association and Fonds de la Recherche de l'Institut de Cardiologie de Montreal, awarded to Dr. Z Wang, and by the National Nature Science Foundation of

China (30430780), the Foundation of National Department of Science and Technology of China (2004CCA06700), awarded to Dr. B Yang. Dr. Z. Wang is a senior research scholar of the Fonds de Recherche en Sante de Quebec.

[1]The abbreviations used are: AMO-1 and AMO-133, anti-miRNA oligonucleotides specific for the muscle-specific miRNAs *miR-1* and *miR-133*, respectively; AP, antigenic peptide; Ctl, control; DA, distamycin A; DM, diabetes mellitus; ERG, *ether-a-go-go* related gene; rbERG, rabbit ERG; HERG, human ERG; I_{Kr}, rapid delayed rectifier K^+ current; miRNA, microRNA; MT, mutant; NC, negative control; SRF, serum response factor; SRF-siRNA, small interference ENA against SRF.

Keywords: *miR-133*, ERG, I_{Kr}, SRF, diabetes, QT prolongation

3.8 Figures and Figure Legends

Fig. 1. Upregulation of the muscle-specific microRNAs *miR-1* and *miR-133* and downregulation of ERG (*ether-a-go-go*-related gene) in rabbit hearts of diabetes model (rbERG, n=5 hearts for each group) and in human hearts (HERG, n=6 hearts for each group) from subjects with diabetes mellitus (DM). (**A**) and (**B**) Increases in mRNA levels of *miR-1* and *miR-133*. (**C**) and (**D**) Downregulation of rbERG and HERG protein levels in DM hearts. AP: pretreated with antigenic peptide; Ctl: age-matched and sham-operated control rabbits or patients with healthy hearts. *p<0.05 *vs*. Ctl.

Fig. 2. Post-transcriptional repression of HERG by the muscle-specific microRNA *miR-133*. (**A**) Luciferase reporter activities showing the interaction between *miR-133* and *HERG* gene. HEK293 cells were co-transfected with the chimeric vector carrying luciferase–*HERG* cDNA and *miR-133* (10 nM and 100 nM), mutant *miR-133* (M-*miR-133*, 100 nM), *miR-133*-specific antisense inhibitor oligonucleotides (AMO-133, 100 nM) or *miR-1* (100 nM). Ctl: control cells transfected with the chimeric vector only. AMO-133 was co-transfected with *miR-133* (100 nM). *p<0.05 *vs*. Ctl; +p<0.05 *vs*. *miR-133* (100 nM); n=5 for each group. (**B**) Luciferase reporter activities verifying the interactions of *miR-1* and *miR-133* with their respective exact binding

sequences (standards) in HEK293 cells. AMO-1: *miR-1*-specific antisense inhibitor; *miR-1* standard or *miR-133* standard: the chimeric vectors carrying luciferase gene and the exact *miR-1* or *miR-133* target sequence. AMO-1 (100 nM) was co-transfected with *miR-1* (100 nM). *p<0.05 *vs.* Ctl; n=4 for each group. (**C**) Western blot analysis of HERG protein levels with membrane protein samples isolated from SKBr3 cells. Cells were co-transfected with the chimeric vector and *miR-133* (10 or 100 nM), M-*miR-133*, AMO-133 or *miR-1* (100 nM). "AP+" represents pretreatment of the antibody with its antigenic peptide. AMO-133 (100 nM) was co-transfected with *miR-133* (100 nM). *p<0.05 *vs.* Ctl; +p<0.05 *vs.* *miR-133* (100 nM); n=5 for each group. (**D**) Failure of *miR-133* (10 and 100 nM) to affect mRNA level of HERG in SKBr3 cells. The concentration of M-*miR-133*, AMO-133 and *miR-1* used for these experiments was 100 nM. AMO-133 was co-transfected with *miR-133* (100 nM). n=5 for each group. (**E**) Whole-cell patch-clamp recordings of rapid delayed rectifier K^+ current (I_{Kr}, encoded by rbERG) in left ventricular myocytes isolated from diabetic (DM) and healthy rabbits (Ctl). Current recording was made 24 h after transfection. I_{Kr} in display was elicited by a 2-s depolarizing voltage step to a test potential of +10 mV from a holding potential of -60 mV (see **Supplemental Figure 3** for the full range of voltages tested). AMO-133: Ctl or DM cells treated with AMO-133 (100 nM) alone; +AMO-133: Ctl cells co-transfected with *miR-133* (100 nM) and AMO-133; *miR-133* and *miR-1*: Ctl cells treated with *miR-133* (100 nM) and *miR-1* (100 nM) alone, respectively. *p<0.05 *vs.* Ctl or DM; +p<0.05 *vs.* *miR-133* (100 nM) alone; n=8 cells for each group.

Fig. 3. Role of serum response factor (SRF) in enhancing expressions of *miR-1/miR-133* in the heart of diabetic rabbits. (**A**) Overexpression of SRF in hearts (left ventricular wall) of diabetes mellitus (DM), determined by Western blot analysis. +AP: antigenic peptide treatment of the anti-SRF antibody. *p<0.05 *vs.* Ctl (normal heart); n=8 hearts for each group. (**B**) Reversal of increased *miR-1/miR-133* levels by SRF inhibitor distamycin A (DA) in left ventricular myocytes isolated from DM rabbits. The myocytes were incubated with DA (100 nM) in normal culture medium for 36 h before extraction of RNA samples. *p<0.05 *vs.* Ctl, +p<0.05 *vs.* DM; n=4

hearts for each group. (**C**) Reversal of increased *miR-1/miR-133* levels by the siRNA targeting SRF (SRF-siRNA) in left ventricular myocytes isolated from DM rabbits. The cells were transfected with SRF-siRNA (30 nM) or negative control siRNA (NC siRNA, 30 nM) and 36 h after RNA samples were extracted. *$p<0.05$ *vs.* Ctl, +$p<0.05$ *vs.* siRNA alone; n=4 for each group. (**D**) Increase in I_{Kr} induced by SRF-siRNA in left ventricular myocytes isolated from DM or healthy control (Ctl) rabbits. The cells were transfected with SRF-siRNA (30 nM) or negative control siRNA (NC siRNA, 30 nM) and 36 h after, patch-clamp recordings were performed. I_{Kr} in display was elicited by a 2-s depolarizing voltage step to a test potential of +10 mV from a holding potential of -60 mV (see **Supplemental Figure 3** for the full range of voltages tested). DA: distamycin A (100 nM). n=7 cells for each group except for DA group (n=5 cells). (**E**) Verification of the efficiency of SRF-siRNA in silencing SRF in left ventricular myocytes isolated from DM rabbits, determined by quantitative real-time RT-PCR methods. *$p<0.05$ *vs.* Ctl, +$p<0.05$ *vs.* siRNA alone; n=3 samples for each group.

Figure 1

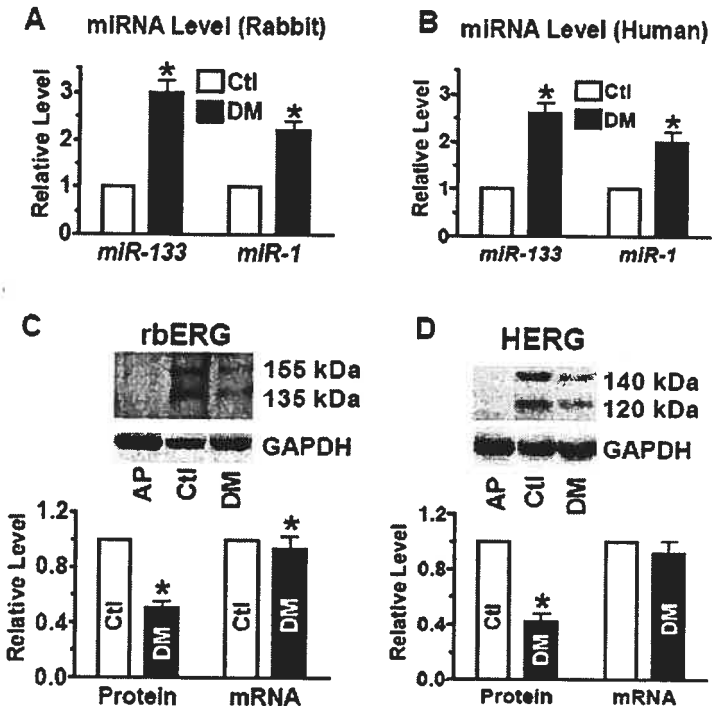
A
miRNA Level (Rabbit)
Relative Level
Ctl
DM
miR-133
miR-1
B
miRNA Level (Human)
C
rbERG
155 kDa
135 kDa
GAPDH
AP
Ctl
DM
Protein
mRNA
D
HERG
140 kDa
120 kDa

Figure 2

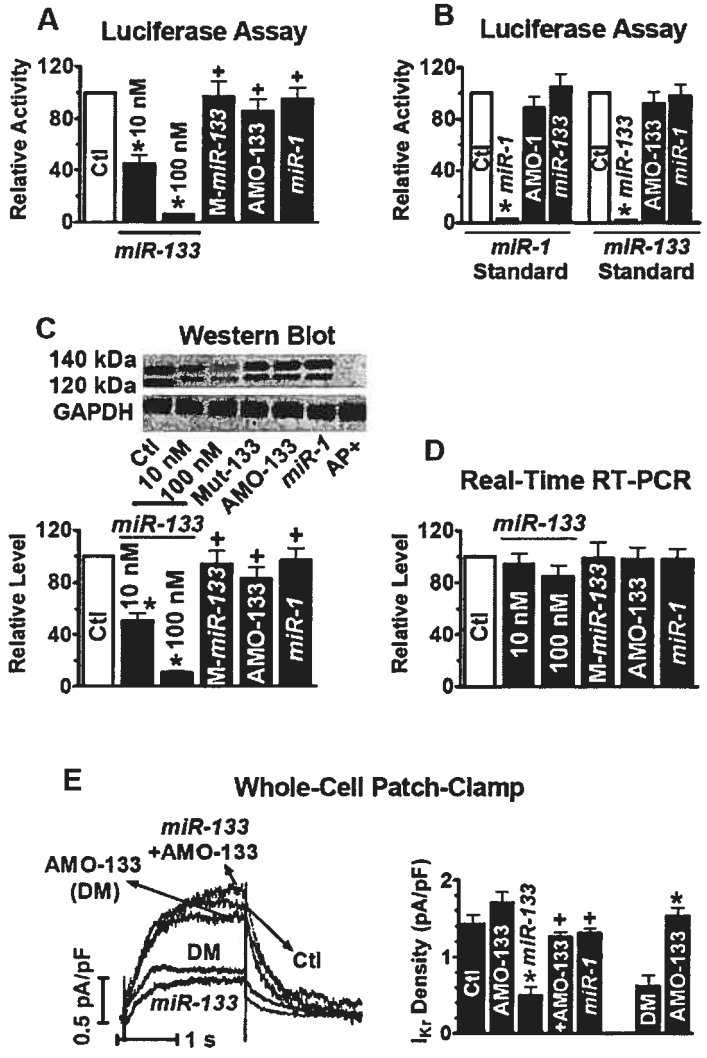
A
Luciferase Assay
Relative Activity
120
80
40
0
Ctl
10 nM
100 nM
M-miR-133
AMO-133
miR-1
miR-133
B
Luciferase Assay
Relative Activity
Ctl
miR-1
AMO-1
miR-133
Ctl
miR-133
AMO-133
miR-1
miR-1 Standard
miR-133 Standard
C
Western Blot
140 kDa
120 kDa
GAPDH
Ctl
10 nM
100 nM
Mut-133
AMO-133
miR-1
AP*
miR-133
Relative Level
D
Real-Time RT-PCR
miR-133
Relative Level
E
Whole-Cell Patch-Clamp
miR-133
+AMO-133
AMO-133
(DM)
DM
Ctl
miR-133
0.5 pA/pF
1 s
I_{Kr} Density (pA/pF)

Figure 3

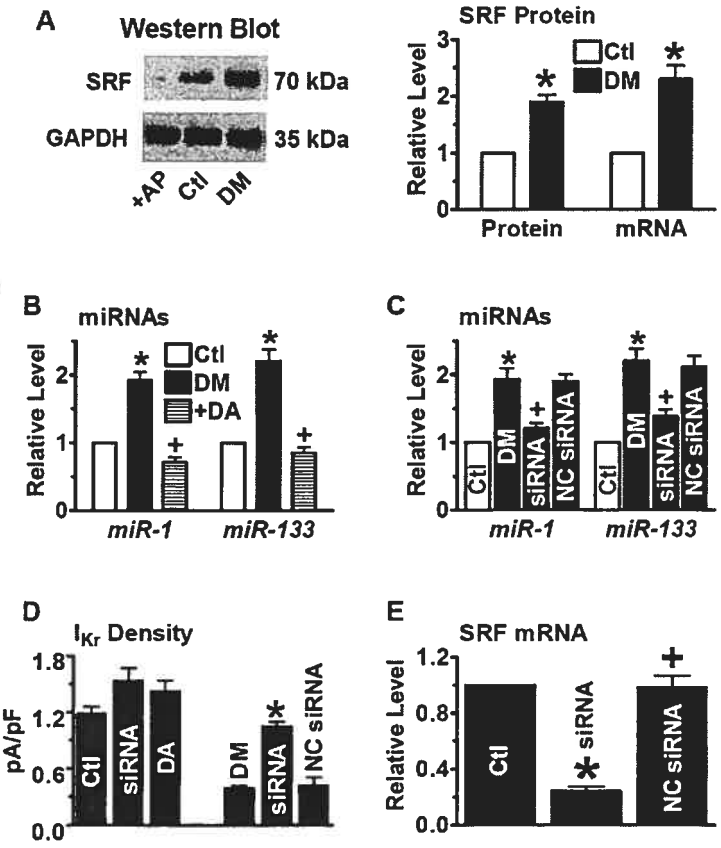
A
Western Blot
SRF
70 kDa
GAPDH
35 kDa
+AP
Ctl
DM
SRF Protein
Relative Level
Ctl
DM
Protein
mRNA
B
miRNAs
Relative Level
Ctl
DM
+DA
miR-1
miR-133
C
miRNAs
Relative Level
Ctl
DM
siRNA
NC siRNA
miR-1
miR-133
D
I_{Kr} Density
pA/pF
Ctl
siRNA
DA
DM
siRNA
NC siRNA
E
SRF mRNA
Relative Level
Ctl
siRNA
NC siRNA

3.9 Supplementary Materials

For

MICRORNA *MIR-133* REPRESSES HERG K^+ CHANNEL EXPRESSION CONTRIBUTING TO QT PROLONGATION IN DIABETIC HEARTS*

Jiening Xiao,[†§¶] Xiaobin Luo,[†§¶] Huixian Lin,[†§¶] Yanjie Lu,[‡¶] Yiqiang Zhang,[†§] Baofeng Yang,[‡¶] and Zhiguo Wang,[†§¶]

[†]Research Center, Montreal Heart Institute, Montreal, PQ H1T 1C8 Canada; [§]Department of Medicine, University of Montreal, Montreal, PQ H3C 3J7 Canada; [‡]Department of Pharmacology (State-Province Key Laboratories of Biomedicine-Pharmaceutics) and [¶]Institute of Cardiovascular Research, Harbin Medical University, Harbin, Heilongjiang 150086, P.R. China

Running Title: Role of *microRNA-133* in diabetic QT prolongation

Address correspondence to: Dr. Zhiguo Wang, Research Center, Montreal Heart Institute, 5000 Belanger East, Montreal, PQ H1T 1C8, Canada; Tel.: (514) 376-3330. Fax: (514) 376-1335. E-mail: [redacted] Prof. Baofeng Yang, Harbin Medical University, Heilongjiang 150086, P. R. China; Tel.: +86 (451) 8667-9473; E-mail: [redacted]

Experimental Procedures

Rat Model of Myocardial Infarction – Male Wistar rats of 230-270 g were randomly divided into control and myocardial infarction (MI) groups. Myocardial infarction was established as previously described (1). The rats were anesthetized with diethyl ether and were placed in the supine position with the upper limbs taped to the table. Chest skin was cleaned with 70% ethanol and a 1–1.5 cm incision was made along the left side of the sternum. The muscle layers of the chest wall were bluntly dissected to avoid bleeding. The thorax was cut open at the point of the most pronounced cardiac pulsation. Using forceps to widen the chest, the abdomen and the right side of the chest were pressed to push the heart out of the thoracic cavity. The left anterior descending (LAD) coronary artery was occluded and then the chest was closed back. All surgical procedures were performed under sterile conditions. Two days after occlusion, the heart was removed and the tissues in ischemic zone were dissected for RNA extraction with with Ambion's *mir*Vana miRNA Isolation Kit for measurement of *miR-1* and *miR-133* levels. Control animals underwent open-chest procedures without coronary artery occlusion. Use of animals was in accordance with the regulations of the ethic committee of Harbin Medical University.

Cell Isolation and Primary Cell Culture – Neonatal rat ventricular cardiomyocytes were isolated and cultured as described previously (2). Briefly, 1-3 days old rats were decapitated and their hearts were aseptically removed. Their ventricles were dissected, minced and trypsinized overnight at 4°C. The next day, cells were dissociated with collagenase and pre-plated twice for 60 min at 37°C. The non-adherent cardiomyocytes were removed and plated in 24-well plates in DMEM/F-12 medium (Invitrogen) containing 10% FBS and 0.1 mM bromodeoxyuridine (Sigma). $1x\ 10^5$ cells/well were seeded in 24-well plate for further experiments. This procedure yielded cultures with ~95% myocytes, as assessed by microscopic observation of cell beating.

Angiotensin II-Induced Hypertrophy and Cell Surface Area Analysis of Cardiomyocytes – Isolated neonatal rat ventricular cells were cultured for 24 h in serum-containing medium after which they were serum-starved for 24 h before

treatment. To induce hypertrophy, cells were stimulated by angiotensin II (1 μM) for 36 h in serum-free culture medium (3,4). Cell surface area was analyzed using a Leica inverted microscope equipped with a Polaroid digital camera at 200×magnification. Cell area was measured using Mocha software (SPSS Inc., Chicago, IL). The cells were collected for total RNA isolation using the Ambion's *mir*Vana miRNA Isolation Kit for measurement of *miR-1* and *miR-133* levels.

Preparation of Animal Model of Congestive Heart Failure (CHF) – The procedures for producing CHF dogs have been previously described in detail (5). Briefly, mongrel dogs (25 to 33 kg) were used for our study. The right ventricle was stimulated at 240 bpm for 3 weeks, followed by 2 weeks at 220 bpm. Dogs were anesthetized with morphine (2 mg/kg SC) and α-chloralose (120 mg/kg IV load, 29.25 mg/kg/h infusion), and a median sternotomy was performed. The heart was quickly removed and the left ventricular endocardium was dissected. The tissue was used for extracting RNA with Ambion's *mir*Vana miRNA Isolation Kit for measurement of *miR-1* and *miR-133* levels.

REFERENCES

1. Yang, B. Lin, H., Xu, C., Liu, Y., Wang, H., Han, H., and Wang. Z. (2005) *Cell. Physiol. Biochem.* **16,** 163–174.
2. Pang, L., Koren, G., Wang, Z., and Nattel, S. (2003) *FEBS Lett.* **546,** 349–354.
3. Lebeche, D., Kaprielian, R., and Hajjar, R. (2006) *J. Mol. Cell. Cardiol.* **40,** 725–735.
4. Rajapurohitam, V., Javadov, S., Purdham, D.M., Kirshenbaum, L.A., and Karmazyn, M. (2006) *J. Mol. Cell. Cardiol.* **41,** 265–274.
5. Li, D., Petrecca, K., Feng, J., Wang, Z., Petrecca, K., Shrier, A., and Nattel, S. (2000) *Circulation* **101,** 2631-2638.

FIGURE LEGENDS

Supplementary Fig. 1. Sequences of the muscle-specific miRNAs and their putative target sites in human *ether-a-go-go*-related gene (HERG) and rabbit *ether-a-go-go*-related gene (rbERG). (**A**) The sequences of wild-type and mutant *miR-1/miR-133* and their respective antisense inhibitors oligonucleotides (AMO-1 and AMO-133). Boldface letters indicate the 'seed site' critical for miRNA::mRNA binding and interaction; lower-case letters indicate the base substitution mutations made to the sequences; italics in the AMOs indicate the locked nucleotides (the ribose ring is constrained by a methylene bridge between the 2'-*O*- and the 4'-C atoms, to confer a higher thermal stability, discriminative power and a longer half-life). AMO-1 and AMO-133 specifically target *miR-1* and *miR-133*, respectively. (**B**) and (**C**) The complementarity between *miR-133* and the putative target sites in HERG gene (**B**) and rbERG gene (**C**). The matched base pairs are bold and connected by "|". The GenBank accession numbers of the genes are indicated in the brackets and the positions of the target sites are labeled by the numbers. Note that there are multiple putative target sites for *miR-133* in HERG and rbERG.

Supplementary Fig. 2. Comparison of *miR-1* and *miR-133* expression levels in various cell lines indicated. *MiR-1* and *miR-133* expression levels were determined by real-time RT-PCR using the *mir*Vana™ qRT-PCR miRNA Detection Kit (Ambion) in conjunction with SYBR Green I. H9c2, rat ventricular cell line (n=6 batches of cells); SKBr3, human breast cancer cell line (n=6 batches of cells); HEK293, human embryonic kidney cell line (n=7 batches of cells). *MiR-1* and *miR-133* levels are expressed as relative levels by normalizing to the values obtained from H9c2 cells. *$p<0.05$ *vs*. H9c2.

Supplementary Fig. 3. Whole-cell patch-clamp recordings of the rapid delayed rectifier K^+ current (I_{Kr}, encoded by rbERG) in left ventricular myocytes isolated from diabetic (DM) and healthy control (Ctl) rabbits. Current recording was made 24 h after transfection. I_{Kr} was elicited by the voltage protocols shown in the inset at an

interpulse interval of 10 s. (**A**) The data on current-voltage (I-V) relationships were obtained from 8 cells for each group. AMO-133 (Ctl): healthy control cells treated with AMO-133 (100 nM); AMO-133 (DM): DM cells treated with AMO-133 (100 nM); +AMO-133 (Ctl): Ctl cells co-transfected with *miR-133* (100 nM) and AMO-133 (100 nM); *miR-133* (Ctl) and *miR-1* (Ctl): Ctl cells treated with *miR-133* (100 nM) and *miR-1* (100 nM) alone, respectively. The differences of I_{Kr} density (pA/pF) between DM or *miR-133* and other groups were statistically significant at voltages from -20 mV to +40 mV. (**B**) Increase in I_{Kr} induced by SRF-siRNA in left ventricular myocytes isolated from DM or Ctl rabbits. The cells were transfected with SRF-siRNA (30 nM) or negative control siRNA (NC siRNA, 30 nM) and 36 h after, patch-clamp recordings were performed. DA: distamycin A (100 nM). n=7 cells for each group except for DA group (n=5 cells).

Supplementary Figure 1

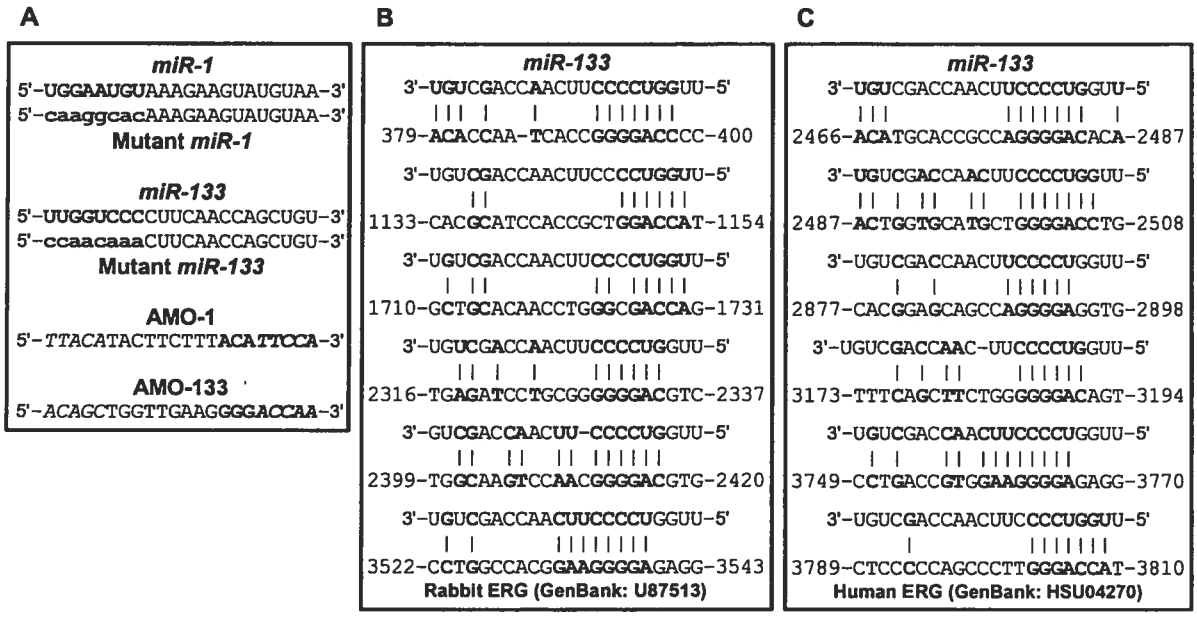

Supplementary Figure 2

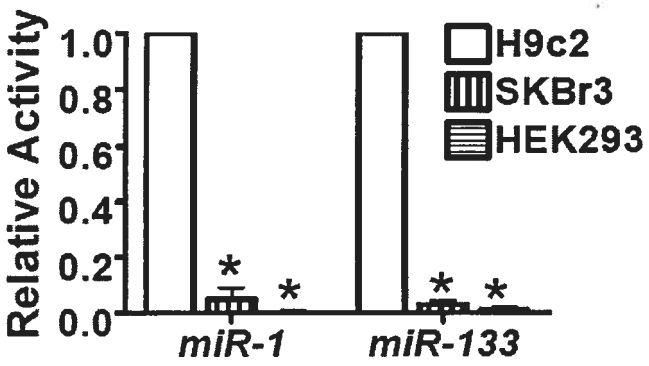

Supplementary Figure 3

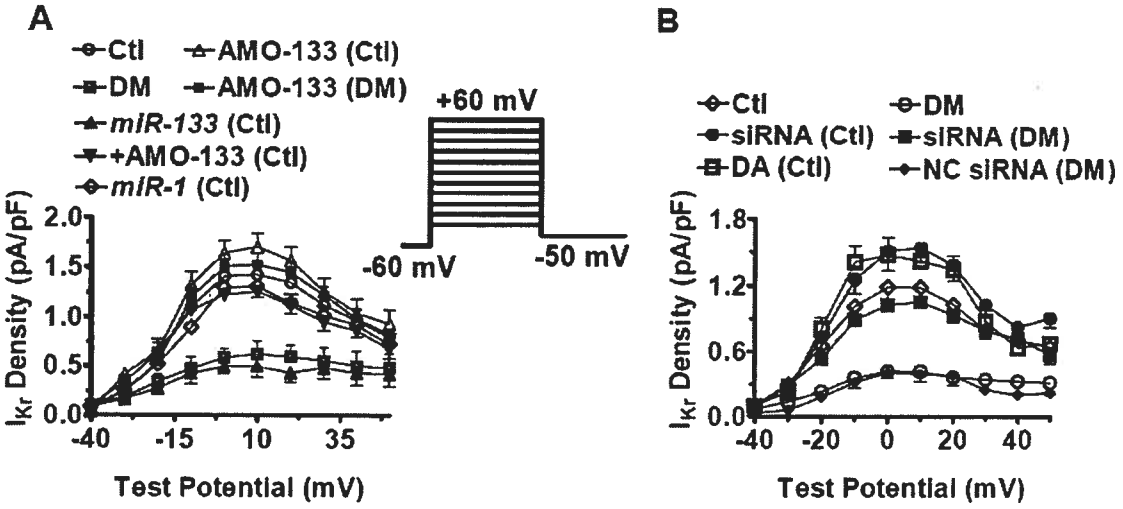

PART III. OVERALL DISCUSSION AND CONCLUSIONS

1. Major findings

HERG1 and *KCNQ1* genes encode two major repolarizing K^+ channel (I_{Kr} and I_{Ks}, respectively) α-subunits that critically determine the repolarization rate and repolarization reserve in cardiac cells thereby the likelihood of arrhythmias. Expressions of these genes are regionally heterogeneous and change dynamically depending on differentiation status and pathological states of the heart. Therefore, elucidating the expression controls of *HERG1* and *KCNQ1* genes will greatly advance our understanding of the molecular mechanisms underlying the electrical remodeling during the developmental stages and pathological processes. In this thesis, we have conducted studies on the transcriptional and post-transcriptional controls of *HERG1* and *KCNQ1* expressions. A number of novel findings are highlighted below.

First, our study identified the core promoter regions of *HERG1a/HERG1b* and *KCNQ1a/KCNQ1b* genes, which control their transcriptions. **Second,** our study revealed the transcription factor Sp1 as a common transactivator for the promoters of *HERG1*, *KCNQ1* and *KCNE1* genes; Sp1 plays an essential role in driving *HERG1*, *KCNQ1* and *KCNE1* transcription and shows an interventricular difference of its expression in the heart. **Third,** our study unraveled a novel aspect of cellular function of miRNAs: post-transcriptional repression of ion channel genes; *miR-133* post-transcriptionally repressed HERG1 and KCNQ1, whereas KCNE1 was validated to be the target for repression by *miR-1*. **Moreover,** evidence was provided indicating that *miR-1/miR-133* exist heterogeneously in the different regions of the heart. **And finally,** our study demonstrated that the interplay between Sp1 and *miR-1/miR-133* determines the expression levels of *HERG1* and *KCNQ1* genes and the unique regional expression profiles of Sp1 and *miR-1/miR-133* may be one of the mechanisms for the well-recognized regional differences of I_{Kr} and I_{Ks}.

2. Summary and Conclusion

2.1 Identification of the core promoter regions of *HERG1* and *KCNQ1* isoforms

The long QT syndrome genes *HERG1* and *KCNQ1*, encoding K^+ channels critical to cardiac repolarization, are both comprised of two isoforms: HERG1a and HERG1b, and KCNQ1a and KCNQ1b, respectively. A number of K^+ channels have been investigated on their genomic structures for the transcriptional regulation, with their promoter regions identified and characterized. However, as already mentioned in the **Introduction** section, the majority of these studies have been conducted with rat and mouse genes, and the acquired information may not be applicable to human counterparts due to the interspecies differences especially at the 5'-untranslated region (5'-UTR) of the genes. Research on promoters of human K^+ channel genes has been sparse despite that two recent studies independently reported the transcriptional control of human *KCNE1* gene encoding a family of single-transmembrane-domain K^+ channel β-subunit that modulate the properties of several K^+ channel α-subunits[1-4].

The promoter for regulation of gene transcription is characterized as the region upstream of its transcription start site (TSS). A TSS for specific gene transcription is normally determined by identification of its complete 5'-UTR. We identified two distinguished TSSs for *HERG1b* and for *KCNQ1a* genes and one TSS for *HERG 1a* and for *KCNQ1b* genes (Chapter 1, Fig. 1). It has been believed that the four isoforms *HERG1a/HERG1b* and *KCNQ1a/KCNQ1b* represent alternatively spliced variants of, *HERG1* and *KCNQ1* genes, respectively[5-8]. However, our results suggest that this view needs to be modified; the four isoforms most likely represent independent transcripts for they each have their own unique transcription start site and promoter region (Chapter 1, Fig. 1,2 and 3).

2.2 Sp1 as the essential transactivators for *HERG1*, *KCNQ1* and *KCNE1* genes

Based on our study, the promoter regions of *HERG1*, *KCNQ1* and *KCNE1* genes all share a common feature, being GC rich in their proximal promoter regions. Computational analysis of these proximal promoter regions reveals multiple Sp1 consensus binding sites and the absence of TATA binding site (Chapter 1, Fig. 1; Chapter 2, Fig. 1). Sp1 is a widely distributed member of a multigene family of zinc-finger transcription factors that bind DNA in mammalian cells primarily via interaction with GC-boxes[9-12]. The binding of Sp1 to GC-boxes is shown to significantly enhance the transcription levels of the genes whose promoters contain no TATA site[13-15]. Consistent with previous reports, our study showed Sp1 to act as transactivator for *HERG1*, *KCNQ1* and *KCNE1* genes. Several lines of evidence were obtained in support of our conclusion. First, there are multiple Sp1 binding sites within the core promoter regions, which are responsible for Sp1 activation of *HERG1*, *KCNQ1* and *KCNE1* genes transcriptional activities, characteristic of 'house-keeping' genes (Chapter 1, Fig. 1; Chapter 2, Fig. 1). Second, the inhibition of Sp1-DNA interaction by mithramycin significantly down-regulated both promoter activities of *HERG1a/HERG1b*(not shown in this thesis from unpublished data), *KCNQ1a* and *KCNE1*(Chapter 2, Fig. 3) as well as the endogenous transcriptions of *HERG1*(not shown in this thesis from unpublished data), *KCNQ1* and *KCNE1*(Chapter 2, Fig. 3). In contrast, overexpression of Sp1 boosted up their promoter activities (Chapter 2, Fig. 3). Third, in a Sp1-null environment (SL-2 cell) the core promoter constructs failed to show any activities whereas when co-transfected with Sp1, SL-2 cells allows promoter activation (Chapter 2, Fig. 3).

Taken together, we can make a conclusion that Sp1 serve as an essential transactivator for HERG1, KCNQ1 and KCNE1 genes. Moreover, the ion channels gene promoters that have been identified to date (including the promoters in this study), regardless of animal species, share the same general structural features common to the housekeeping-type promoters. That is, the promoter lack consensus TATA boxes and are GC-rich with multiple Sp1 consensus elements.

2.3 HERG1, KCNQ1 and KCNE1 are targets for post-transcriptional repression by the muscle-specific microRNAs *miR-1* and *miR-133*

Having generated a tremendous amount of excitement about miRNAs in many areas of biology, research over the past five years has put miRNAs at centre stage. Indeed, miRNA-mediated gene regulation is now considered a fundamental layer of genetic programs that operates at the post-transcriptional level. Based on computational prediction, HERG is shown to be the target of *miR-133*, whereas, neither KCNQ1 nor KCNE1 were considered as candidate targets for *miR-1/miR-133*, despite that they both have substantial complementarity to the miRNAs, likely due to unfavorable free energy status. By detailed analysis (basing on the complimentarity) of the 3'UTR of *HERG1* and *KCNQ1*, we identified 6 putative *miR-133* binding sites for *HERG1* (Chapter 3, Supplemental Fig. 1) and four of that for *KCNQ1* (Chapter2, Fig. 4A). Similarly, the 3'UTR of *KCNE1* was found containing three putative *miR-1* binding sites (Chapter2, Fig. 5A). These multiple sites may cooperate with one another to confer significant effects of the miRNAs.

In order to verify HERG1, KCNQ1 and KCNE1 are indeed the cognate targets of *miR-1/miR-133* for post-transcriptional repression, we took the following two approaches. First, we used a cell-based luciferase reporter gene system to test the effect of *miR-1/miR-133* on 3'UTR of each gene by overexpressing or silencing these miRNAs, which has been reported to be an effective way to study the function of miRNAs[16-18]. Second, we determined the effects of *miR-1/miR-133* on endogenous expression of HERG1, KCNQ1 and KCNE1 at both protein and mRNA levels in culture cells. Our experimental data convincingly demonstrated that the expression levels of HERG1, KCNQ1 and KCNE1 are importantly regulated by *miR-133* and *miR-1*, respectively. Consistent with the principle of action of miRNAs, *miR-133* and *miR-1* decreased HERG1, KCNQ1 and KCNE1 protein levels without significantly affecting their mRNA levels (Chapter 2, Fig. 4&5; Chapter 3, Fig. 2). Moreover, our study is, to date, the first study to elucidate that the expression of ion channel genes could be regulated not only on their 5'UTR but also on the 3'UTR of the mRNA.

2.4 The spatial distribution patterns of Sp1 and *miR-1/miR-133* and the potential roles in regional heterogeneity of I_{Kr} and I_{Ks}

One of the most important findings in this study is the heterogeneous distribution of Sp1 and miRNAs in adult human hearts. We assessed the expression level of Sp1 and *miR-1/miR-133* at three different axes in the heart (interventricular, transmural and apical-basal) and we found that there is an interventricular difference of the expression of Sp1 (RV>LV) at both protein and mRNA levels (Chapter2, Fig 7), whereas neither *miR-1* nor *miR-133* showed any appreciable interventricular difference (Chapter 2, Fig. 7). Intriguingly, both *miR-1* (Epi>Mid; Base>Apex) and *miR-133* (Mid>Epi; Base>Apex) appeared to have characteristic differences in their expressions in transmural and apical-basal axes (Chapter 2, Fig. 7), whereas, in the same axes, both protein and mRNA levels of Sp1 were found to be consistently identical (Chapter 2, Fig. 7). Considering the effects of Sp1 and *miR-1/miR-133* we have demonstrated on regulation of *HERG1*, *KCNQ1* and *KCNE1* genes, it is quite reasonable for us to question whether the heterogeneous distributions of Sp1 and *miR-1/miR-133* may have correlation to regional asymmetries of I_{Kr} and I_{Ks}.

For I_{Kr}, there is not obvious transmural difference, whereas, a debatable interventricular difference in the canine heart is reported[19]. As in our studies, we tried to reproduce the interventricular difference of I_{Kr} and found that, indeed, there exist interventricular gradients of *HERG1* transcripts in human heart (Chapter 1, Fig. 7). One possible mechanism underlying this interventricular difference is through regulating the target genes activated by dose-response transcriptional regulators binding. In this scenario, differences in the levels of transcription factors result in the activation or repression of diverse target genes, allowing finer control of the spatial and temporal events of organogenesis. A recent study revealed that a transcription factor (repressor) Irx5 encoded by the Iroquois homeobox gene can repress expression of the gene encoding Kv4.2 and is expressed with an opposite transmural gradient to Kv4.2 is in mice[20]. Besides Irx5, another two transcription factor genes, Irx3 and Etv1, were also found to be expressed in transmural gradients across the ventricular walls of rat and canine hearts[21]. Whether these two factors play roles in regional differences of K^+ channels remained unknown, we have made a

comprehensive survey of *HERG1*, *KCNQ1* and *KCNE1* genes' 5'-flanking regions using the *MatInspector* program and did not find any consensus sites as candidates for Irx3, Irx5 or Etv1 binding. Instead, our data point to the critical role of transactivator Sp1 in *HERG1* transcription. First, Sp1 is an essential driving factor for *HERG1* transcriptions. Moreover, Sp1 expression demonstrates the same pattern of interventricular gradient of *HERG1* expression, at both mRNA and protein levels, and this is in agreement with the finding that there is not interventricular difference of *miR-133*. It is thus possible to conclude that the interventicular dispersion of I_{Kr} may be determined by Sp1.

For I_{Ks}, there is a well-recognized spatial heterogeneity in its distribution in the heart, similar to the study of I_{Kr}, we first qualitatively reproduced the results reported in previous published studies: (1) KCNQ1 and KCNE1 distribute with significant interventricular gradients (RV>LV) at both mRNA and protein levels [22], (2) the protein levels of both KCNQ1 and KCNE1 are higher in apical than in basal area[23], despite that their mRNA levels are not significantly different, and (3) KCNQ1 protein level is greater in Epi than in Mid[24], whereas that of KCNE1 is the opposite, and there is not transmural difference in mRNA levels of KCNQ1 and KCNE1[25]. Clearly, in addition to the regional difference of KCNQ1 and KCNE1 expressions, there is also a consistent discrepancy between the protein and mRNA expressions of these genes (Chapter 2, Fig. 6). Intriguingly, the distribution patterns of Sp1 and *miR-1*/*miR-133* seem to provide a reasonable explanation for the observations and this can be sorted out as following. First, the interventricular difference of Sp1, which drives KCNQ1 and KCNE1 expressions, corresponds exactly to the interventricular differences of KCNQ1 and KCNE1, at both mRNA and protein levels. By comparison, *miR-1* and *miR-133* do not show any chamber-dependent difference. These suggest that the higher abundance of Sp1 in RV likely contributes to the higher abundance of KCNQ1 and KCNE1 in the same chamber. Second, there is no difference of Sp1 expression either across the LV wall or along the apical-basal axis, coincident with the uniformity of distributions of KCNQ1 and KCNE1 transcripts in these two axes. Most strikingly, the *miR-133* level was found much greater in Base than in Apex and in Mid than in Epi. Considering the fact that *miR-133* represses

KCNQ1 proteins leaving its transcripts unaltered, it is not difficult to understand why KCNQ1 protein levels have the opposite patterns of transmural and apical-basal gradients to those of *miR-133* but KCNQ1 mRNA does not have transmural and apical-basal gradients. The same logic can be applied to *miR-1* and KCNE1; the characteristic regional distributions of *miR-1*, Base>Apex and Epi>Mid, can be one of the causal factors for the converse transmural and apical-basal gradients of KCNE1 protein levels (Chapter 2, Fig.7). It seems reasonable to come to a conclusion that the combination and interplay of the characteristic spatial distributions of Sp1 and *miR-1/miR-133* account, at least partially, for the regional heterogeneity of I_{Ks}-encoding genes and the disparity between protein and mRNA expressions of these genes.

3. Potential implications

In brief, the present studies have several important pathophysiological implications.

It is well known that the normal heterogeneities of I_{Kr} and I_{Ks} are crucial for determining the normal cardiac repolarization dispersion and abnormal repolarization dispersion is a prerequisite for arrhythmias to occur and to sustain (such as *torsade de pointes*). The normal heterogeneity of cardiac repolarization can be changed under pathological conditions, which renders the heart a loss of the intrinsic antiarrhythmic mechanism and a vulnerability to arrhythmogenesis. For example, enlarged interventricular differences have been shown to cause acquired LQTS [26;27]. Our finding that Sp1 and *miR-133/miR-1* as a potential mechanistic link for the special heterogeneities between ion channel expressions and cardiac repolarization suggests a new approach for antiarrhythmic therapy via interfering expressions of Sp1 and *miR-133/miR-1*. In the other word, Sp1 and *miR-133/miR-1* might prove novel antiarrhythmic targets.

Second, the results from present studies also have some important implications in channelopathy under various disease conditions. In our study, *miR-133* was found to be responsible for the disparate alterations of HERG protein and mRNA, which had been observed along with the I_{Kr}/HERG channelopathy in diabetic hearts. Moreover, it is important to note here that the phenomenon of disparate

changes of HERG expression at protein and mRNA levels have also been observed in failing heart and ischemic myocardium. For example, several studies found that I_{Kr} current density was significantly diminished in myocytes from failing hearts that is also electrophysiologically characterized by repolarization slowing and QT prolongation similar to diabetic hearts, despite that the mRNA level of HERG was barely altered under these conditions[28]. Whether these disparate changes of ERG protein and mRNA in failing hearts and ischemic myocardium are consequent to upregulation of *miR-133* expression is worthy of detailed studies. Our recent paper further demonstrated that *miR-1* is an arrhythmogenic or proarrhythmic factor that is detrimental to the ischemic heart[29]. Taken together, it is possible to speculate that *miR-1/miR-133* may have important pathophysiological function in the heart and may play an essential role in disease-induced ion channel dysfunction.

Third, as already described in the **Introduction**, expression of *HERG* and *KCNQ1* in cardiac cells changes in its abundance during the early developmental stages with *HERG* and *KCNQ1* highly expressed in the fetal heart and dissipate in the adult stage.[30;31] Similarly, in neural crest neurons, HERG1 currents are transiently expressed at very early stages of their neuronal development, disappearing at later stages to be substituted by inward rectifier-like currents[32]. Coincidently, Sp1 expression also undergoes similar developmental alterations. Ubiquitously expressed, this nuclear protein has been implicated in the activation or suppression of a large number of genes and is shown to be involved in cellular process such as cell cycle regulation, chromatin remodeling, prevention of CpG island methylation, and apoptosis. Together this fact with the findings in the present studies, it is suggested that Sp1 might be an important factor in developmental control of ion channel genes.

4. Possible limitations of the present study

It should be noted that there are some limitations in the present study. First, the exact roles of *HERG1b* and *KCNQ1b* in cardiac repolarization and their functional relationships with *HERG1a* and *KCNQ1b*, respectively, were not investigated in this study. Second, we did not investigate the regional difference of MirP-1 in the present study and its possible role in determining the functional

dispersion of I_{Kr}. And finally, our data did not provide enough information to conclusively establish the pathophysiological roles of Sp1 and *miR-1* and *miR-133*, and further studies using *in vivo* genetic engineering of Sp1 and *miR-1/miR-133* are absolutely needed to fully establish to unravel this issue.

5. Future Directions

Given the potential important roles of Sp1 and *miR-1/miR-133* in determining the regional heterogeneities of I_{Kr} and I_{Ks}, the exact pathophysiological function of Sp1 and *miR-1/miR-133* will need to be clarified. To achieve this goal, we could probably use an *in vivo* engineered Sp1- or *miR-1/miR-133*- knockout mice, but the problem here will be how to examine the functional properties of HERG1 and KCNQ1, since it has been shown that I_{Kr} and I_{Ks} are undetectable in the small adult rodent. Another aspect which will be worth of further investigation is whether Sp1, per se, is also affected by *miR-1/miR-133* or even some other miRNAs, although, according to our data, the distribution profile of Sp1 in the heart were converse to those of *miR-1* and *miR-133* and it is unlikely that the regional difference of Sp1 is determined by either *miR-1* or *miR-133*.

6. References

1. Mustapha Z, Pang L, Nattel S. Characterization of the cardiac KCNE1 gene promoter. *Cardiovasc Res*. 2007;73:82-91.

2. Lundquist AL, Turner CL, Ballester LY, George AL, Jr. Expression and transcriptional control of human KCNE genes. *Genomics*. 2006;87:119-128.

3. McDonald TV, Yu Z, Ming Z, Palma E, Meyers MB, Wang KW, Goldstein SA, Fishman GI. A minK-HERG complex regulates the cardiac potassium current $I_{(Kr)}$. *Nature*. 1997;388:289-292.

4. Sanguinetti MC, Curran ME, Zou A, Shen J, Spector PS, Atkinson DL, Keating MT. Coassembly of K(V)LQT1 and minK (IsK) proteins to form cardiac $I_{(Ks)}$ potassium channel. *Nature*. 1996;384:80-83.

5. Lees-Miller JP, Kondo C, Wang L, Duff HJ. Electrophysiological characterization of an alternatively processed ERG K^+ channel in mouse and human hearts. *Circ Res*. 1997;81:719-726.

6. Crociani O, Guasti L, Balzi M, Becchetti A, Wanke E, Olivotto M, Wymore RS, Arcangeli A. Cell cycle-dependent expression of HERG1 and HERG1B isoforms in tumor cells. *J Biol Chem*. 2003;278:2947-2955.

7. Demolombe S, Baro I, Pereon Y, Bliek J, Mohammad-Panah R, Pollard H, Morid S, Mannens M, Wilde A, Barhanin J, Charpentier F, Escande D. A dominant negative isoform of the long QT syndrome 1 gene product. *J Biol Chem*. 1998;273:6837-6843.

8. Pereon Y, Demolombe S, Baro I, Drouin E, Charpentier F, Escande D. Differential expression of KvLQT1 isoforms across the human ventricular wall. *Am J Physiol*. 2000;278:H1908-H1915.

9. Black AR, Black JD, Azizkhan-Clifford J. Sp1 and kruppel-like factor family of transcription factors in cell growth regulation and cancer. *J Cell Physiol*. 2001;188:143-160.

10. Samson SL, Wong NC. Role of Sp1 in insulin regulation of gene expression. *J Mol Endocrinol*. 2002;29:265-279.

11. Pugh BF, Tjian R. Mechanism of transcriptional activation by Sp1: evidence for coactivators. *Cell*. 1990;61:1187-1197.

12. Kadonaga JT, Courey AJ, Ladika J, Tjian R. Distinct regions of Sp1 modulate DNA binding and transcriptional activation. *Science*. 1988;242:1566-1570.

13. Rudge TL, Johnson LF. Synergistic activation of the TATA-less mouse thymidylate synthase promoter by the Ets transcription factor GABP and Sp1. *Exp Cell Res*. 2002;274:45-55.

14. Skak K, Michelsen BK. The TATA-less rat GAD65 promoter can be activated by Sp1 through non-consensus elements. *Gene*. 1999;236:231-241.

15. Azizkhan JC, Jensen DE, Pierce AJ, Wade M. Transcription from TATA-less promoters: dihydrofolate reductase as a model. *Crit Rev Eukaryot Gene Expr*. 1993;3:229-254.

16. Chan JA, Krichevsky AM, Kosik KS. MicroRNA-21 is an antiapoptotic factor in human glioblastoma cells. *Cancer Res*. 2005;65:6029-6033.

17. Cheng AM, Byrom MW, Shelton J, Ford LP. Antisense inhibition of human miRNAs and indications for an involvement of miRNA in cell growth and apoptosis. *Nucleic Acids Res*. 2005;33:1290-1297.

18. Krutzfeldt J, Rajewsky N, Braich R, Rajeev KG, Tuschl T, Manoharan M, Stoffel M. Silencing of microRNAs in vivo with 'antagomirs'. *Nature*. 2005;438:685-689.

19. Volders PG, Sipido KR, Carmeliet E, Spatjens RL, Wellens HJ, Vos MA. Repolarizing K^+ currents I_{TO1} and I_{Ks} are larger in right than left canine ventricular midmyocardium. *Circulation*. 1999;99:206-210.

20. Costantini DL, Arruda EP, Agarwal P, Kim KH, Zhu Y, Zhu W, Lebel M, Cheng CW, Park CY, Pierce SA, Guerchicoff A, Pollevick GD, Chan TY, Kabir MG, Cheng SH, Husain M, Antzelevitch C, Srivastava D, Gross GJ, Hui CC, Backx PH, Bruneau BG. The homeodomain transcription factor Irx5 establishes the mouse cardiac ventricular repolarization gradient. *Cell*. 2005;123:347-358.

21. Rosati B, Grau F, McKinnon D. Regional variation in mRNA transcript abundance within the ventricular wall. *J Mol Cell Cardiol*. 2006;40:295-302.

22. Ramakers C, Vos MA, Doevendans PA, Schoenmakers M, Wu YS, Scicchitano S, Iodice A, Thomas GP, Antzelevitch C, Dumaine R. Coordinated down-regulation of KCNQ1 and KCNE1 expression contributes to reduction of $I(_{Ks})$ in canine hypertrophied hearts. *Cardiovasc Res*. 2003;57:486-496.

23. Szentadrassy N, Banyasz T, Biro T, Szabo G, Toth BI, Magyar J, Lazar J, Varro A, Kovacs L, Nanasi PP. Apico-basal inhomogeneity in distribution of ion channels in canine and human ventricular myocardium. *Cardiovasc Res*. 2005;65:851-860.

24. Szabo G, Szentandrassy N, Biro T, Toth BI, Czifra G, Magyar J, Banyasz T, Varro A, Kovacs L, Nanasi PP. Asymmetrical distribution of ion channels in canine and human left-ventricular wall: epicardium versus midmyocardium. *Pflugers Arch*. 2005;450:307-316.

25. Pereon Y, Demolombe S, Baro I, Drouin E, Charpentier F, Escande D. Differential expression of KvLQT1 isoforms across the human ventricular wall. *Am J Physiol*. 2000;278:H1908-H1915.

26. Verduyn SC, Vos MA, van der ZJ, Kulcsar A, Wellens HJ. Further observations to elucidate the role of interventricular dispersion of repolarization and early afterdepolarizations in the genesis of acquired torsade de pointes arrhythmias: a comparison between almokalant and d-sotalol using the dog as its own control. *J Am Coll Cardiol*. 1997;30:1575-1584.

27. Verduyn SC, Vos MA, van der ZJ, van der Hulst FF, Wellens HJ. Role of interventricular dispersion of repolarization in acquired torsade-de-pointes arrhythmias: reversal by magnesium. *Cardiovasc Res*. 1997;34:453-463.

28. Tsuji Y, Opthof T, Kamiya K, Yasui K, Liu W, Lu Z, Kodama I. Pacing-induced heart failure causes a reduction of delayed rectifier potassium currents along with decreases in calcium and transient outward currents in rabbit ventricle. *Cardiovasc Res*. 2000;48:300-309.

29. Yang B, Lin H, Xiao J, Lu Y, Luo X, Li B, Zhang Y, Xu C, Bai Y, Wang H, Chen G, Wang Z. The muscle-specific microRNA *miR-1* regulates cardiac arrhythmogenic potential by targeting GJA1 and KCNJ2. *Nat Med*. 2007;13:486-491.

30. Wang L, Feng ZP, Kondo CS, Sheldon RS, Duff HJ. Developmental changes in the delayed rectifier K^+ channels in mouse heart. *Circ Res*. 1996;79:79-85.

31. Wang L, Duff HJ. Identification and characteristics of delayed rectifier K^+ current in fetal mouse ventricular myocytes. *Am J Physiol*. 1996;270:H2088-H2093.

32. Arcangeli A, Rosati B, Cherubini A, Crociani O, Fontana L, Ziller C, Wanke E, Olivotto M. *Eur J Neurosci*. 1997;9:2596-2604.

APPENDIX

Appendix 1. Additional Publications

1. Lin H, Xiao J, **Luo X**, Xu C, Gao H, Wang H, Yang B, Wang Z. Overexpression HERG K^+ channel gene mediates cell-growth signals on activation of oncoproteins Sp1 and NF-kB and inactivation of tumor suppressor Nkx3.1. ***J Cell Physiol*** 2007 Feb 20;212(1):137-147.

2. Zhang Y, Xiao J, Wang H, **Luo X**, Wang J, Villeneuve LR, Zhang H, Bai Y, Yang B, Wang Z. Restoring depressed HERG K^+ channel function as a mechanism for insulin treatment of the abnormal QT prolongation and the associated arrhythmias in diabetic rabbits. ***Am J Physiol*** 2006 291(3):1446-1455.

3. Yang B, Lin H, Xiao J, Lu Y, **Luo X**, Li B, Zhang Y, Xu C, Bai Y, Wang H, Chen G, Wang Z. The muscle-specific microRNA *miR-1* causes cardiac arrhythmias by targeting *GJA1* and *KCNJ2* genes. ***Nat Med*** 2007 Apr;13(4):486-491.

4. Xiao J, Yang B, Lin H, Lu Y, **Luo X**, Wang Z. (2007) Novel approaches for gene-specific interference via manipulating actions of microRNAs: Examination on the pacemaker channel genes *HCN2* and *HCN4*. ***J Cell Physiol*** 2007 Aug;212(2):285-92.

5. Zhang Y, Lin H, Xiao J, **Luo X**, Bai Y, Wang J, Zhang H, Yang B, Wang Z. (2007) Abnormal QT prolongation and the associated arrhythmias in diabetic rabbits: HERG K+ channelopathy as the result of metabolic perturbations. ***Cell Physiol Biochem*** 2007;19(5-6):225-38

Appendix 2. Accord de coauteurs

Appendix 2. Accord de coauteurs

ANNEXE II

ACCORD DES COAUTEURS ET PERMISSION DE L'ÉDITEUR

A) Déclaration des coauteurs d'un article

Lorsqu'un étudiant n'est pas le seul auteur d'un article qu'il veut inclure dans son mémoire ou dans sa thèse, il doit obtenir l'accord de tout les coauteurs à cet effet et joindre la déclaration signée à l'article en question. Une déclaration distincte doit accompagner chacun des articles inclus dans le mémoire ou la thèse.

1. **Identification de l'étudiant et du programme**
   Xiaobin Luo
   2ème cycle en sciences biomédicales, sans option
2. **Description de l'article**

Luo X, Xiao J, Lin H, Lu Y, Li B, Yang B, Wang Z. (2006) Transcriptional activation by stimulating protein 1 and post-transcriptional repression by muscle-specific microRNAs of I_{Ks}-encoding genes and potential implications in regional heterogeneity of their expressions. ***J Cell Physiol*** (In Press).
List of the authors:
Xiaobin Luo, Jiening Xiao, Huixian Lin, Yanjie Lu, Baoxin Li, Baofeng Yang, Zhiguo Wang.
This paper is accepted to be published in Journal of Cellular Physiology on Dec 21, 2006

Luo X, Lin H, Lu Y, Li B, Xiao J, Yang B, Wang Z. (2007) Genomic structure, transcriptional control and tissue distribution of human *ERG1* and *KCNQ1* genes. ***Genomics*** (in Preparation).
List of the authors:
Xiaobin Luo, Huixian Lin, Yanjie Lu, Baoxin Li, Jiening Xiao, Baofeng Yang, Zhiguo Wang.
This paper is now in preparation and will be submitted to ***Genomics*** journal in the middle of February 2007.

3. **Déclaration de tous les coauteurs autres que l'étudiant**

À titre de coauteur de l'article identifié ci-dessus, je suis d'accord pour que **Xiaobin Luo** inclue cet article dans **son mémoire de maîtrise** qui a pour titre **Transcriptional activation by Sp1 and post-transcriptional repression by muscle specific microRNA mir-133 of expression of human ERG1 and KCNQ1 genes and potential implication in Arrythmogenesis**.

Jiening Xiao [redacted] Feb. 8. 07
Coauteur Signatur

Huixian Lin [redacted] Feb. 8. 07
Coauteur Signatur

Yanjie Lu [redacted] 08/02/07
Coauteur Signatur

Baoxin Li [redacted] Feb. 8. 07
Coauteur Sign

Baofeng Yang [redacted] for Prof. Baofeng Yang 09/02/2007
Coauteur Signature

Zhiguo Wang [redacted] 08/02/2007
Coauteur Signat

SIGNATURE DES COAUTEURS

Titre du 1er article :

Transcriptional activation by stimulating protein 1 and post-transcriptional repression by muscle-specific microRNAs of I_{Ks}-encoding genes and potential implications in regional heterogeneity of their expressions

Signature des coauteurs :

[redacted]

XIAO, Jiening

[redacted]

LIN, Huixian

[redacted]

LU, Yanjie

[redacted]

LI, Baoxin

[redacted] for Prof. Baofeng Yang

YANG, Baofeng

[redacted]

WANG, Zhiguo

SIGNATURE DES COAUTEURS

Titre du 2ème article :

Genomic structure, transcriptional control and tissue distribution of human *ERG1* and *KCNQ1* genes

Signature des coauteurs :

[redacted]
LIN, Huixian

[redacted]
LU, Yanjie

[redacted]
LI, Baoxin

[redacted]
XIAO, Jiening

[redacted] for Prof. Baofeng Yang
YANG, Baofeng

[redacted]
WANG, Zhiguo

SIGNATURE DES COAUTEURS

Titre du 3ème article :

MicroRNA miR-133 Represses HERG K+ Channel Expression Contributing to QT Prolongation in Diabetic Hearts.

Signature des coauteurs :

[redacted]

XIAO, Jiening

[redacted]

ZHANG, Yiqiang

[redacted]

LIN, Huixian

[redacted] for Baofeng Yang

YANG, Baofeng

[redacted] for Ying Zhang

ZHANG, Ying

[redacted]

WANG, Zhiguo

[redacted]

LU, Yanjie

[redacted]

WANG, Ning

ANNEXE II

ACCORD DES COAUTEURS ET PERMISSION DE L'ÉDITEUR

A) Déclaration des coauteurs d'un article

Lorsqu'un étudiant n'est pas le seul auteur d'un article qu'il veut inclure dans son mémoire ou dans sa thèse, il doit obtenir l'accord de tout les coauteurs à cet effet et joindre la déclaration signée à l'article en question. Une déclaration distincte doit accompagner chacun des articles inclus dans le mémoire ou la thèse.

1. **Identification de l'étudiant et du programme**
   Xiaobin Luo
   2ème cycle en sciences biomédicales, sans option
2. **Description de l'article**

Xiao J, Lin H, **Luo X**, Bai Y, Wang H, Lu Y, Yang B, Wang Z.(2007) Critical roles of transcription factor Sp1 in driving the promoter activities of *HERG1* genes and in determining the interventricular dispersion of their expressions. (to be submitted)
List of the authors:
Jiening Xiao, Huixian Lin, Xiaobin Luo,Yunlong Bai, Huizhen Wang, Yanjie Lu, Baofeng Yang, Zhiguo Wang.

Xiao J, **Luo X**, Lin H, Zhang Y, Lu Y, Wang N, Zhang Y, Yang B, Wang Z. MicroRNA miR-133 Represses HERG K+ Channel Expression Contributing to QT Prolongation in Diabetic Hearts.***J Biol Chem.*** 2007 Apr 27;282(17):12363-7.
List of the authors:
Jiening Xiao, Xiaobin Luo, Huixian Lin, Ying Zhang, Yanjie Lu, Ning Wang, Yiqiang Zhang, Baofeng Yang, Zhiguo Wang.
This paper is published in the ***Journal of Biological Chemistry*** on April 27, 2007

3. **Déclaration de tous les coauteurs autres que l'étudiant**

À titre de coauteur de l'article identifié ci-dessus, je suis d'accord pour que **Xiaobin Luo** inclue cet article dans **son mémoire de maîtrise** qui a pour titre **Transcriptional activation by Sp1 and post-transcriptional repression by muscle specific microRNA mir-133 of expression of human ERG1 and KCNQ1 genes and potential implication in Arrythmogenesis**.

Jiening Xiao [redacted]
Coauteur Signature Date

Huixian Lin [redacted]
Coauteur Signature Date

Ying Zhang [redacted] 09/02/2007
Coauteur Signature Date

Ning Wang [redacted] 08/02/2007
Coauteur Signature Date

Yunlong Bai [redacted] 09/02/2007
Coauteur Signature Date

Yiqiang Zhang [redacted]
Coauteur Signature Date

Yanjie Lu [redacted] Feb. 8, 07
Coauteur Signature Date

Huizhen Wang [redacted] 10/02/2007
Coauteur Signature Date

Baofeng Yang [redacted] 09/02/2007
Coauteur Signature Date

Zhiguo Wang [redacted] 08/02/2007
Coauteur Signature Date